Lateral persistency of precession-driven floodplain cycles and their relation to fluvial sandbodies

MSc Thesis

Jasper de Lanoy

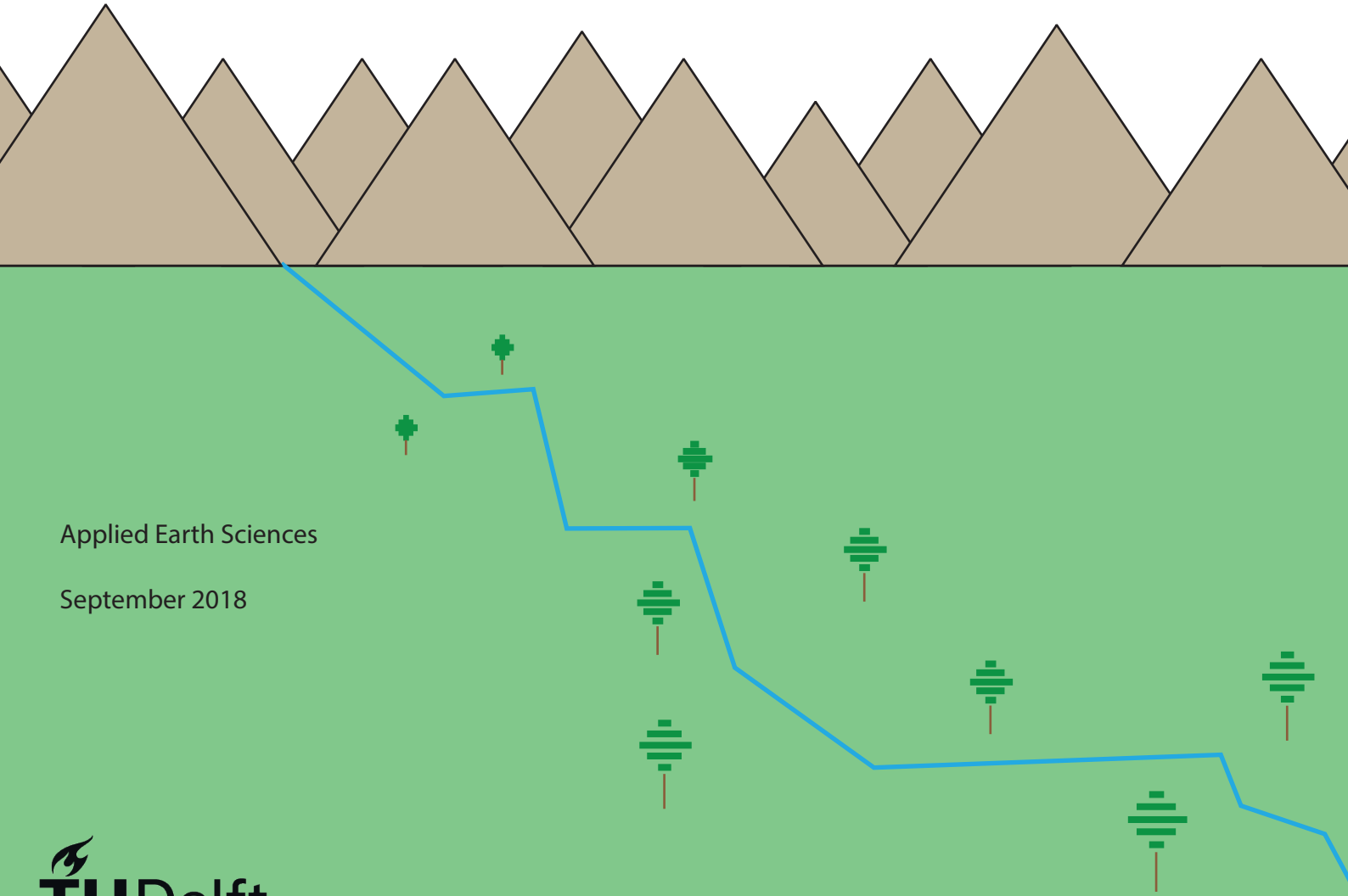

Applied Earth Sciences

September 2018

TU Delft

Lateral persistency of precession-driven floodplain cycles and their relation to fluvial sandbodies

MSc thesis

by

Jasper de Lanoy

to obtain the degree of Master of Science
at the Delft University of Technology,
to be defended publicly on September 26, 2018 at 11:00 AM.

Department of Geoscience & Engineering, section Applied Geology

Student number:	4225368	
Project duration:	November, 2017 – September, 2018	
Thesis committee:	Dr. H.A. Abels,	TU Delft, section Applied Geology - daily supervisor
	Dr. J. E. A. Storms,	TU Delft, section Applied Geology
	Dr. R. C. Lindenbergh,	TU Delft, department of Geoscience & Remote Sensing

An electronic version of this thesis is available at `http://repository.tudelft.nl/`.

TU Delft

Abstract

Accurately predicting the subsurface architecture is essential in finding potential reservoirs for subsurface engineering purposes. The architecture of the deposits is determined by both autogenic (internal) and allogenic (external) controls on the fluvial system and its deposition of sediments. However, the extents to which each of the two controls have an influence and how they interact in fluvial systems, is not sufficiently known for predicting the architecture of the deposits. Allogenic astronomical cycles have a trend which can be extracted from the deposits, leaving autogenic variability. This thesis means to find the lateral and vertical persistency of externally-driven floodplain deposits and their relation to the fluvial sands. Photogrammetry panels of the Early Eocene Willwood Formation (Bighorn Basin, USA) have been interpreted, a formation in which previous studies have found a pattern matching precession, one of the astronomical cycles. The formation consists of two floodplain facies in successions, together with a sandstone channel facies. Previous researches focused on the floodplain successions stratigraphically and only limited on the sandstones; this thesis means to find the lateral and vertical persistency of the floodplain successions and how these sandstones relate to the successions. The two floodplain facies, overbank deposits and heterolitics, form successions with an average thickness of 6.9m and standard deviation of 1.3m, measured over a maximum distance of 3.0km parallel and 2.8km perpendicular to the paleoflow direction. The longer the distance along which the successions are measured, the larger the range and standard deviation of an individual succession is and the more the average thickness converges to the average thickness of 6.9m. The average thickness over the 28 successions indicates a cyclicity period of 20.9kyr, matching precession cyclicity. The sandstones are subdivided into two classes based on their thickness: minor and major. The minor sands are observed to occur in the heterolitics layer of the floodplain successions. The average major sandbody thickness is 14.0m with a standard deviation of 3.9m, based on 13 bodies. Though most being multistory, it is thicker than results from previous research in the area. Opposed to the minor sands, there is not sufficient data and information on the major sands to confirm a depositional model. For the floodplain successions steps have been made to predict their behavior; once there is sufficient data to determine the role of the sandstones, prediction of the full alluvial architecture is enabled.

Keywords: Willwood Formation, Bighorn Basin, autogenic, allogenic, fluvial deposits, Milankovitch Cycles, orbital climate change

Contents

Preface

A lifetime long we spend our time on this earth. And everything we'll ever have and everyone we'll ever love will spend their time on this earth. The one object that is always there, the most essential to life, hides so many beautiful secrets. It's a waste not learn, puzzle and discover what those are.

For the past years, I have spent my time studying Applied Earth Sciences. Starting with Geological Mapping and Oral Presentation courses, passing Calculus and Algebra courses, Mechanics and Thermodynamics, to Sedimentology and Fieldworks, every step of the way has been a small piece of the puzzle. Here I would like to present to you the last, completing piece of the puzzle. This piece, which completes my puzzle, is only a small piece of the greater puzzle that is called geology. And that is a puzzle we can continue working on for decades to come.

When I started this master, Petroleum Engineering and Geosciences, it was focused on finding and extracting oil and gas. My specialization, Reservoir Geology, could be used to find and characterize potential reservoirs. My motivation to start this master was because of the geology and I am happy that I can finish it with a thesis full of geology. The past years, the oil and gas industry has been losing its importance, but the battle for energy and the battle against climate change continues. Knowledge that has been used in the past to find oil, can now be used for geothermal energy and storage of CO_2. And I am convinced that there are more sustainable opportunities yet to be found. I am glad to say that apart from this, I found Reservoir Geology to be much more fundamental than this. It is not only about finding a use to it, it also tries to explain how the world has been, how it is and from that how it will be.

Though this project involved months of working behind a computer, in a quiet room on the TU Delft campus, it has proven to be more than just a project. Once I had gotten the chance to visit the Bighorn Basin, the project 'came to life'. Despite the visit was not for geological purposes, it helped as inspiration and motivation to continue with the thesis. Now it was no longer a bunch of rocks as seen behind the computer. The Bighorn Basin is no longer just a geological term. It is where people live, gateway to Yellowstone National Park, home of Buffalo Bill and a part of my memory forever. During my travels I truly asked myself, why do people go to Wyoming, because it is ... empty. However, along the way, the answer became clear, step by step. That reminded me of life as a geologist. You go to places no one goes, you see things no one sees and you find treasures no one finds.

My gratitude towards everyone involved in this project, in special my supervisor Dr. Hemmo Abels and commmittee members Dr. Joep Storms and Dr. Roderik Lindenbergh, but also PhD-candidate Youwei Wang and PostDoc-candidate Pierre-Olivier Bruna, is large. I would also like to thank Abenezier Feleke, for his advice regarding the approach of the project and help with the software. Furthermore my dad, for travelling with me to the Bighorn Basin. Even larger is my gratitude to everyone involved in my life for never questioning my love for rocks and just being there. This, however, is not the moment to get all emotional about ending my student career and leaving my life in Delft; I'll have another thesis to write before that moment comes.

List of Figures

List of Tables

1 Introduction

How to predict what is in the subsurface, if you can't see it and it was formed millions of years ago? That is the most essential challenge an applied geologist has. This thesis is to resolve a part of this challenge, set in the field of fluvial sedimentology. An outcrop study is used to determine the alluvial architecture in the Willwood Formation in the Bighorn Basin (Wyoming, USA). In the end it leads to two things: knowledge about sedimentary systems and predictive value of the subsurface. The first is more of a scientific use; discovering how the systems works and have worked in the past. The latter, predictive value of the subsurface, is essential for many geoscience industries.

The key to understanding and predicting the alluvial architecture is in understanding the deposition of the sediments. Since river systems are dynamic systems, which are influenced by numerous controls, predicting behaviour is far from straightforward (Miall, 1988). These controls are classified into two classes: controls inside the system (autogenic controls) and controls from outside the system (allogenic controls). Autogenic controls include channel migration, diversion and meandering and bar migration (Beerbower, 1964, Stouthamer and Berendsen, 2007). Allogenic controls include tectonics, base-level changes and climate (Stouthamer and Berendsen, 2007), which are interdependent (Shanley and McCabe, 1994). For this thesis, the focus in on climate change controlling fluvial architecture. But how does climate influence fluvial deposits, i.e. the alluvial architecture? Alluvial architecture is defined as "The geometry, proportion and spatial distribution of fluvial deposits in the alluvial succession" (Gouw, 2007). As Slingerland and Smith, 2004 describe, flow will seek a path with the highest gradient advantage and/or the greatest flow efficiency; i.e. an avulsion will occur, an autogenic process. A recent study, Nicholas et al., 2018, suggest there is more to avulsion than only topographic metrics. It still considers super-elevation as a necessary and important factor, but the likelihood of an avulsion is not necessarily largest when super-elevation is largest. Hydrodynamics, such as sediment delivery, influence the likelihood of an avulsion. One of the controls on sediment supply is climate, an allogenic control. External controls influence deposits upstream by impacting the composition of sediment, sediment flux, water discharge and relief, downstream they can impact geometry of sequences, erosional surfaces and floodplain characteristics (Hajek et al., 2012).

As Stouthamer and Berendsen, 2007 recognize, an event like avulsion is controlled by autogenic and allogenic controls, but their relative roles are not well known. To determine whether sedimentation is influenced by autogenic controls or allogenic controls, one should determine whether the sediment deposits change with a similar trend as the allogenic controls (in this case climate), as has been done in Stouthamer and Berendsen, 2007. If changes show a similar trend, they are likely to be allogenic; if they do not show a similar trend, they are likely autogenic. Therefore, an allogenic control with a known trend is necessary. A relevant control to study is climate, for which astronomical cycles (Milankovitch Cycles) are used as a measure. This is done for three reasons: 1. They are cyclic with an approximate constant cycle length. 2. Orbital climate change (casued by the astronomical cycles) is largely predictable (Abdul Aziz et al., 2008, Abels et al., 2013). 3. It is argued that allogenic changes are only recorded into sediments when the cycles of allogenic change are larger than the time that the sedimentary system needs to respond to these changes (Kim et al., 2014) or that the allogenic forcing must be of greater amplitude and/or timescale than the time necessary for deposition and removal from the surficial zone of reworking (Foreman and Straub, 2017). The

astronomical cycles are not on a sufficiently large timescale such that they can always be recognized; only in basins with a short compensation timescale (Foreman and Straub, 2017). Precession, one of the astronomical cycles, causes changes in seasonality (Fischer and Bottjer, 1991) and and it is that seasonal distribution of e.g. precipitation that is important for deposition of fluvial sediments (Vandenberghe, 2003). One of the difficulties in recognizing this trend in the deposits, is the long timescale that is needed. For recognition of the astronomical cycles in fluvial deposits, intervals of 800kyr+ should be evaluated. In the field this is close to impossible, because this relates to possibly hundreds of meters of sediments. Large amounts of data should therefore be evaluated, which is not sufficiently done in current literature (Hajek et al., 2012, Abels et al., 2013). Also, the question arises whether such a 1D measurement give a realistic representation of the area or that lateral variability plays a large role. Furthermore, the relationship of the fluvial sandstones with respect to the floodplain successions is yet unknown. This thesis means to find answers to fill these gaps.

For this thesis, a main research question is set, which is further specified by sub-research questions. The main research question of the thesis is:

Research question

What is the lateral and vertical persistency of externally-driven floodplain successions and how do the fluvial sandstones relate to these successions?

The goal of this thesis is to determine whether any predictive value regarding the alluvial architecture can be derived from the relation between autogenic and the allogenic control. The necessary descriptive and explanatory knowledge is obtained with subquestions. The subquestions formed to answer the main research question are:

- Is the amount of data available sufficient and easy to interpret and model?
- What is the lateral persistency of the floodplain successions and how is this related to the channel belt?
- What is the geometry and frequency of the sands and how are the sands related to the channel belt?
- Can the floodplain successions and sands be combined into a model and linked to the astronomical cycles?
- Can the alluvial architecture be predicted?

A location where numerous researches have been performed on (among others) autogenic and allogenic controls on fluvial sedimentation, is the Willwood Formation in the Bighorn Basin (USA). The fluvial depositional origin and lateral relations have been developed in Bown and Kraus, 1987. The Willwood Formation is late-Paleocene, early-Eocene and consists of alternations between three facies: sandstones and two floodplain facies (alternating overbank mud-deposits with paleosols and heterolotic deposits lacking paleosols) (Kraus and Gwinn, 1997, Abdul Aziz et al., 2008, Abels et al., 2013). The floodplain facies are most distinct by their color: In the overbank deposits, paleosols have formed, characterized by their red color. The heterolitic deposits, interpreted as avulsion deposits (Kraus and Gwinn, 1997 based on Smith et al., 1989), do not have this paleosol development and therefore lack the red color.

More recently, evidence has been found that the successions are related to the astronomical cycles (Abels et al., 2013). Successions have been measured to have an average thickness of 7.1m (Abels et al., 2013), fitting precession cycles. Furthermore, it proposes a depositional model (figure 1.1). Abels et al., 2013 finds an average thickness relatable to precession, but has no information about lateral variability and consistency. Sandstones have been evaluated in Foreman, 2014 and an average sandstone thickness of ca. 8m is found, though with a high variation.

Regarding the floodplain successions, the depositional model as described by Abels et al., 2013 (figure 1.1) is expected to fit with the results. That is to say, successions that can be linked to precession, of which the heterolitics facies represents an environment in which the channel is unstable and an overbank facies in which

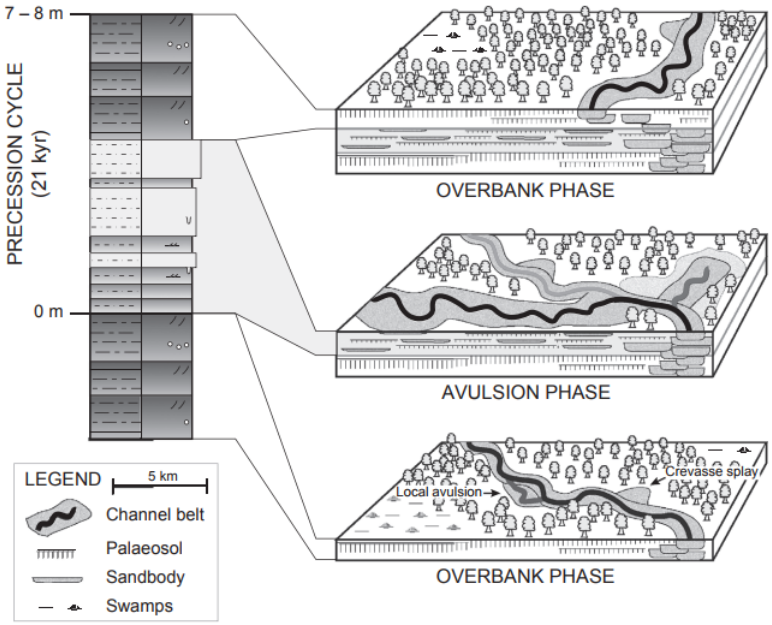

Figure 1.1: The depositional model by Abels et al., 2013. It shows the development of a succession and how it is related to precession.

the channel is stable. It is hypothesized that the variability of the successions thickness is limited, allogenic controls exert the main controls on the environment. I.e., the same trend that is seen in the astronomical cycles, can be seen in the deposits. Regarding the sands, it is hypothesized that the base of a major sandstone is somewhere halfway in the heterolitics phase. It then stays stable during the overbank phase. In the next heterolitics phase, the river avulses and there is not a lot of new sedimentation. However, the channel was topographically higher than the floodplain during the overbank phase, due to its levees and bars. Therefore, one would expect that the sand is slightly higher than the end of the overbank phase, approximately halfway up the heterolitics phase. All in all, the total thickness of the major sandstone is half a heterolitics phase, a full overbank phase and half a heterolitics phase; i.e. ca. the full thickness of a single succession. When the channels erodes down, it might even exceed the thickness of a single succession.

Testing the hypotheses and answering the research question is done by evaluating photopanels. No fieldwork is executed, the only source of data are the photopanels. This methodology has the advantage that a much larger area can be evaluated. Previous researches are often limited to ca. 7 to 15 successions, while this thesis is able to provide over 30 successions. In addition to that, they are followed laterally, which is also not done by previous researches. Detailed study of local events, such as a local avulsion, is outside the scope of this thesis. The focus is on the laterally consistent successions. The sands and their internal structure will not be studied in detail, only their relation to the stratigraphy is determined. Furthermore, the depositional model proposed in Abels et al., 2013 is evaluated and in relation to that, the stratigraphic position of the sandstones. Finally, this is a rather different methodology than used in other researches. Is it suitable and can a stratigraphic model be made? However, the photogrammetry panels and modelling are used as a tool; in depth analysis of those are outside the scope of this thesis.

A background description of the area and geology can be found in Chapter 2. The approach to this research is described in the methodology, Chapter 3. The results are described in Chapter 4. How do the results and their interpretation fit in the scientific world, how reliable are the results and how can they be improved? This is summarized in the discussion in Chapter 5. The conclusions are presented in Chapter 6.

2

Regional Geology

This chapter presents a description of the area: the geography, regional geology and deposition.

2.1. Geography

This research focuses on the northern section of the Bighorn Basin, just north of the McCullough Peaks (figure 2.1). The Bighorn Basin is located in the north-west of Wyoming (USA), east of Yellowstone National Park (figure 2.2). The basin is bounded by several mountain ranges: the Absaroka Range and the Beartooth Mountains in the west, the Bighorn Mountains in the east, the Pryor Mountains in the north-east and the Owl Creek Mountains in the south. Several rivers traverse the basin, of which the Bighorn River is the main channel, flowing towards the north. The Shoshone River is located close to the research area.

Figure 2.1: Overview of the outcrops in the area to show the scale and outline of the outcrops, facing the McCullough Peaks (seen in the back on the right).

The Bighorn Basin nowadays includes agricultural land and badlands. The area is hilly but walkable. Dimensions of outcrops can go to kilometers in length and about 200 meters in height. Vegetation is not abundantly present and consists mainly of small bushes. These characteristics make the area useful to geologists.

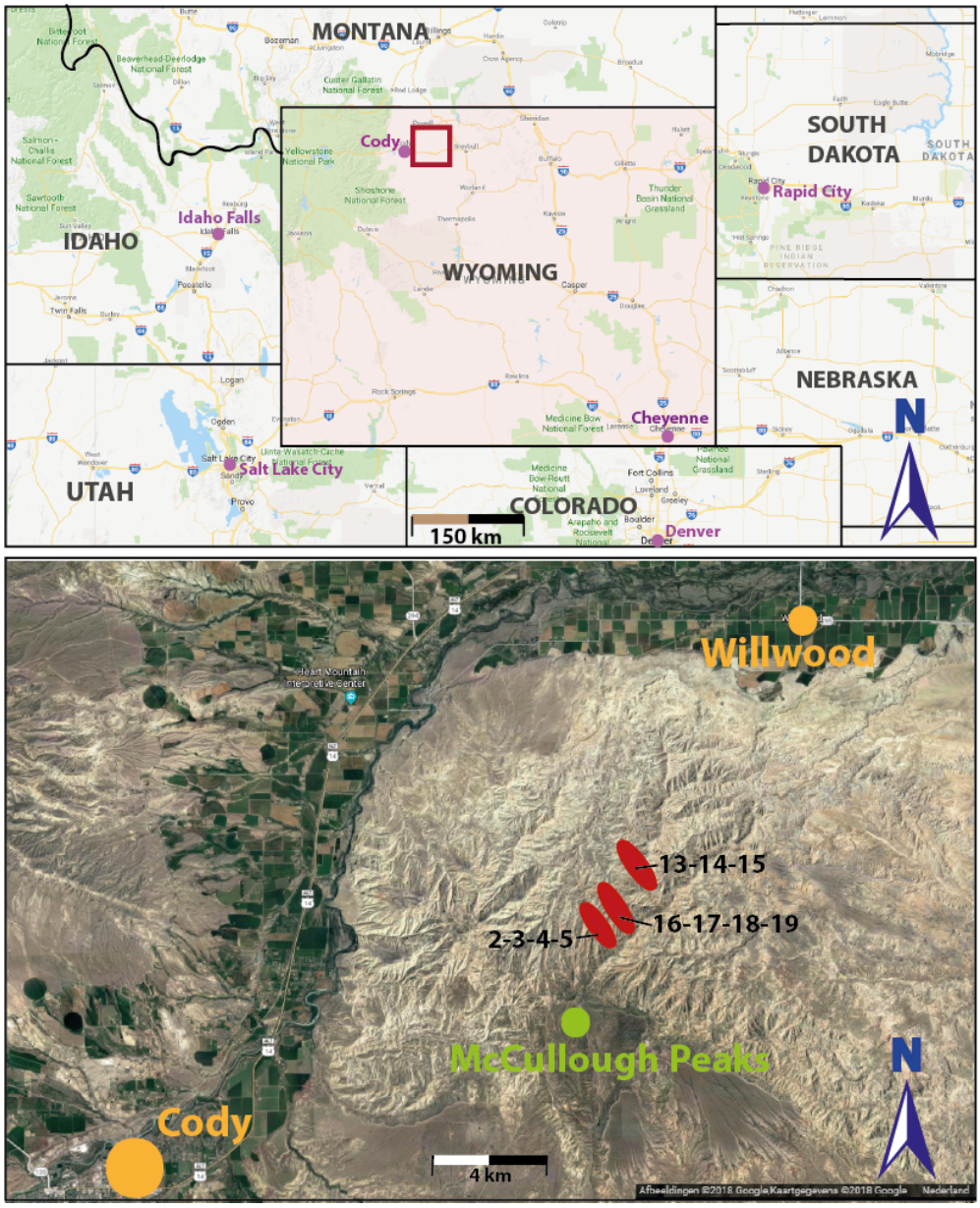

Figure 2.2: The location of the research area. In the upper map, the approximate research area is shown in the red box. The lower map shows the approximate location of the individual photopanels at a much smaller scale. Some relevant cities are shown on both maps. Background of both maps is retrieved from Google Maps, Google LLC, 2018.

2.2. Regional Geology of the area

The Bighorn Basin has its origin in the Laramide Orogeny. The Laramide Orogeny took place 75MA to 40MA in the area now known as the Rocky Mountains (Lawton, 2008). The orogeny consists of basement cored uplifts and led to the formation of basins, of which the Bighorn Basin is one of many (Lawton, 2008). The main source of sediment of the basin are the bounding mountain ranges; Beartooth, Bighorn and Owl Creek Mountains (Clyde et al., 2007; Abels et al., 2013). The Absaroka Mountains, which are found to the west of the basin, were formed after deposition of the Willwood Formation and have a volcanic origin (Kraus and Gwinn, 1997). The average tectonic subsidence rate near the McCullough peaks is 250m/my (Clyde et al., 2007). Most of the outcrops are of the Willwood Formation (figure 2.3); a stratigraphic column is shown in figure 2.4. This Early Eocene Willwood Formation is the subject of this thesis and consists mainly out of finer fluvial material (Abels et al., 2013).

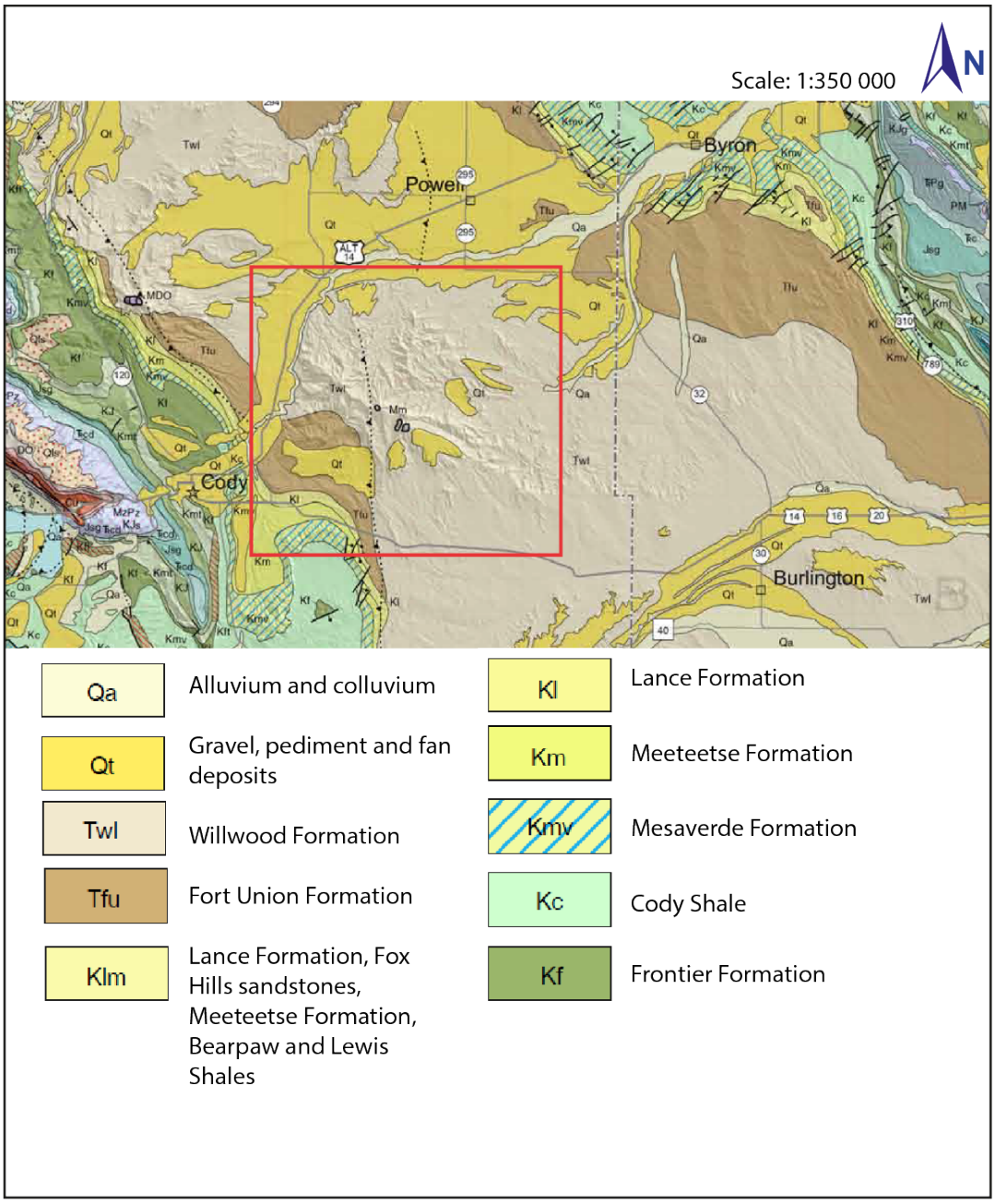

Figure 2.3: The geological map of the area. Adjusted from Wyoming State Geologic Survey (Wyoming State Geological Survey, 2018). All formations from the Quartenary start with Q, formations from the Tertiary with T and formations from the Cretaceous with Q. Note this is not the full legend, only a small, relevant part. The approximate research area is marked with the red box.

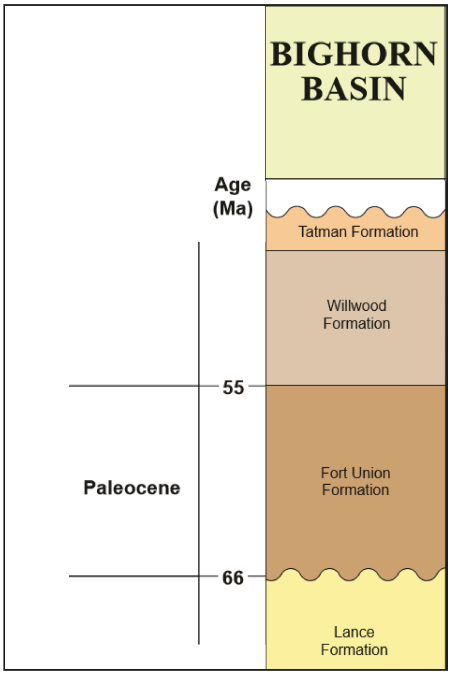

Figure 2.4: The stratigraphic column of the area with the relevant interval. Adjusted from Wyoming State Geologic Survey (Wyoming State Geological Survey, 2018). The stratigraphy is also confirmed by Neasham and Vondra, 1972.

2.3. Deposition

The depositional model of the Willwood Formation is as follows:

It is believed that the Willwood Formation is a fluvial deposition (e.g. Neasham and Vondra, 1972; Willis and Behrensmeyer, 1995). The climate where the formation has been deposited is identified as warm (13°C - 18°C as a yearly average) and frost free, seasonal rainfall and with vegetation as an evergreen, broad-leaved forest (Kraus and Gwinn, 1997).

Fluvial sedimentation

How is sediment deposited in the first place and what are the controls? Clastic sediment is formed by weathering. In fluvial sedimentology, most sediment is eroded by rivers and also deposited by rivers. The type of sediment that is deposited in each of the elements is dependent on the flow speed. Inside the channels itself, the flow speed of the water is high, having sufficient energy to transport coarse grains. When the river floods, on the edges the coarsest grains are deposited, creating the levees. As the water spreads out, flow speed and energy decreases, depositing the finer grained material.

The Willwood Formation is seen as a fluvial depositional environment (Willis and Behrensmeyer, 1995). This means that different sedimentary elements can be found, such as floodplains, bars, channels, crevasse splays, levees, etc. Since the flow speed is different during deposition of all these sedimentary elements, the grainsize of the sediment is different as well.

Based on a moving average paleocurrent map, the sand grain size and shape and the maximum conglomerate clast size, Seeland, 1998 created an Early Eocene flow pattern map, indicating the flow direction to the north-east (figure 2.5). Willis and Behrensmeyer, 1995 identified the Bighorn strata as river deposits, with the main river flowing south to north along the basin axis and smaller channels transverse to the main river and basin axis, similar to Seeland, 1998.

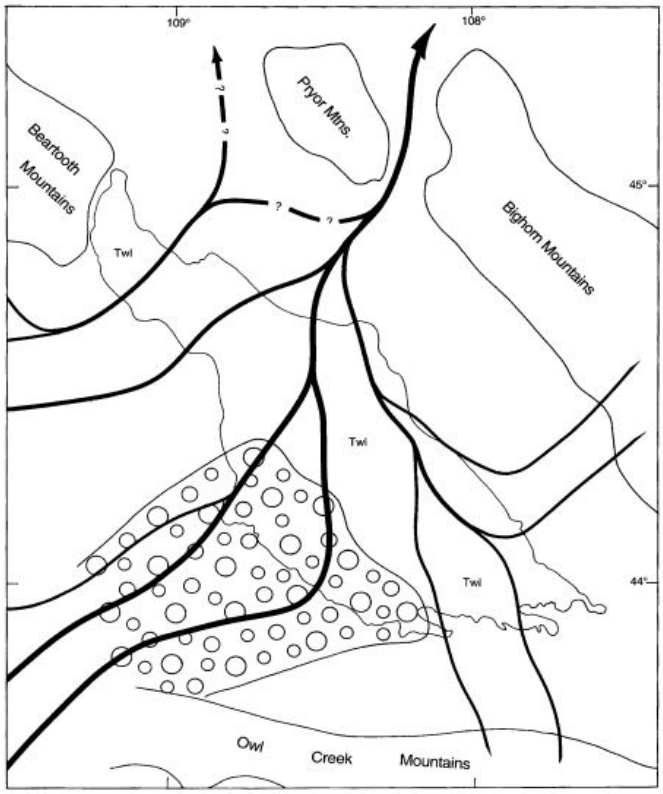

Figure 2.5: The flow pattern map shows the approximate flow direction of the river system responsible for the deposition of the Willwood Formation (Seeland, 1998).

Willwood Formation

The Willwood Formation is of late-Paleocene, early-Eocene age and consists of a sandstones facies and alternations between two floodplain facies: overbank mud-deposits with paleosols and heterolotic deposits lacking paleosols (Kraus and Gwinn, 1997, Abdul Aziz et al., 2008, Abels et al., 2013). The floodplain facies can be distinguished based on their color. In the overbank deposits, paleosols have formed, characterized by their red color. The heterolitic deposits, interpreted as avulsion deposits (Kraus and Gwinn, 1997 based on Smith et al., 1989), do not have this paleosol development and therefore lack the red color. Color analysis of the area has been done in multiple studies, e.g. Abdul Aziz et al., 2008 and Abels et al., 2013. The red color of the paleosols is not always similar, some are more purple, others more brown etc. This is caused by differences in sediment accumulation and drainage of the soil (Kraus and Gwinn, 1997, Owen et al., 2017). Paleosols developed more strongly further away from the coeval channel body (Bown and Kraus, 1987). A subdivision is made between moderately- to well-drained and poorly drained paleosols by Owen et al., 2017. The moderately- to well-drained paleosols have more rootlets, slickensides, mottling and burrows. They have the more reddish colour, due to oxidation. Poorly drained paleosols on the other hand, have fewer rootlets etc., but do have more organic matter and are more grey to purple in color. So, the purple paleosols were less well drained than the red paleosols (Kraus and Riggins, 2007).

A lithological description of both the overbank deposits and the heterolitic deposits is given in Abels et al., 2013. A summary of these descriptions is given here:

The overbank deposits:

- claystones to sandy siltstones
- paleosols present (red, purple)
- matrixcolors include black, purple, olive, light grey, (dark) reddish brown and bright yellowish brown
- mottling, carbonate nodules, organic matter and slickensides present in some, but not all deposits

The heterolitics:

- claystones to sandy siltstones
- weak paleosol development

The distinctive colors of the paleosols are either brown, red, purple or grey. The purple paleosols are distinctive and easy to correlate. Some of the most distinctive purple paleosols in the area evaluated, have been described and numbered by Abels et al., 2012 and are referred to as Purple -2 to Purple 4.

The channel facies present (the sands) in the Bighorn Basin, is described in Owen et al., 2017, where the Fort Union Formation and Willwood Formation in the Bighorn Basin have been studied. First of all, the scale of interest must be determined. For the purpose of this thesis, this excludes ripples and other small bedform features. Sandstone bodies and mainly the stratigraphy are the scales of interest. This is roughly in the scale of several meters. Owen et al., 2017 makes a hierarchical distinction of the scales: (from small to large) bedform, barform, channel body, system and basin. Bedforms are below our scale of interest, basins are above our scale of interest. The middle three are all of interest, with the main focus on the system: "Single depositional system composed of channel bodies that show different stratigraphic stacking patterns through space and time" (Owen et al., 2017). In the system hierarchy, it is not just about the sandstones, but also about the successions.

Owen et al., 2017 describes 6 facies associations present in the Fort Union Formation and Willwood Formation in the Bighorn Basin: 1. Gravelly braided stream, 2. Heterolitic, dominantly braided, 3. Heterolitic, dominantly meandering, 4. Fine-grained channel fill, 5. Lacustrine, 6. Paleosols. The ones present in the area of evaluated in this thesis are mainly facies 3 and facies 6.

3

Data description and research methodology

This chapter describes how the data is obtained from the field and how this has been adjusted (by others), in order to come to the initial data which was needed to start this project. Furthermore, a description of all steps taken in order to obtain the results is given. All in all, it means to give a clear overview of the steps taken, such that it is understandable and reproducible.

3.1. Description and evaluation of the photopanels

This section describes the original data and all work done by others. An analysis of this is necessary to determine the reliability of the data and therewith the results.

Description of the photopanels and their location

Several different sections of one area have been photographed, after which they have been made into photopanels. In total, 12 successful photopanels have been made; i.e. of 12 sections there exists useable data (figure 3.1).

The numbering is taken from the original fieldwork, to prevent confusion. Panel 15.1 and 15.2 were originally one photopanel. However, for processing reasons they have been split into two.

Photography with a drone

The photopanels have been made photographing from a drone (DJI Phantom 4 Pro) with a built-in DJI camera and GPS device. Photographing with the drone has been done in a systematic way. That is to say, the outcrop is approached perpendicularly; when the full height is captured, the drone is flown parallel to the outcrop for a small distance, after which it is flown back perpendicularly. This process repeats. However, drones were flown by hand and sometimes from large distances, meaning that it is not always as systematic as intended. Furthermore, all sections were only flown once, which means that shadows can be an issue.

The main advantage of using a drone is that inaccessible areas can be photographed up close and from the front of the outcrop, providing the best view. You are not dependent on where you can walk.

Photogrammetry with Agisoft

After the fieldwork, the photos have been used to create photopanels. This is done with photogrammetry. This work has been done by PhD-candidate Youwei Wang. Since the photogrammetry itself was not part of the thesis, further elaboration is only given in Appendix A. Dimensions of the panels differ, roughly a height of 100m per panel and 300m to 500m in width is indicative.

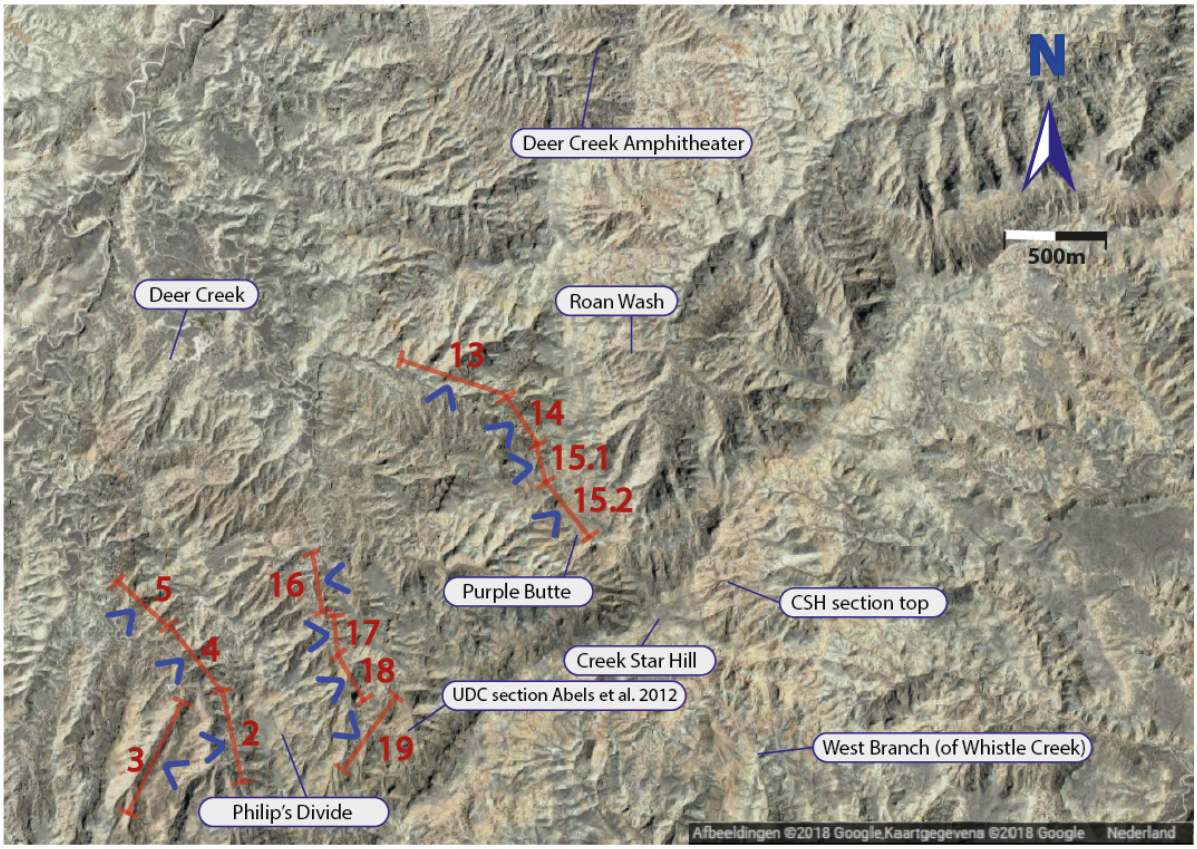

Figure 3.1: The location of the 12 photopanels. Each marker shows the side from which the outcrop is faced. Satellite photo by Google Maps, Google LLC, 2018.

Photogrammetry - how does it work

Photogrammetry is the creation of a three-dimensional model, based on photographs. In short this means that when the exact same object/spot is photographed from multiple positions, the location (in 3D) with respect to the camera can be estimated (Bemis et al., 2014). By georeferencing, the object can be assigned world coordinates. The result is a georeferenced 3D model. A more extensive explanation of how photogrammetry works can be found in Appendix A.

One cannot blindly rely on models such as the photopanels, since they are never equal to reality. There are deviations from the reality, as well as errors and gaps in the data.

From Agisoft, it can be retrieved how accurate the photopanels are (table 3.1). The table also offers an interesting statistic. The panel with the largest surface per photo is by far panel 13, though it is not the one with the largest root mean square (rms) error. A possible reason for this could be the shape of the facade that is photographed. Some panels are straightforward; laterally extensive walls with few features, while others are more hilly, have side canyons and caves. For panel 15.1 and 15.2, the overall rms error is remarkably high, also taking into account that they are one of the smallest panels. The root mean square error is not robust, meaning it is susceptible to outliers. Therefore an additional statistic is shown, the Median Absolute Deviation (MAD), which is robust. When using the MAD, panel 15.1 and 15.2 no longer have a significantly higher MAD than the others. So the large differences in rms error are mainly caused by a outliers, which is confirmed when analyzing the data individually.

The reason panel 15 was split up into panel 15.1 and 15.2 were the bad photogrammetry results; they were unable to be aligned. By splitting the panel up and decreasing the amount of photos used (decreasing photo

Table 3.1: Data of the photopanels as retrieved from Agisoft.

Panel	overall rms error (m)	MAD (m)	surface (m^2)	number of photos
2	1.95	0.61	171 309.8	832
3	1.64	0.50	229 239.2	1173
4	1.67	0.49	91 743.5	514
5	1.73	0.55	131 042.2	442
13	2.34	0.72	379 227.0	670
14	2.18	0.64	135 633.8	498
15.1	6.13	0.72	62 830.5	406
15.2	5.98	0.68	55 102.0	649
16	2.67	0.75	196 790.6	553
17	2.60	0.79	58 297.9	394
18	2.05	0.69	98 471.8	513
19	2.57	0.75	270 295.0	938

(a) An example of the resolution in panel 14

(b) An example of the resolution in panel 15.1

Figure 3.2: A comparison of the resolution between panel 14 and 15.1. In both subfigures, the same location is shown. Note the loss of detail in the photopanel.

density), the results improved (but are still not comparable to the rest). For panel 16, also fewer photos have been used. Panel 15.1 has a large overlap with panel 14, so resolutions can be compared. Visually it can be seen that the resolution of panel 14 is higher than the resolution of panel 15.1 (figure 3.2). This implies that using a lower photo density deteriorates the resolution.

Since the models are not a 100% match with reality, it is important that the original photos are consulted during the interpretation as well. How this is done, will be explained more in the next section.

3.2. Interpretation of the photopanels

The floodplain succession boundaries and the sandstones have to be interpreted from the panels. The succession boundaries are defined as the transition from overbank facies to the heterolitics phase on top. This is a definition based on a color transition, since the only data that is available are the photopanels. To come to an interpretation that can be used to build a model of the area, the following steps have to be made:

Step 1. Choose the correct coordinate system. Initially, all coordinates in Agisoft are in the WGS84 coordinate system. Interpretation of the photopanels is done in Lime VOG software. Lime is not able to handle spherical coordinate systems such as WGS84, so the coordinates are converted into a Cartesian coordinate system. The system chosen is NAD83 - Wyoming West Central (EPSG: 32157), since the Bighorn Basin falls within the Wyoming West Central section. The conversion can be done in Agisoft. Afterwards, the model is exported into an .obj file, which is suitable for Lime.

Step 2. The geological features can be interpreted in Lime. On the photopanel, lines can be drawn. Interpretations are made that are relevant for the scope of this project. These are succession boundaries and channel bodies. The succession boundaries that are interpreted are the boundaries from overbank deposits to heterolitic deposits. In practice, this often means the transition from the reddish paleosols to the grey heterolitics. However, this is not always a clear boundary, so caution must be kept. Important is that they are laterally continuous, if not, they are local events and not relevant for this thesis. Furthermore, the sandstone bodies are interpreted. Regarding the sandstone interpretation, the base of the sandstone body and the top of the sandstone body is marked. When both are known, thicknesses of the bodies can be calculated later on. Interpretation in Lime can be difficult due to limitations from the model, as retrieved in Agisoft. An example of this is low resolution. Another issue that arises, is the presence of shadows and gaps. When photographing the outcrop, one is limited by the weather conditions. Since a 3D area is photographed and modelled, this means that shadow can be present in the photos and therefore also in the model (figure 3.3). Also, since the area is three-dimensional, photos with the drone should be taken in every direction. When this does not happen, gaps can arise in the model (figure 3.3). Interpretation is not possible in these sections.

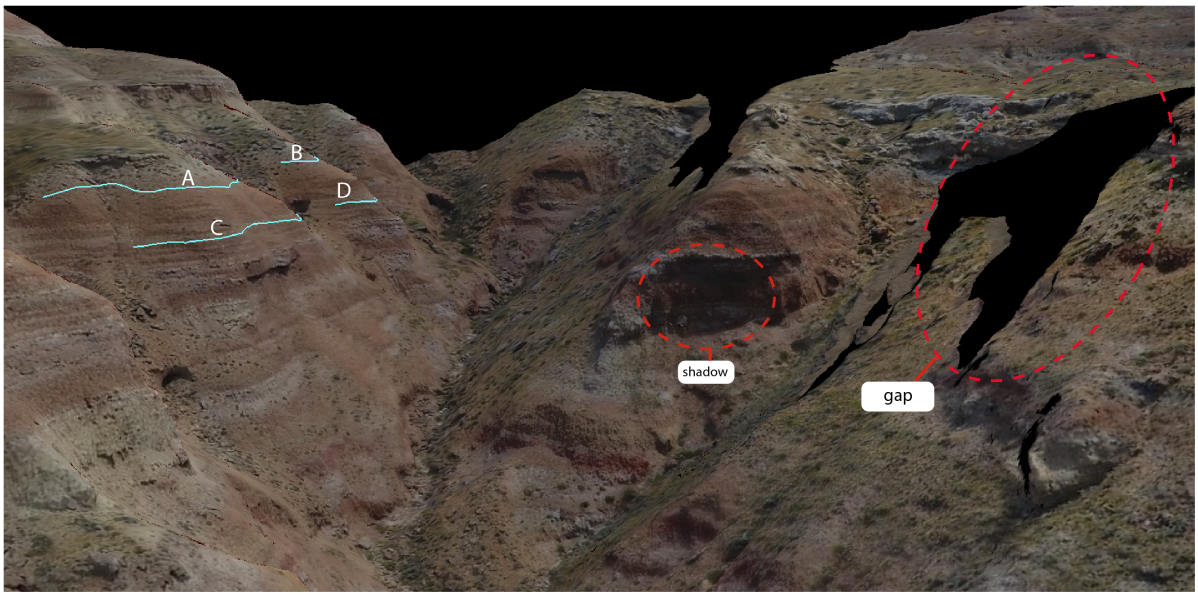

Figure 3.3: An example of two flaws in the photopanels. On the left is shadow, making the outcrop less clearly visible. On the right is a gap in the data. The example is from one of the sidecanyons in panel 13. Note that the gap can be prevented by better drone photography, while the shadow is weather dependent. Lines A to D partly mark two succession boundaries, to indicate the methodology. All other succession boundaries are not shown in the figure.

Since numerous photopanels are used in the interpretation, it is important to keep the interpretation structured. Since the succession boundaries are only marked when they are actually visible, this means that each panel has multiple lines for each succession boundary, while there are already numerous succession boundaries in each panel. In figure 3.3, this is shown as line A and B marking the same succession boundary and line C and D marking the same succession boundary. Each line is a piece of a succession boundary and it is vital to classify all pieces to the correct succession boundary. When modelling in Gocad, they have to be assigned individually to a feature. Proper identification of each single line is therefore important.

What makes interpretation difficult, is that not every color transition is a succession boundary. Geological knowledge is needed. All in all, a potential succession boundary should not be interpreted if:

- The succession boundary is not laterally continuous
- There is a sandstone on top which might have eroded the actual succession boundary (partly). Only when laterally can confirmed that the boundary seen is in fact the top of the succession, it is interpreted.
- There is any doubt which cannot reasonably be solved.

Step 3. The panels have to be correlated with each other, such that the data can be combined and a single model can be made for the entire area. In other words, lines marking the same succession boundary should be matched with each other, such that the lateral outline of that succession boundary becomes clear. At first, the panels are correlated in 3 sets. The sets are based on their geographic location. The sets are as follows:

- Panel 2, 3, 4, 5
- Panel 13, 14, 15.1, 15.2
- Panel 16, 17, 18, 19

Within these sets, there is a small overlap between some of the panels, making correlation easier and very reliable. Only the set of panel 13, 14, 15.1, 15.2 is fully connected (figure 3.1). After completion, a correlation between the sets of panels is made, forming one large model containing all data.

Correlation is rather easy when there is overlap between panels. However, this is not always the case. Within the sets, the panels are close to each other, such that most of the successions are recognizable, enabling correlation. The main difficulty is when correlating between the sets of panels, e.g. between the set of 2, 3, 4, 5 and the set of 13, 14, 15.1, 15.2. In the top sections, the distinctive purple layers as described by Abels et al., 2012 are present. These are distinctive layers, some of which can be found in all sets. This is the starting point for correlation between the sets. On stratigraphically lower intervals, the succession boundaries are less distinctive, so visual correlation becomes more difficult. Then the assumption has to be made that the succession on top in one set of panels, is the same succession as the succession on top of that same correlated layer in the other set of panels. This is done with extreme caution, as soon as doubt arises if this still holds, correlation is stopped until a new visual correlation can be made. It is not right to correlate numerous boundaries based on their subsequent thickness only, since that only holds under the assumption that thickness stays constant. This assumption is tested in this research, so it cannot be used. Therefore, the visual correlation is essential; a sufficient amount of visually correlated boundaries must be present to obtain reliable results.

Step 4. Thicknesses of the successions are measured in each panel. To get statistical relevant and reproducible data, every 30 meters the thickness between two succession boundaries is measured. In Lime, a line is drawn between the two succession boundaries, as perpendicular to both boundaries as possible (line a in figure 3.4). The thickness recorded is then the difference in Z-location, i.e. line b in figure 3.4. The approximately 30 meter distance to the next point is measured from the point in the middle of the succession (the red dot in figure 3.4) to again the middle of the succession. Since it is a 3D model, the 30 meters can be in any direction and not necessarily along the surface. Therefore, at all times there is (at least) ca. 30 meters between all of the measurements in the sample. If there is no measurement possible after the previous point, e.g. due to a succession boundary not being visible there, this measurement point is skipped and 30 meters further the next measurement is taken. If that point is also not usable, the first next possible location is used and the 30 meter interval is restarted. The measurements are done per panel; however, there is overlap between some of the panels. When combining data after correlation, duplicates are removed, so there are no double measurement of the same location.

Step 5. The thicknesses of sandstone bodies are measured. The thickness measured is the maximum thickness of that specific sandstone body, so only one measurement per body. Similar to the successions, the difference in Z-location is recorded as the thickness.

After these measurements, the interpretation is finished and a start can be made with building a model.

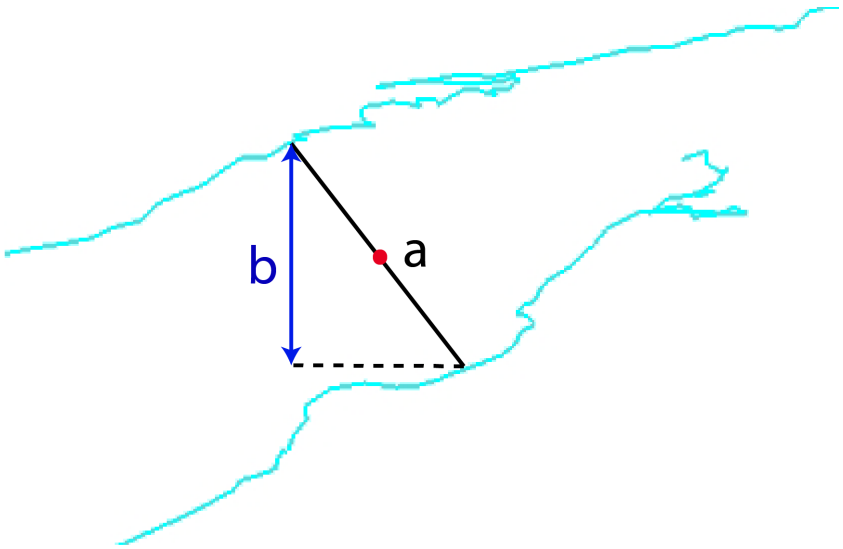

Figure 3.4: Schematic depiction of how the thickness is measured in Lime. Line a represents the measurement that is taken in Lime. Line b represent the Z-difference, i.e. the thickness that is recorded. The red dot represents the middle of the succession, of which the distance of 30 meter to the next measurement is taken.

3.3. Building a model

All interpretations in Lime are imported into Skua-Gocad, from now on referred to as Gocad. In Gocad, these interpretations are used as input to create a structural model. In other words, whereas Lime was just marking what could be seen, Gocad is filling those gaps where the successions cannot be seen. The description of the steps is continued from the previous section.

Step 6. The lines are exported from Lime as .asc files. Unfortunately, they are not directly usable. The Z-location (height) of the panels in Agisoft has a few meter deviation from reality (regardless of the coordinate system it is in). Consequence: the exact same point which is present in two panels, is a few meters higher in one panel than in the other. This is likely to be caused by an error in the GPS of the drone. Some separate GPS measurements were taken in the field, which confirm the deviation. With Matlab, the lines in the .asc files are adjusted in such a way that this deviation is removed. Since the separate GPS measurements are not sufficient to do all this, the decision is made to make sure that all panels correlate with each other and are changed in order to honor this correlation. I.e., when two points are present in multiple panels, they are set to the same height. Internal consistency within the panels is assumed, so all lines within that panel are changed in the exact same manner. One panel is chosen as base, the Z-location is changed according to the GPS measurements and all other panels are changed to fit this initial panel. This is done for all three sets of panels separately, since there is no overlap between the sets. For some panels, also the X- and Y- coordinates had to be adjusted (slightly) to honor consistency. The changes made to the lines are shown in appendix C.

Step 7. With all lines adjusted, they can be imported into Gocad. Two approaches have been evaluated: 1. Making a single model for the entire area. 2. Making a model for each set, so in total 3 separate models. The choice has been made to make three separate models in Gocad, for two reasons. First of all, there is quite a distance between the sets and there could be faults or other features in between which cannot be captured by the model. Second of all, the Z-location (height) of the panels is not accurate, as described in step 6. Since in each set a different base point is chosen to which the panels are connected, consistency with the other sets is lost. Furthermore, results of the single model approach showed bad results.

Each line that corresponds with the same succession boundary and/or sandstone body, is assigned to the same feature. This is also a feedback step to the interpretation. If lines of succession boundaries are correlated with each other, but do not show up at the same height in the model, the Lime interpretation should be rechecked and adjusted if necessary. When there is consistency, a stratigraphic column is made and finally Gocad builds a surface through each of the lines of a feature.

Step 8. Remove all duplicates. Since there is overlap in some of the panels, a part of the same succession boundary is interpreted twice. The lines never overlap 100%, so after checking if the lines are drawn where they were supposed to, one of them has to be removed. If it is not removed, Gocad has issues interpreting the data.

Step 9. In the previous step all data has been imported and sorted. Gocad can now build a model. A stratigraphic column has to be made. The model is made with a data bounding box. Resolution has to be maximized within the abilities of the computer. The result is a 3D model, which can be used to determine thickness, variability etc. of the all successions.

Step 10. Validation of the model. The resulting model is validated and checked with the statistics from Lime; they should correspond more or less. Furthermore, they can be correlated with literature.

4

Results

This chapter describes the results that have been obtained with the methodology described in Chapter 3. At first, a description is given of the interpretation and correlation of the panels. The next section describes the results of the direct measurements versus the modelled results and concludes with a preferred option. The results from the preferred option are described in the next two sections; the first presenting the successions, the latter presenting the sands. A distinction is made between qualitative results and quantitative results.

4.1. Geologic interpretation of the photopanels

In all 12 photopanels the succession boundaries have been evaluated and marked. An example (panel 5) is shown in figure 4.1, all others can be found in Appendix B.

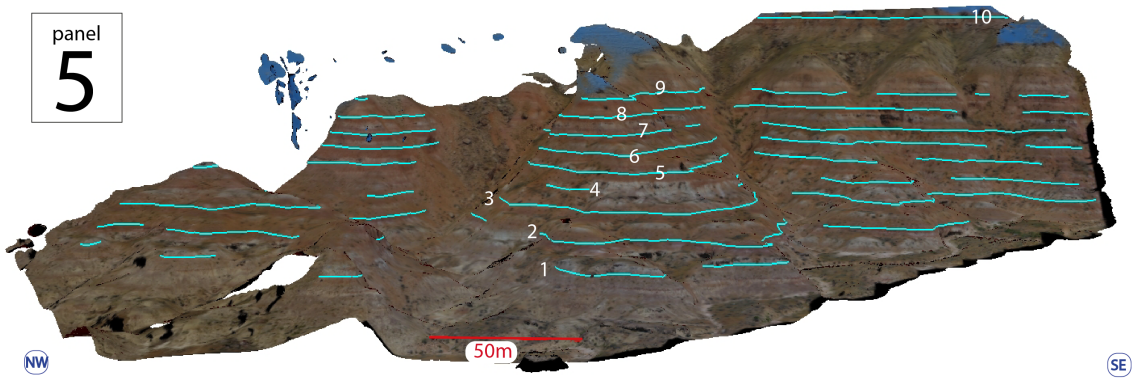

Figure 4.1: The geologic interpretation of panel 5. The succession boundaries have been marked with blue lines and numbered from bottom to top. The red line indicates a length of 50m.

Interpreting the panels is not straightforward. Even with the original photos, it can be difficult to determine where the succession boundaries are. Sometimes, two transitions follow each other closely, making it uncertain which of the two is the true succession boundary (figure 4.2). Such a difficulty, as described above, is seen at approximately 2 in 10 succession boundaries. The difference between the two options is in the range of ca. 0.5m to 2.5m.

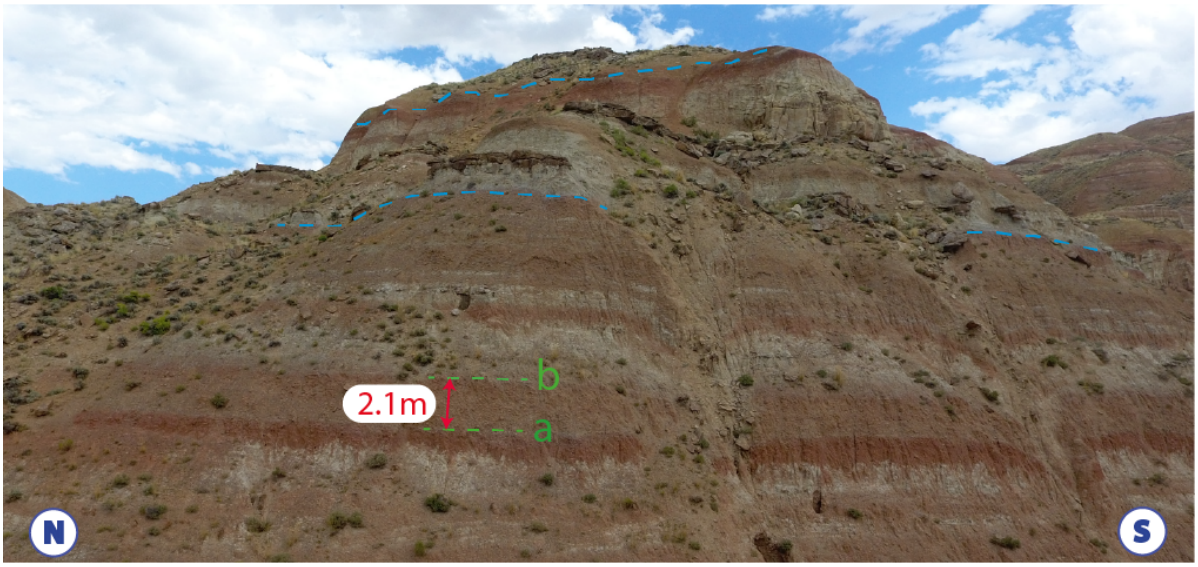

Figure 4.2: An example of two options for the succession boundary (panel 18). The lower option (a) is a more distinct soil, the upper option (b) is a the higher soil. The difference between the two is 2.1m. In this case, option b has been chosen. The other succession boundaries are marked with blue dashed lines.

Boundaries are only interpreted as being a succession boundary, when they are laterally continuous. At what distance a succession can be said to be laterally continuous is not yet known, this will be one of the outcomes of this thesis. For now, it is assumed to be as exceeding 1km in width, unless the amount of data available is less than 1km. In that case, it is interpreted as laterally continuous if it is present for the full width of the data available. If a distinct paleosol is present which seems to be a boundary, but is not laterally continuous, it is not interpreted as being a succession boundary (figure 4.3).

Figure 4.3: A strictly local event (panel 3). A bright red-brown soil is distinctively observable, in the figure marked by the green dotted line underneath. However, this event is only locally (180m in width) present, (though it continues beyond the green marker), so it is not used in the interpretation. The succession boundaries are marked with blue dashed lines.

Furthermore, sandstones can interrupt and erode floodplain successions and their boundaries. If a sandstone erodes into the preceding succession, the actual succession boundary is no longer present and no interpretation is made. When a floodplain succession boundary cannot be unambiguously be determined, it is left uninterpreted to prevent faulty results.

4.2. Correlation of the successions

The correlation between the panels is done visually, i.e. by reviewing the original photos and the photogrammetry panels in Lime software. The original photos provide the best resolution, while the photogrammetry panels provide largest overview and ability to view in 3D. There are a few measurable variables that can help

identifying the same layers; i.e. they support a visual correlation. Sometimes there are clear layers visible, which can be used as markers. Also, their Z-location (height) can be helpful when correlating. The dip of the layers is limited (maximum dip-angle measured is 2.3°). This means that the same layer can be expected within an approximate range of the same Z-location in a nearby panel.

What stands out during the correlation is that identification of a succession boundary is easiest based on purple paleosols. They are distinct and not subject to large variations. Other distinctive color patterns or layers can be used as marker as well. Since thicknesses of individual successions are variable, correlation based on thickness is not possible. The correlation result (figure 4.4) shows which boundaries have been correlated with each other. Their spatial relation and the amount of overlap indicates why certain boundaries have been easier to correlate compared to others (figure 4.5). Most succession boundaries / successions have been matched successfully. When no correlation could be made, a gap is left open. Correlation is a time consuming and manual exercise, but essential for evaluating the floodplain successions. Correlation with literature is included in section 4.4.

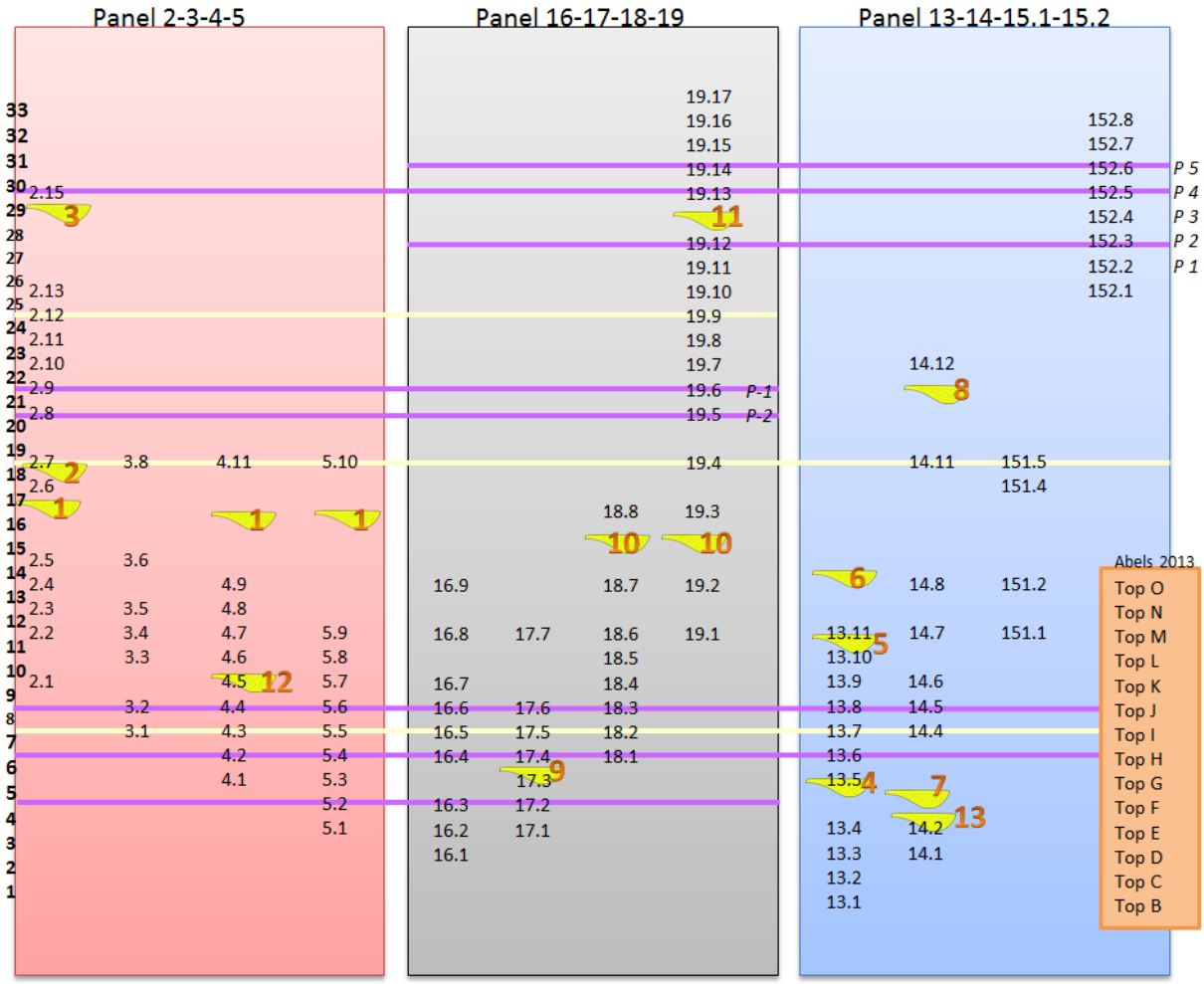

Figure 4.4: The correlation of all succession boundaries, sorted per set and the sets ordered according to the geographic location (SW to NE). The numbering of the succession itself is on the left, each succession being between two succession boundaries. The major sandstone intervals have also been added, they are described further on. The boundaries on which the correlation is based are marked by lines. When the line is purple, the boundaries have a distinctive purple paleosol and made correlation easy. When the line is white, the correlation is not based on a purple paleosol, but on another property. Please note that there are more purple paleosols in the outcrops, but those have not been used for correlation purposes. In orange are the successions as found by Abels et al., 2013. The purple paleosols as defined by Abels et al., 2012 are also shown as P1, P2 etc. Also note that this figure shows all succession boundaries, not the successions itself.

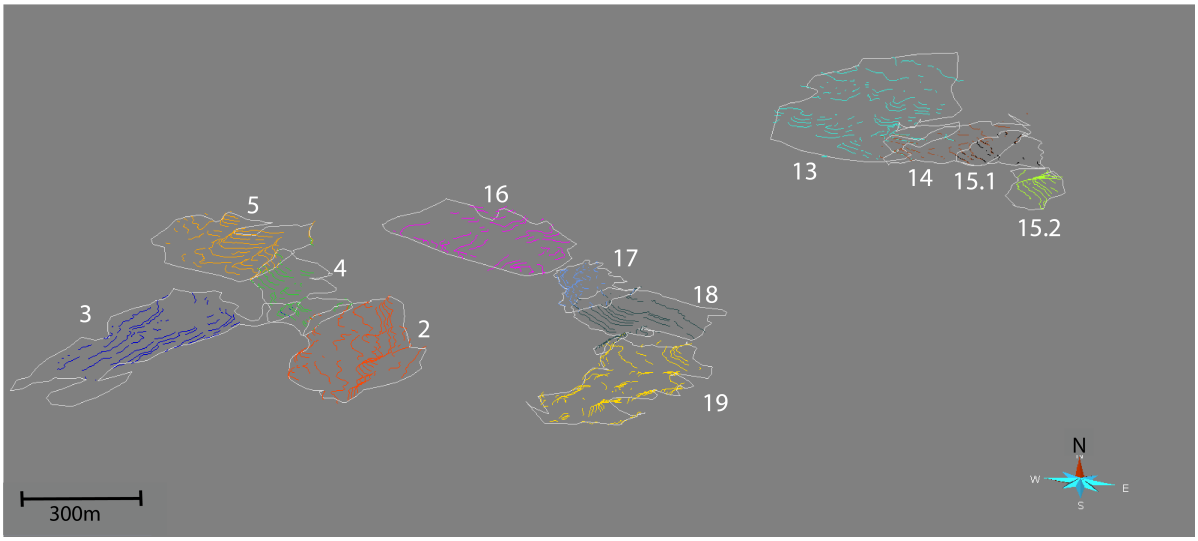

Figure 4.5: This figure provides an overview from Gocad, in which all panels are shown. The interpreted succession boundaries are shown, for each panel a different color. As can be seen, some panels have overlap, making correlation easier. Note: this is a fish-eye view.

4.3. Direct vs. modelled results

The results on the succession thickness can be obtained in two ways:

1. Direct, via measurement in the Lime panels
2. Modelled, via the model made in Gocad

Firstly, a model is evaluated in which all data is combined; i.e. all panels are combined into a single model. The modelled results are compared to the direct Lime measurements (figure 4.6).

To improve the modelling results, the decision has been made to split the modelling up into three parts: one model for each of the sets of panels. The sets are, as described in Chapter 3, as follows:

- Panel 2, 3, 4, 5
- Panel 13, 14, 15.1, 15.2
- Panel 16, 17, 18, 19

The direct results of the set of panel 13-14-15.1-15.2 is compared to the model of that set (figure 4.7). This set has been chosen because it is the only set in which each panel overlaps with one another. The variability of the modelled surfaces decreases when interpolating and extrapolating (figure 4.8). This occurs when Gocad is forced to fit data, as well as when Gocad is forced to smooth the fit. The standard deviation of the first succession is higher due to edge effects and should be ignored.

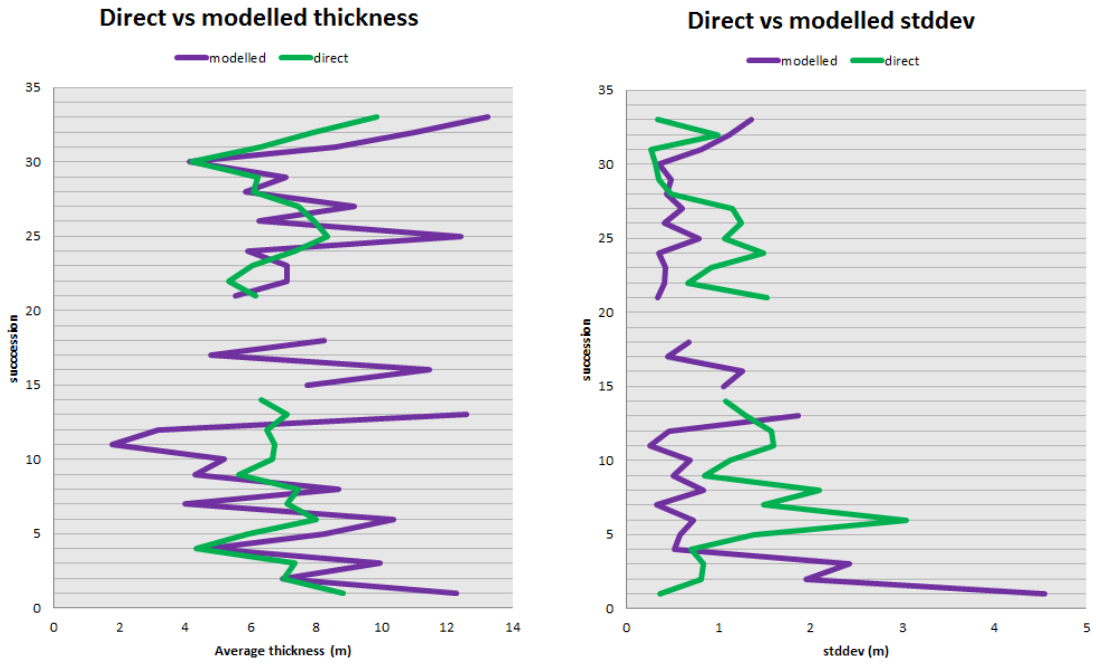

(a) The average thickness

(b) The standard deviation

Figure 4.6: A comparison of the modelled results and the direct results, when all panels are combined into a single model. Note that the modelled data has fewer gaps than the direct measurements, since those succession boundaries are identified but are not in proximity to each other. Direct measurements were therefore not possible. Also note that the standard deviation of the model at the lower succession is influenced by edge effects and is therefore not representative in the lower section.

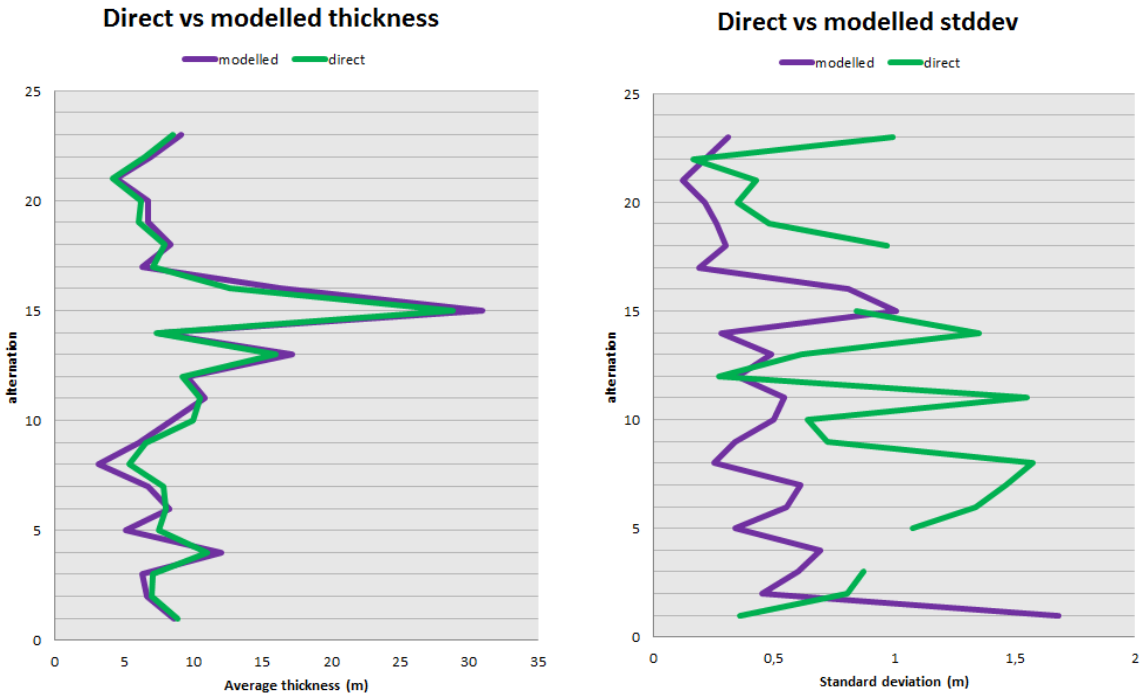

(a) The average thickness

(b) The standard deviation

Figure 4.7: A comparison of the modelled results and the direct results, when only the set of panel 13-14-15.1-15.2 is considered. Note that the standard deviation of the model at the lower succession is influenced by edge effects.

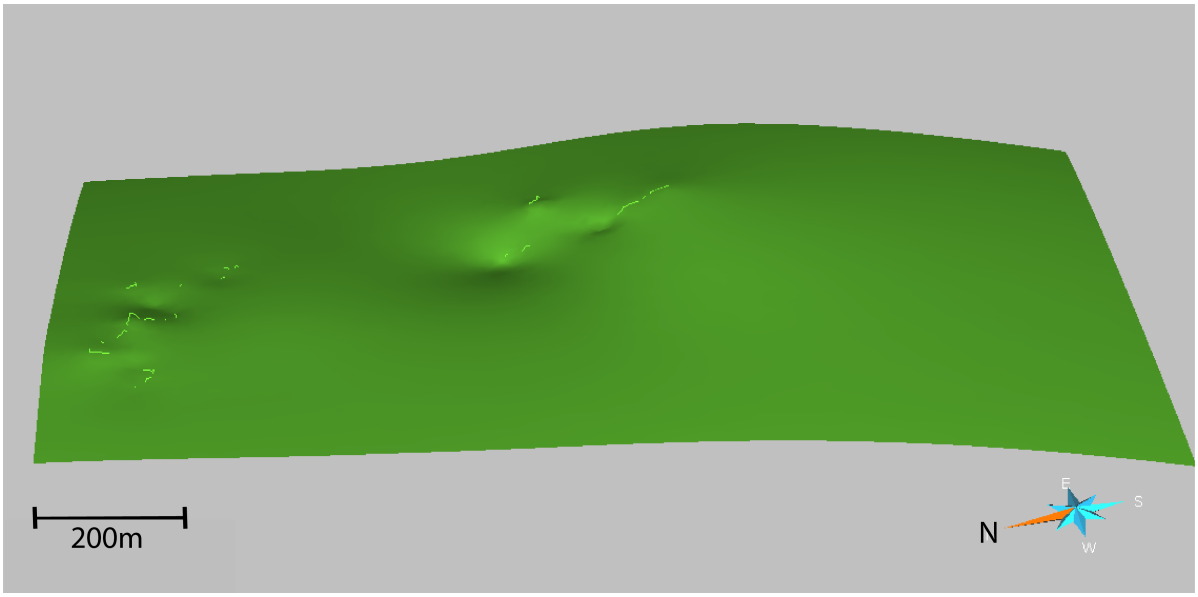

Figure 4.8: This figure shows the surface of a succession boundary, including the horizons as they have been interpreted. The variability is only present where the horizons have been interpreted; where the model interpolates and extrapolates, the variability is smaller. The Z-axis is exaggerated by a factor 10.

Sensitivity analysis of the parameters in Gocad

For the sensitivity analysis, the settings in Gocad have been varied. Based on the results, the optimal settings have been determined. The most important choices that have to be made are to what extent the model should smooth the successions or fit the data, as well as whether large unit thickness variations are allowed. In the sensitivity analysis, there are six variants: a model with a global smooth, a model with fitting the data, a model with a medium setting (between global smooth and fit data); all with large unit thickness variations allowed and all without large unit thickness variations allowed (table 4.1).

Table 4.1: The sensitivity analysis of the model in Gocad, in which the modelling results are compared to the direct results. The smaller the deviations and errors are, the better is the fit of the model. The visual quality is evaluated in a qualitative way, ranging from + (best) to - (worst)

	global smooth no large var.	**global smooth large var.**	**fit data no large var.**	**fit data large var.**	**medium no large var.**	**medium large var.**
deviation average (m)	21.8	24.2	31.2	19.0	22.9	20.6
deviation stddev (m)	10.7	13.5	10.7	13.7	13.4	14.4
max error (m)	3.7	3.5	6.4	3.3	3.7	3.6
visual quality (+ / +- / -)	+	+-	-	+-	+	-

The parameters have been calculated as follows:
'Deviation average', with *dm* being the modelled thickness and *dd* being the directly measured thickness:

$$\sum_{i=1}^{n} \sqrt{(dm_i - dd_i)^2}$$

A similar methodology holds for the 'deviation standard deviation (stddev)', with *stddevm* being the modelled standard deviation and *stddevd* being the standard deviation of the direct measurements:

$$\sum_{i=1}^{n} \sqrt{(stddevm_i - stddevd_i)^2}$$

The maximum error is largest difference between the modelled thickness and the directly measured thickness

for the same succession.

The visual quality of the model is essential, since a model can produce thicknesses which are close to the direct results, but that does not necessarily mean that the model is a good representation of reality. The four extremes are shown in figure 4.9. Overall, it is concluded that 'global smooth, no large unit thickness variation allowed' the preferred option is; it has the best visual quality and low deviations and errors.

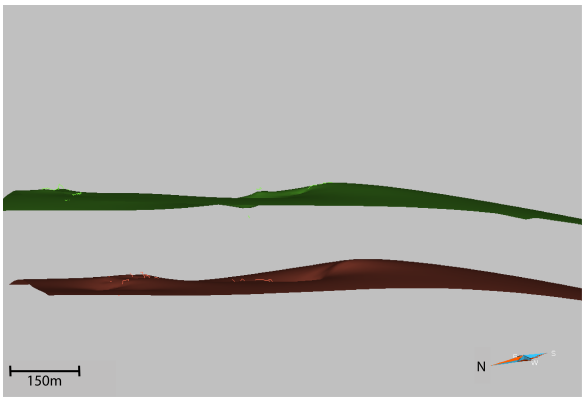

(a) Global Smooth, no large thickness variation allowed

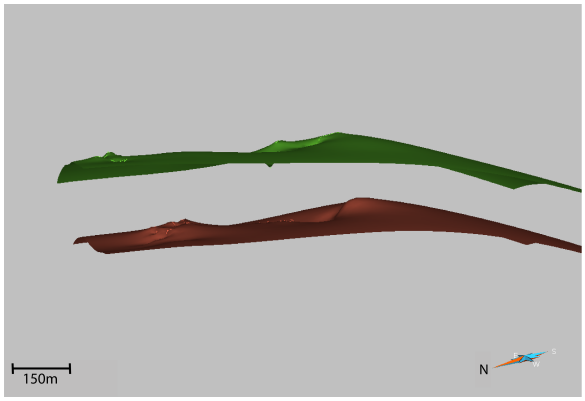

(b) Fit Data, no large thickness variation allowed

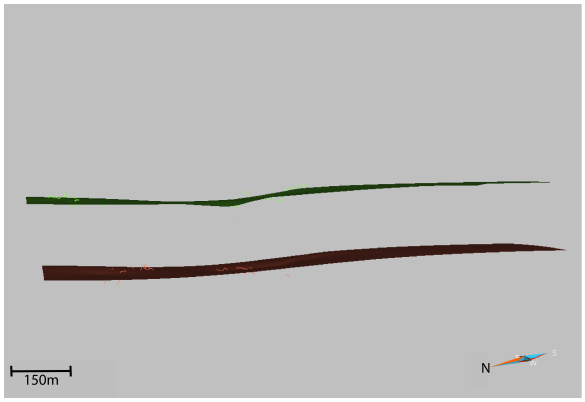

(c) Global Smooth, large thickness variation allowed

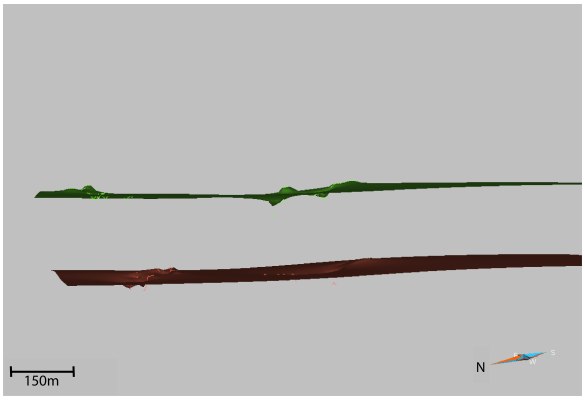

(d) Fit Data, large thickness variation allowed

Figure 4.9: The sensitivity analysis of Gocad. In all subfigures, Z-axis is exaggerated by a factor 10. In all subfigures, the same two succession boundaries are shown.

As will be discussed in Chapter 5, using the direct measurements is determined to be the best method for obtaining the results. Therefore, they are presented in the next sections.

4.4. Succession results

4.4.1. Quantitative results on the successions

The direct measurements in Lime lead to an average thickness for each floodplain succession (table 4.2). For succession 15, 16 and 17, no measurements could be made. The succession boundaries for those successions do not appear in proximity to each other. For succession 19, there is a gap. Here could be actually two or three successions judging by the thickness of the gap. However, to not influence the results, it is left open how many successions there actually are. Succession 20, the average thickness exceeds 14.8m, with not a single measurement below 12.0m. Therefore it is assumed that there is a succession boundary in between, but it has not been observed. The results are therefore removed; it is no longer the result of a single succession. Therefore, there are 28 complete succession and 2 intervals which have no proper recognition of the successions.

Table 4.2: The average thickness, standard deviation, number of measurements per succession and the distance to the paleoflow direction for all successions. The number of the succession refers to the numbering as determined in the correlation, with 1 being the stratigraphic lowest successions and 33 the stratigraphic highest succession. *n* denotes the number of measurements per succession. When no data could be obtained, *xx* is entered in the table. For the distance along the paleoflow direction, it is important to note that not necessarily the specified distance is measured in one line, it can be a combination of distance data at different locations. Furthermore, the distance between the panels is not taken into account.

Succession	average thickness (m)	standard deviation (m)	range (m)	*n*	distance parallel (km)	distance perp. (km)
1	8.8	0.4	1.2	10	0.65	0.56
2	7.0	0.8	2.9	18	0.65	0.56
3	7.4	0.8	2.4	12	1.27	1.33
4	4.3	0.7	2.5	17	0.85	1.07
5	5.9	1.4	4.8	14	0.47	0.70
6	8.0	3.1	7.9	16	1.47	1.55
7	7.1	1.5	5.3	46	2.01	2.29
8	7.5	2.1	8.0	54	2.97	2.77
9	5.7	0.9	3.1	32	2.14	2.40
10	6.7	1.1	4.0	26	1.51	1.63
11	6.7	1.6	6.6	32	2.09	1.74
12	6.5	1.6	4.4	18	1.41	0.76
13	7.1	1.3	3.5	9	0.83	0.66
14	6.3	1.1	2.1	3	0.48	0.36
15	xx	xx	xx	0	xx	xx
16	xx	xx	xx	0	xx	xx
17	xx	xx	xx	0	xx	xx
18	8.7	1.6	6.5	22	1.02	1.03
19	xx	xx	xx	0	xx	xx
20	xx	xx	xx	0	xx	xx
21	6.2	1.5	4.7	23	1.12	0.69
22	5.3	0.7	2.1	21	1.12	0.69
23	6.0	0.9	3.7	17	1.12	0.69
24	7.4	1.5	4.5	16	1.12	0.69
25	8.4	1.1	3.7	9	1.12	0.69
26	7.9	1.2	1.8	2	0.95	0.45
27	7.5	1.2	2.9	7	0.95	0.45
28	6.1	0.5	1.6	8	0.31	0.12
29	6.2	0.4	0.9	6	0.31	0.12
30	4.2	0.3	1.2	13	0.95	0.45
31	6.3	0.3	0.9	12	0.95	0.45
32	7.9	1.0	3.0	9	0.95	0.45
33	9.9	0.3	0.7	3	0.64	0.33

Statistics used for representation of the results

The following statistics of the results are presented:
The average thickness of each succession is calculated, based on the individual measurements (as shown in Appendix D). This leads to a list of average thicknesses, one for each succession. The average thickness as presented in table 4.3 is the average of all successions, so an average of the average per succession.

The 'standard deviation of the average thickness' is calculated as follows: The average thickness of each succession is calculated, leading to a list of average thicknesses, one for each succession. The standard deviation of this list is determined. Statistically, this can be seen as the standard deviation of the population. The standard deviation is then calculated as

$$stddev = \sqrt{\sum_{i=1}^{n} \frac{(x_i - \bar{x})^2}{n}}$$

It is therefore a measure of variability over the successions, so comparing the succession with each other.

The 'average standard deviation individual succession' has the following meaning: The standard deviation of thickness of a single succession is calculated, based on the individual measurements of that succession. Statistically, the measurements can be seen as samples from a population, which is relevant for the standard deviation. The standard deviation is then calculated as

$$stddev = \sqrt{\sum_{i=1}^{n} \frac{(x_i - \bar{x})^2}{n-1}}$$

For each succession this leads to a single value, of which this is the average. It is therefore a measure of the variability within a succession, i.e. the variability of an individual succession.

The standard deviation is not a robust statistic. However, all data entries have been evaluated and determined to be realistic. There are no major outliers. The only outliers have been removed because of geological interpretation and that has been done before the determination of the statistics. Therefore, the standard deviation suffices as a measure of the variability.

The median is the median thickness measurements out of all measurements. On the one hand, the median is a robust statistic, not susceptible to outliers. On the other hand, it is not sorted per succession. For example, when a thinner succession has more measurements than a thicker succession, the median decreases due to the unbalanced number of measurements.

The minimum average thickness is the successions which has, on average, the lowest thickness. The maximum average thickness is the succession which has, on average, the largest thickness. These are measures for variability over the successions.

The minimum and maximum thickness measured are the extreme values, so the minimum and maximum values over all measurements taken. These values are relevant, since they show in what range the succession thicknesses can be expected.

The average range of thicknesses within a succession, are calculated as follows: Of all successions, the range is determined. That is

$$range = max(thickness) - min(thickness)$$

Of this, the average is determined. It is therefore a measure of variability of individual successions.

The thicknesses per succession are relevant for interpretation of the results. However, for now and for comparison with literature, statistics of the measurements are more useful (table 4.3, explained in the purple textbox). These statistics have also been used to check and validate the model which is made in Gocad. Furthermore, it has been used as a feedback step to the interpretation. If a standard deviation of a few meters shows up, it is wise to check the interpretation again and, if necessary, improve this.

Table 4.3: The statistics when all is combined into one model. For a more indepth explanation of the meaning of the statistics, refer to the purple textbox on the previous page.

Statistics	
Average thickness (m)	6.9
Standard deviation of average thickness (m)	1.3
Average standard deviation individual succession (m)	1.1
Median (m)	6.5
Minimum average thickness (m)	4.3
Maximum average thickness (m)	9.9
Minimum thickness measured (m)	3.5
Maximum thickness measured (m)	12.4
Average range of thicknesses within a succession (m)	3.4

The average thickness of a succession is 6.9 meters, with a standard deviation of 1.3. The average standard deviation, which is a measure for the variability of each single succession, is on average 1.1 meter. However, the range of thicknesses measured for a single sequence is in some cases a lot larger. 13 of the successions have a range > 3.0 meter. Of those, four are above 5.0 meter and two are above 7.0 meter. The distance is over which the datapoints are spread, is measured twice: one measurement parallel to the paleoflow direction and one measurement perpendicular to the paleoflow direction. The paleoflow direction has been determined in Chapter 2: north-north-east (NNE). For each panel, the horizontal distances over which the succession boundaries are visible are measured. The space in between the sets of panels is not included. The successions with the largest thickness range and the largest standard deviation also have the largest distance along which the succession has been measured (figure 4.10, figure 4.11). With an increasing floodplain distance along which the data is measured, the spread in average thickness of the successions (figure 4.12) becomes smaller. The data converges towards the average succession thickness of 6.9m.

The histogram of the average succession thickness is shown in figure 4.13, measurements have first been sorted per succession. The distance along the which the successions have been measured perpendicular to the paleoflow direction are included as a redness of the histogram bins. The histogram that does not exclusively includes the averages, but at all measurements that have been taken, is shown in figure 4.14.

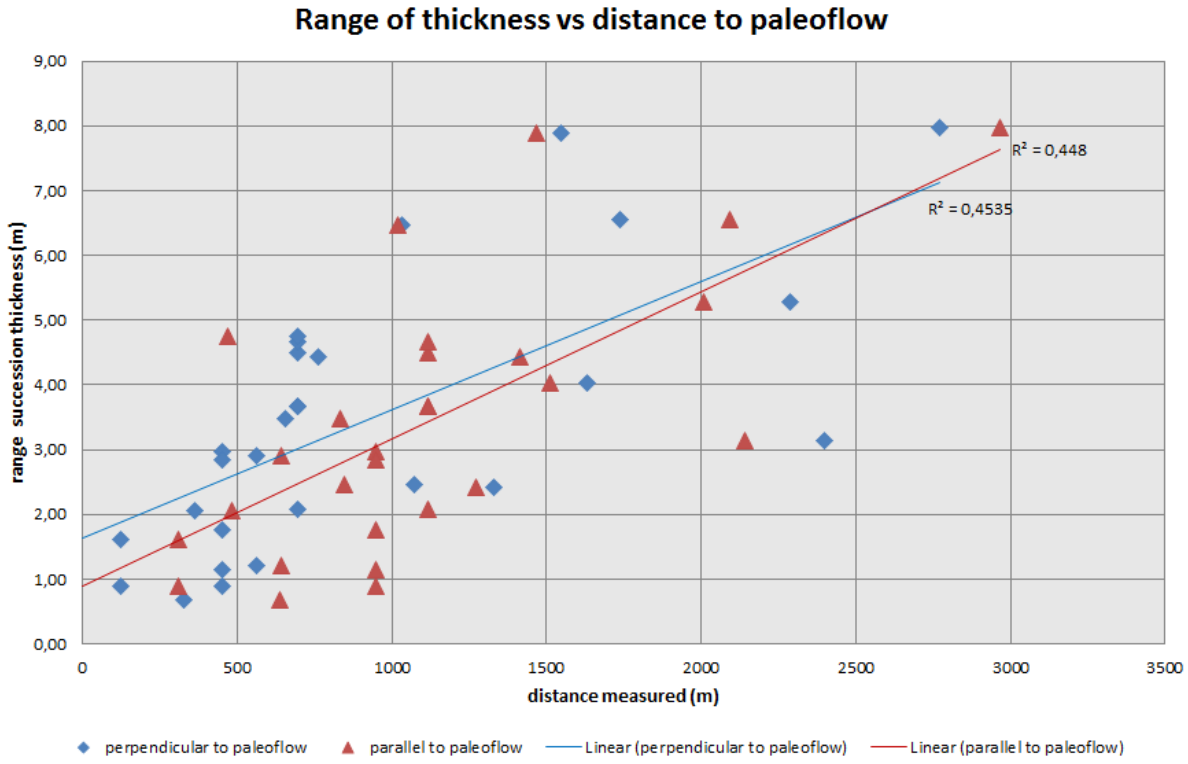

Figure 4.10: The scatterplot of the range of thicknesses of each succession versus the distance along which the succession has been measured. Linear trendlines have been fitted to the data; the R^2 is denoted in the graph.

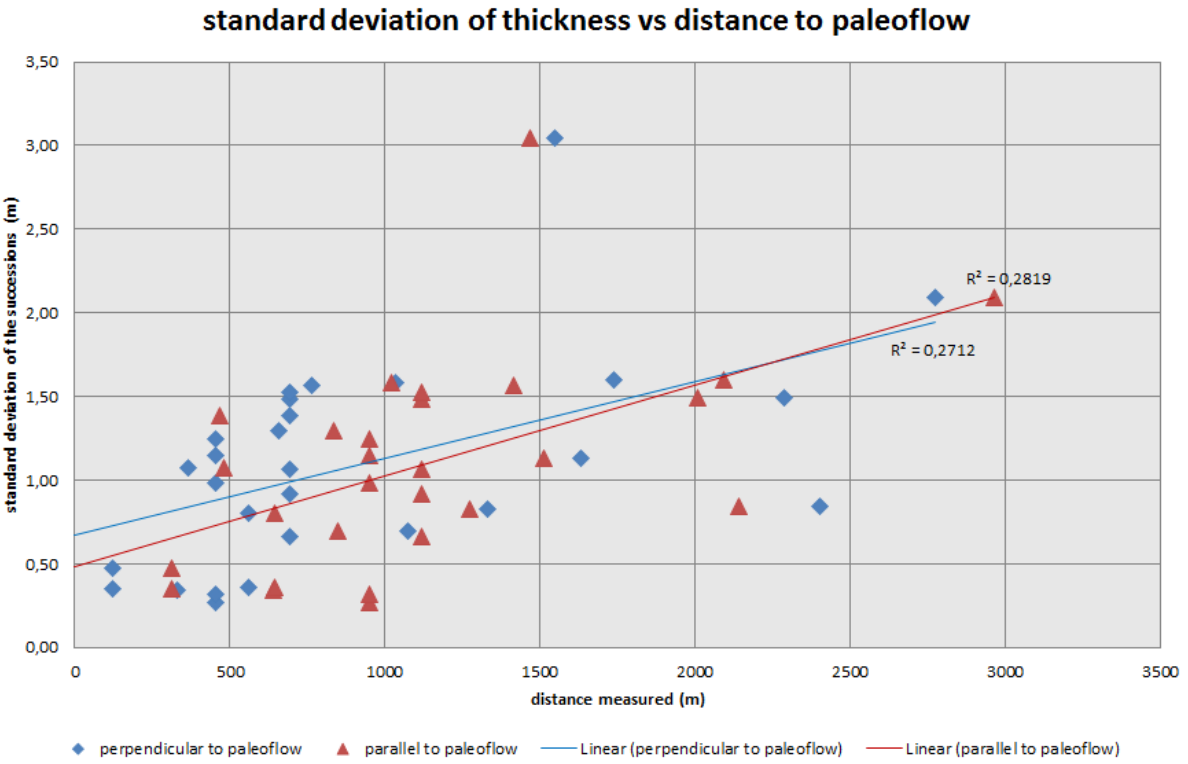

Figure 4.11: The scatterplot of the standard deviation of thicknesses of each succession versus the distance along which the succession has been measured. Linear trendlines have been fitted to the data; the R^2 is denoted in the graph.

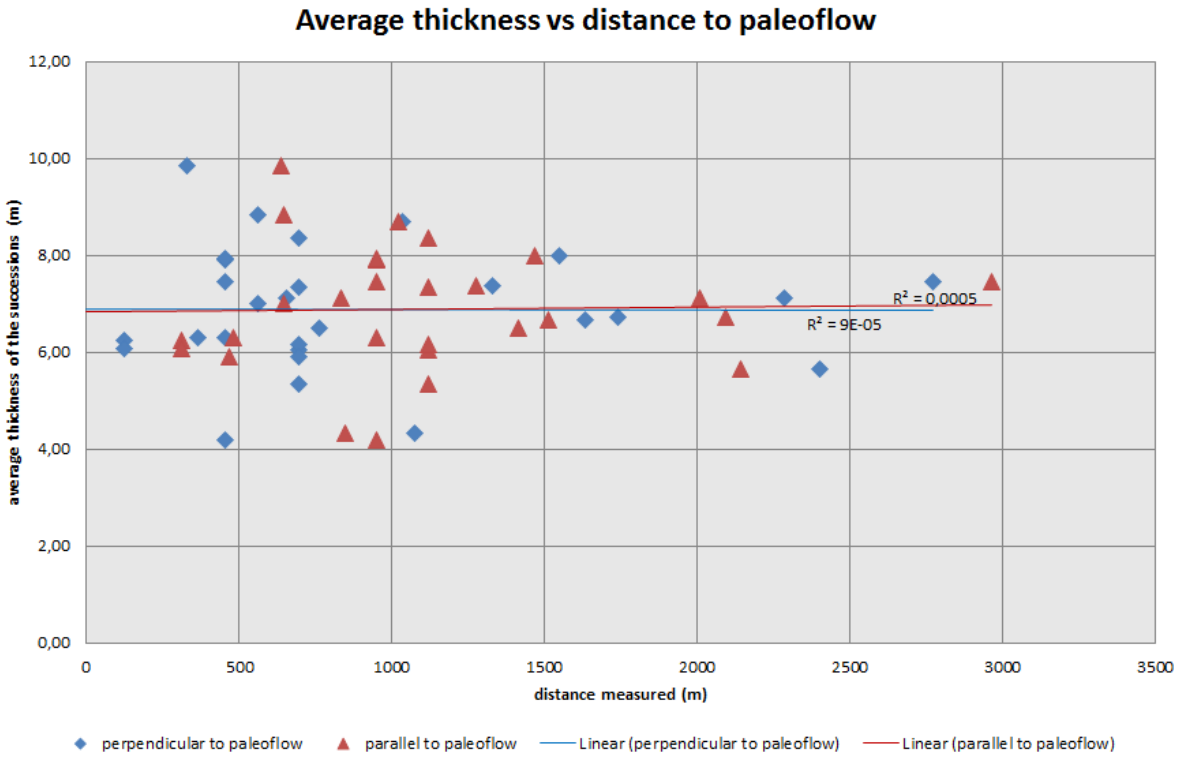

Figure 4.12: The scatterplot of the average thickness of each succession versus the distance along which the succession has been measured Linear trendlines have been fitted to the data; the R^2 is denoted in the graph. Note that the average succession thickness is 6.9m.

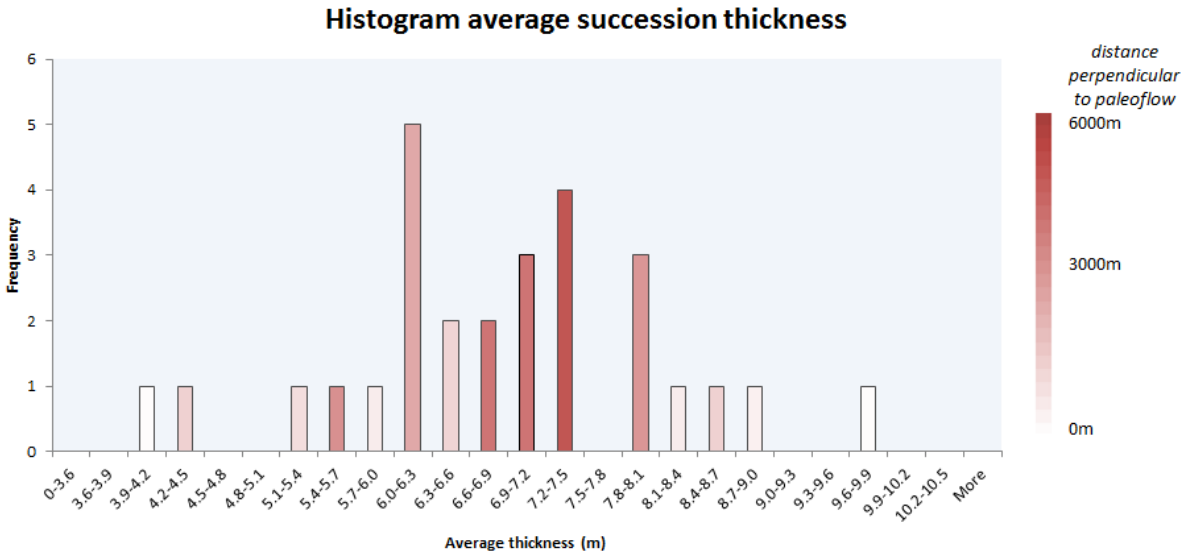

Figure 4.13: A histogram of the average succession thickness. The red color-scale indicates the amount of data the frequency count is based on. The amount of data is represented by the perpendicular distance to the paleoflow direction. In bins with a frequency larger than 1, the perpendicular distances are added up. A bin with a larger frequency is likely to get a darker color, since multiple successions contribute to the distance.

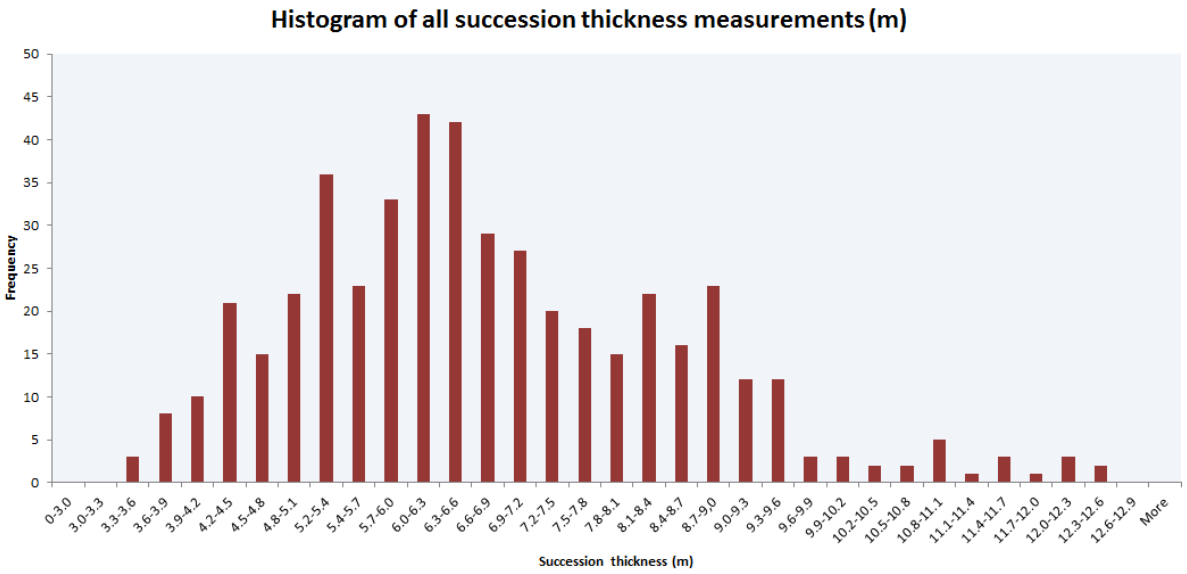

Figure 4.14: A histogram of all the succession thicknesses measured, based on 475 measurements.

Thickness compensation

To determine whether a thin succession is followed by a thick succession and vice versa (i.e. whether thickness differences are compensated in the next or previous succession), first the averages are evaluated. There, no relation between succession thicknesses is found: a thin succession is not specifically followed by a thicker succession or vice versa (figure 4.15). The five successions with the lowest thickness are evaluated in more detail. These are succession 30, 22, 9, 5 and 4. Succession 30 is on top of purple 4, a very distinct purple soil defined by (Abels et al., 2012). Succession 22 is on top of purple -1, also a distinct purple soil (Abels et al., 2012). Succession 9 and 5 are also on top of a purple (figure 4.4). Succession 4 is not on top of a purple, but the purple is in the top of succession 4. There are more purple layers, where no thinner layer is on top. Despite, it is remarkable that 4 of the 5 thinnest layers on average are on top of purple soils. Also, the successions below these 5 thinnest layers are not remarkably thick on average.

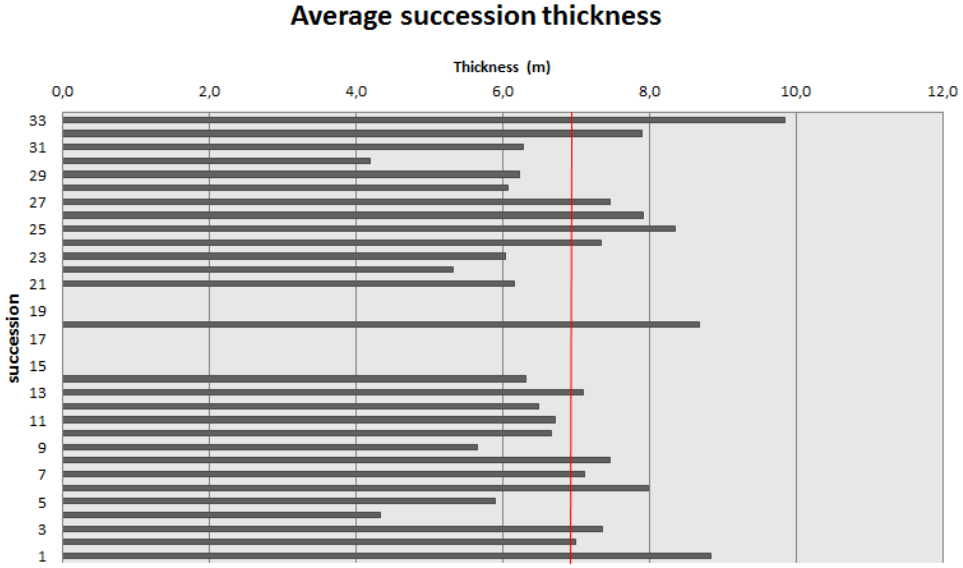

Figure 4.15: The average thicknesses of all successions in stratigraphic order. Note that a thin succession is not necessarily followed by a thick succession and vice versa, when the average thicknesses of each succession are considered. The red line presents the overall average thickness of 6.9m.

However, these are averages. A closer look is taken at the specific locations where a succession is thin or thick. Thin will be defined as the 10th percentile, i.e. anything below 4.7m. Thick will be defined as the 90th percentile of all measurements, anything above 9.5m. There are four sections in which these values appear; those are evaluated separately.

Panel 17
Between boundary 17.1 and 17.2 (succession 4), the succession is thin. However, between boundary 17.2 and 17.3 (succession 5), there is another thin layer. So there are two thin layers on top of each other. On top of those, there is a major sandstone, due to which the succession above can no longer be measured. Since the successions above cannot be seen and the successions below are not present in the panel, a quantitative analysis is not possible.

Panel 16
Between succession boundary 16.5 and 16.6 in panel 16 (succession 8), the succession is thick and significantly thicker than the succession is elsewhere. Between succession boundary 16.6 and 16.7 (succession 9), the succession is 6.1m thick on the same interval. This is lower than average, but not a thin succession according to the definition. In order to quantify, the average thickness is plotted when only the measurement of the thick succession is used (n=1), the average thickness (incl. standard deviation) of the thick succession and the succession below is plotted (n=2), the average thickness when the thick succession and the succession below and above are combined (n=3) and finally the overall average thickness and standard deviation (6.9m and 1.3m) (figure 4.16). Adding another succession (n=4) is not possible, since it is not present in the panel.

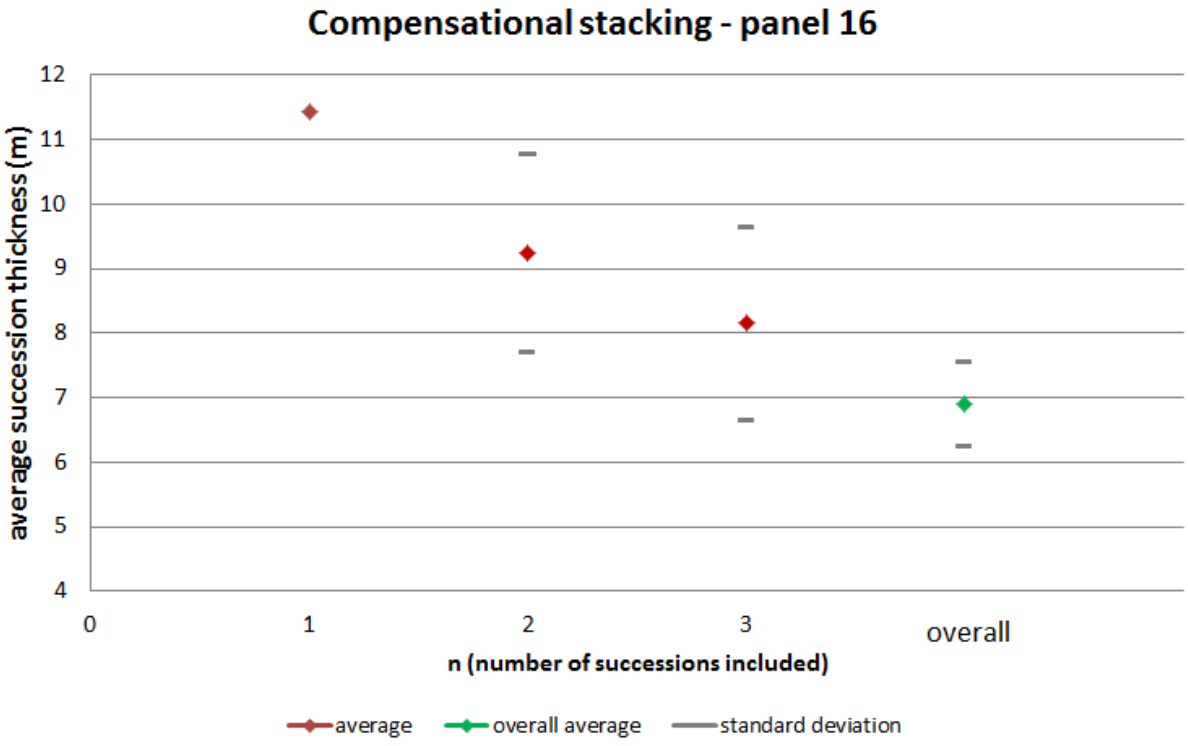

Figure 4.16: The average succession thickness plotted against the number of successions included - locally near the thick succession of panel 16. The grey lines represent the standard deviation. Note that the average succession thickness decreases towards the overall average when more successions are included. The standard deviation between successions cannot be determined when only one succession is included. The standard deviation decreases going from n=2 to n=3, but the difference is small. Note that the average succession thickness presented in this figure is only local and for each succession measured at the exact same lateral position.

Panel 4
In panel 4, between succession boundary 4.7 and 4.8 (succession 12), the succession is thin on a small interval. The succession on top seems to increase in thickness here, compensating the thickness difference. However, it is not significantly thicker than average. When combining the thin succession and the succes-

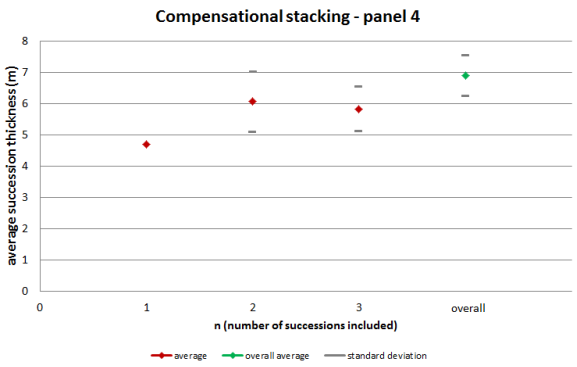

Figure 4.17: The average succession thickness plotted against the number of successions included - locally near the thin succession (12) of panel 4.

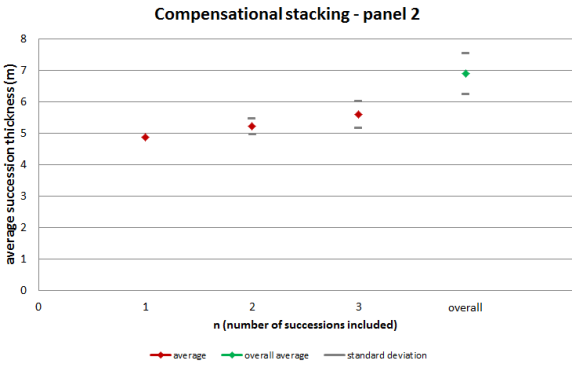

Figure 4.18: The average succession thickness plotted against the number of successions included - locally near the thin succession (21) of panel 2.

sions below and above, the average thickness approaches the overall average (figure 4.17). Adding the third succession lowers the average thickness compared to two succession, this is since the succession below is added in n=2, the succession above (which is relatively thin as well) only in n=3. If the order is reversed, the average thickness increases with increasing *n*. The standard deviation decreases with increasing *n*.

Panel 2

In panel 2, between successions boundary 2.8 and 2.9 (succession 21), the succession is thin in a few of the measurements. Sometimes a measurement is just below the cut-off value and sometimes just below. When combining the thin succession and the two successions above, the average thickness approaches the overall average (figure 4.18). Including the succession below numerically is impossible, since that is an interval not interpreted and the thickness is therefore not known. A graphic representation is shown, where the uninterpreted successions are represented as one bulk, such that the local thickness variations can be evaluated (figure 4.19)

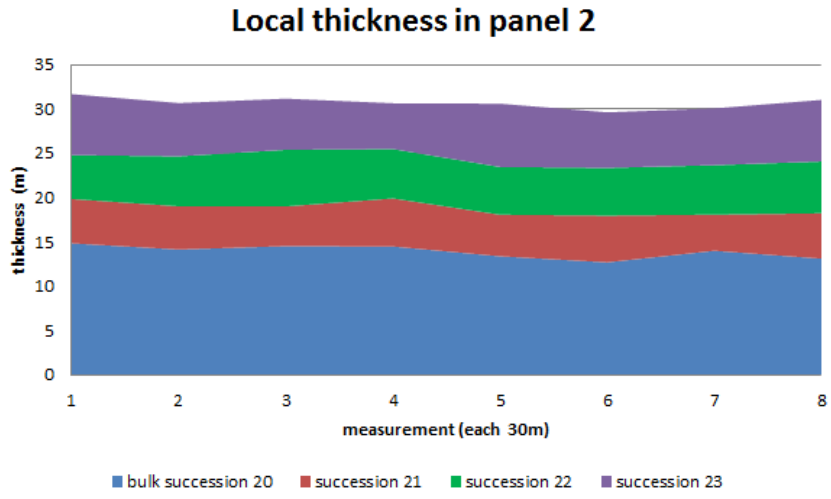

Figure 4.19: Local thickness variation in panel 2. Bulk succession 20 represents the interval where successions are uninterpreted. Note that the total thickness of the column is ca. 30m in all measurements, despite local thickness differences.

What-If analysis

This section describes how the results are when a slightly different approach is used in determining the statistics.

What if - only the laterally extensive successions are included?
First of all, successions 7 to 11 are present in (almost) all panels (figure 4.4) and therefore hold the most lateral information (table 4.4). Furthermore, these are the successions with most data points (thickness measurements), 40% of the total. The average thickness of this subset is 6.7m. The standard deviation of an individual succession is in this section 1.4m on average, which is higher than the 1.1m for the full section. The average thicknesses of successions 7 to 11 are relatively close to the overall average, compared with the full dataset. The standard deviation between the average thicknesses of those successions is only 0.6m.

Table 4.4: The results on the laterally extensive subset (succession 7 to 11). It is important to note that the distance between the panels is not taken into account.

Succession	Average thickness	range (m)	Found in panel	*n*	distance parallel (m)	distance perp. (m)
7	5.3	7.1	4, 5, 13, 14, 16, 17, 18	46	2008	2286
8	8.0	7.5	3, 4, 5, 13, 14, 16, 17, 18	54	2965	2773
9	3.1	5.7	4, 5, 13, 14, 16, 18	32	2142	2400
10	4.0	6.7	4, 5, 13, 18	26	1513	1631
11	6.6	6.7	3, 4, 5, 13, 18	32	2093	1739

What if - the weighted average is taken?
Apart from taking an average thickness of the successions, a weighted average can be taken. This weighted average is based on the number of measurements made. I.e., the more measurements that have been made for a succession, the more that average thickness counts in the total average succession thickness. The resulting weighted average thickness is:

Weighted average succession thickness: 6.8m

What if - literature is included?
Correlation with Abels et al., 2012 is easiest, since some of the logs made fall within panel 19 of this thesis. Some of the distinctive purple layers have been numbered by Abels et al., 2012. This makes a visual comparison easy, Purple 2 (top of succession 27) and Purple 4 (top of succession 30) can be found right away. Purple -1 corresponds to top of succession 21, Purple -2 to top of succession 20. Since they can be recognized visually, they can be correlated with the other panels.

Correlation with Abels et al., 2013 is also possible, though more difficult, since there is no overlap with one of the photopanels. In Abels et al., 2013, each sequence is identified, analyzed and named A to P, with A being the lowest. Of these, B to O have been correlated (figure 4.4). Succession A and P could not be correlated.

Since the Dear Creek Amphitheater (which is evaluated by Abels et al., 2013) is only ca. 1.5km north of panel 13, these results can be included in the results as well. The results are found with a different method by another person, therefore the combined results are made separately and exclusively for this section. Further interpretation is not based on this combined average thickness. For combining average thickness, there are two options: 1. Add the thicknesses from Abels et al., 2013 as single measurements to the measurements made for this thesis. The average thickness does not change. 2. Calculate an average thickness per set of panels and add the thicknesses from Abels et al., 2013 as a fourth set. Then calculate the total average as the average over the four sets. Again, the average thickness does not change, it is also 6.9m (table 4.5). The standard deviation is slightly different, but the calculation method is not comparable (much less measurements, since there are only four).

Table 4.5: Combination of the results of this thesis with Abels et al., 2013 results. In this scenario, the three sets of panels from this thesis and the data of Abels et al., 2013 are used as four separate data entries, i.e. all four get a weight of 0.25, which is used to determine the average thickness of the succession. Note that there are significant thickness differences of individual successions between the sets.

Succession Abels 2013	**Succession #**	**Thickness Abels 2013 (m)**	**Thickness Set 2-3-4-5 (m)**	**Thickness Set 13-14-15.1-15.2 (m)**	**Thickness Set 16-17-18-19**	***Average***
A	xx	6.9	xx	xx	xx	*6.9*
B	xx	4.3	xx	xx	xx	*4.3*
C	1	6.2	xx	8.84	xx	*7.52*
D	2	5.0	xx	7.00	xx	*6.0*
E	3	8.6	xx	7.09	7.74	*7.81*
F	4	10.4	3.90	xx	4.56	*6.29*
G	5	8.8	6.66	xx	3.99	*6.48*
H	6	5.4	5.47	7.47	11.55	*7.47*
I	7	4.85	6.72	8.72	6.28	*6.64*
J	8	8.75	5.99	7.85	8.94	*7.88*
K	9	5.95	5.72	5.35	5.62	*5.66*
L	10	6.95	7.26	6.58	5.27	*6.52*
M	11	9.9	6.58	9.98	5.64	*8.03*
N	12	8.45	6.50	xx	xx	*7.48*
O	13	5.75	7.10	xx	xx	*6.43*
P	xx	7.4	xx	xx	xx	*xx*
average		**7.1**	**6.2**	**7.7**	**6.6**	***6.9***
std. dev.		**1.9**	**0.9**	**1.3**	**2.3**	***1.6***

4.4.2. Qualitative results on the successions

Some succession boundaries are more distinct than others; some overbank deposits have a more intense color. Based on this, a classification has been made (figure 4.20). The classification is qualitative, based on a scale of four options: visible but not distinct is colored green, slightly distinct is colored yellow, distinct is colored orange and very distinct is colored red (see also figure 4.20). Results show that a single succession boundary can have different interpretations of distinctiveness over the panels. Despite, in general there can still be sets identified, as has been done by the blue and green braces. They mark the sets, which are important for relating to precession and eccentricity: three or four distinct successions (the blue braces) followed by one or two less distinct successions (the green braces). Starting from the top, the pattern is clearly visible; two times a set of three distinct successions is seen, interrupted by one less distinct succession. Then, starting from succession 25 downwards, there is no clear pattern visible anymore. From succession 20 downwards, there are succession boundaries missing. Near succession 13, there is enough data to pick up the pattern again. One less distinct succession boundary, followed by four very distinct succession boundaries and again one less distinct succession boundary. Succession 6 and downwards is left open, since the pattern is not clearly visible anymore.

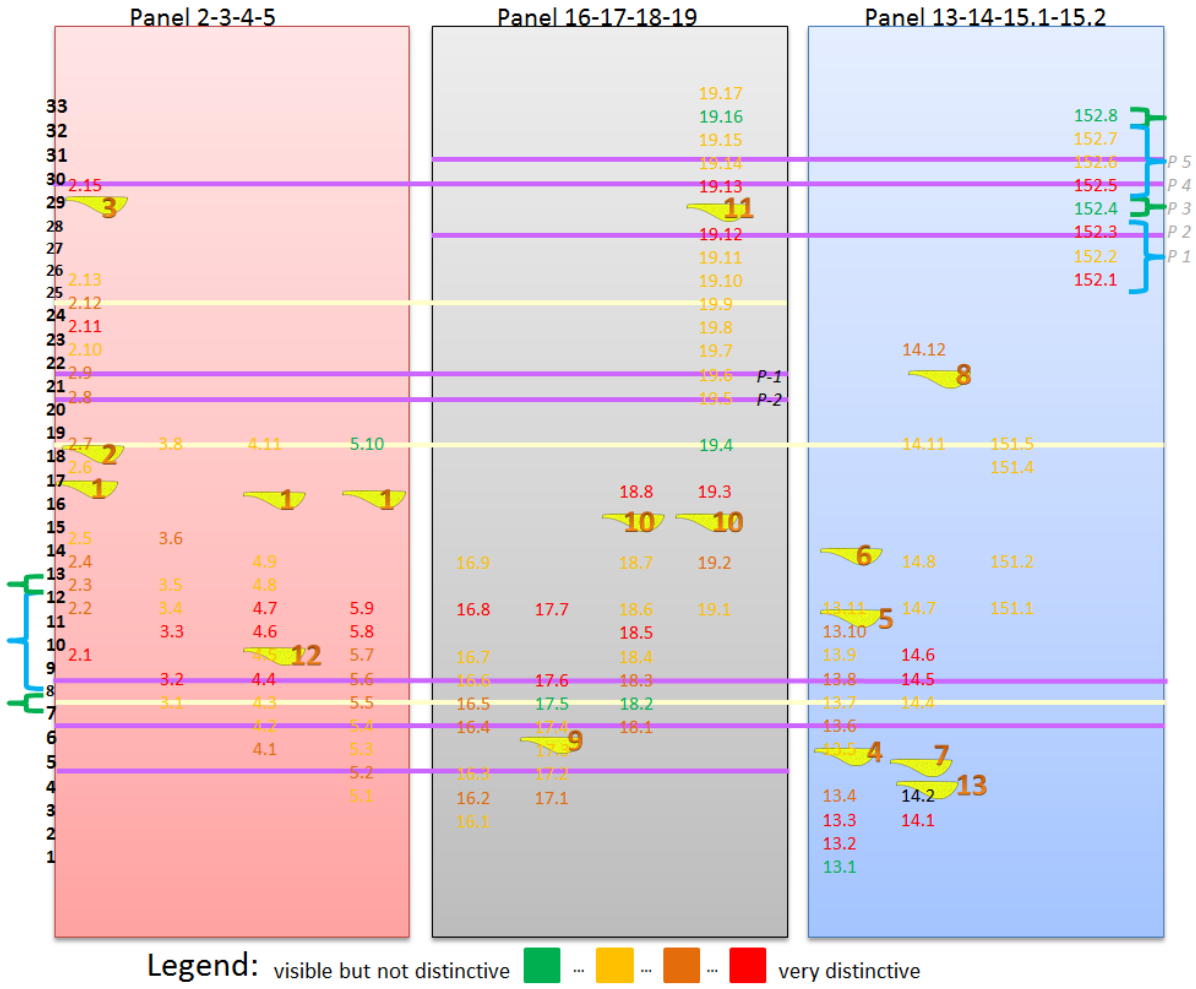

Figure 4.20: The distinctiveness of the succession boundaries. Note that an individual succession (boundary) shows lateral differences in distinctiveness. The purple and white lines represent the successions on which the correlation has been based. Blue braces mark distinctive sets, green braces mark less/non- distinctive sets. Note that this pattern cannot clearly be found in all successions.

4.5. Sandstone results

4.5.1. Quantitative results on the sands

The sands that are found in the panels are divided into two categories: major sandstones and minor sandstones. To determine how the distinction should be made, a closer look is taken at the statistics. Of 94 individual sandbodies the thickness is measured (figure 4.21). These are not all the sandstones present, but a significant portion and they are well distributed among the panels and stratigraphy. There are many sandstones with small thickness, and a few with large thickness. Two clusters are seen: a cluster with a high frequency below 7.0m thickness and a cluster with low frequency above 7.0m thickness. Near the boundary of 7.0m, the three bodies to the left of the boundary and the three bodies to the right of the boundary are evaluated visually, to determine the correctness of this boundary. The sandstone bodies to the left are significantly smaller and less wide than the sandstone bodies to the right and therefore the boundary is kept at 7.0m. To summarize:

- major sandstone: maximum thickness > 7.0m
- minor sandstone: maximum thickness ≤ 7.0m

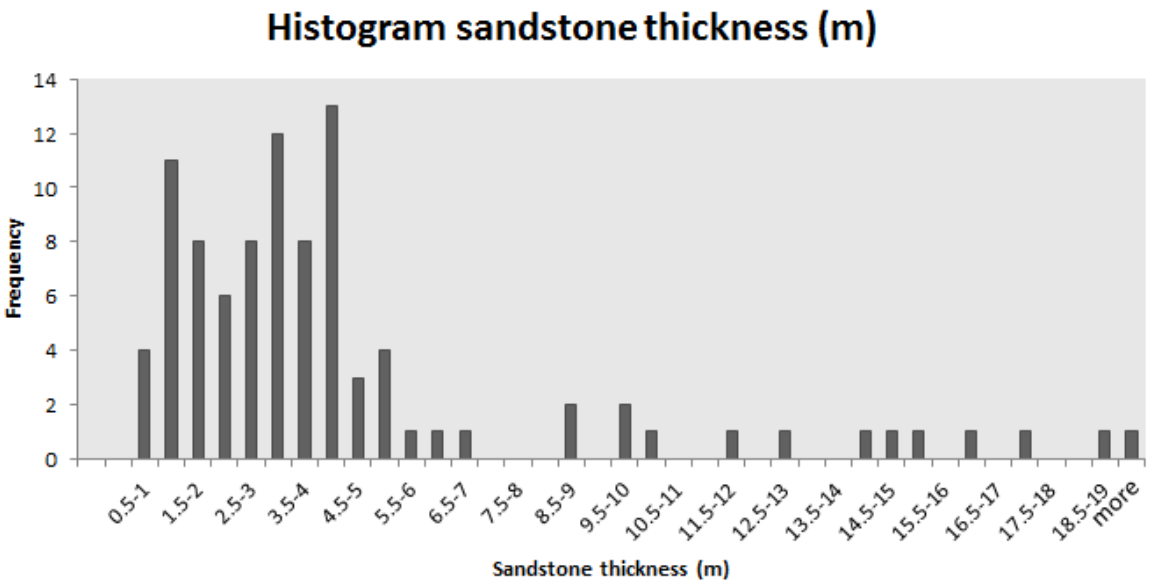

Figure 4.21: The distribution of sandstone thickness, out of 94 measurements. Note that roughly two clusters are seen, one on the left with small thickness and large frequencies and one the right with large thickness and low frequencies.

Major sandstones

The thickness of the major sandstones is measured as a maximum thickness, i.e. there where the thickness is maximum and the top and base are clearly visible. An approximation of their lateral extent is also given, but since they sometimes exceed the area covered by the panels, then no exact measurements can be taken. Major sands are often in the top of the panel. As a consequence, the thickness can no longer be measured, since the top of the sandstone itself is no longer present; or it cannot be confirmed that it is still present.

The average thickness of the major sandstones is 14.0m with a standard deviation of 3.9m (table 4.6). Each major sandstone has been numbered randomly for easy referencing. The results show the panel(s) in which it has been observed, the maximum thickness measured and the minimum lateral extent. When a type could be determined, it is also shown in the table. Some major sandstones are multistory sandstone bodies. If identification was possible, the number of stories is also mentioned under type. Examples of these major sandstones are shown in figures 4.22, 4.23.

For the multistory sandstones, it is tried to disentangle them. In other words, if possible it is measured what the thickness of each of the stories is (table 4.7). Of four major sandstones, it has been possible to determine the thickness per story.

First of all, a new average can be calculated, where the major sandstones that can be split up, are entered as two separate measurements. This results in an average thickness of 11.6m. Second of all, an average can be measured in which only the major sandstones are used, which are without a doubt single story. When this is done, major sandstones 2, 12 and 13 are used, as well as major sandstone 3, 6 and 8 which were split up as seen in table 4.7. This results in an average single story thickness of 9.6m.

Table 4.6: The results from the major sandstones. The sandstones have been numbered at random, for further reference. Under *type* is denoted as what type of sandstone body it is interpreted and/or how many stories the major sandstone body has. If no interpretation could be made, a '-' is entered under *type*.

Major SST	panel	approx. height (m)	max thickness (m)	min width (m)	type
1	2, 4, 5	1542	17.1	892	2 stories, channels
2	2	1553	10.0	171	channel, single
3	2	1613	14.3	174	2 stories
4	13	1515	16.1	440	2 stories, splaychannel
5	13	1550	15.1	345	-
6	13	1570	18.7	364	2 stories
7	13, 14	1511	10.1	237	channel
8	14	1610	22.9	288	2+ stories, channel + bar
9	17	1485	11.7	247	-
10	18, 19	1535	14.9	501	-
11	19	1630	9.7	238	-
12	4	1514	9.0	66	single story
13	14	1498	13.0	75	single story
Average			**14.0**	**311**	
Std.deviation			**3.9**	**208**	
Median			**14.3**	**247**	

Table 4.7: The maximum thickness results of the major sandstones which have been split per story. Thicknesses do not necessarily add up to the total thickness from table 4.6, since maximum thickness is measured.

Major SST	total thickness (m)	thickness lower SST (m)	thickness upper SST (m)
3	14.3	7.5	7.0
6	18.7	10.5	7.0
8	22.9	unknown	13.2

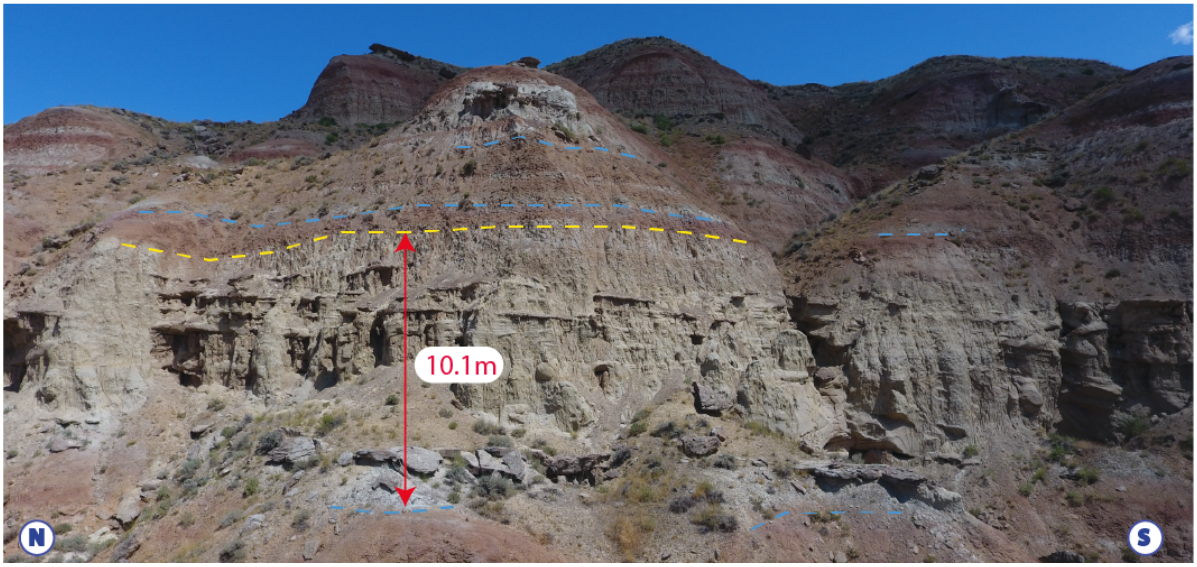

Figure 4.22: An example of a smaller major sandstone as found in the research area (panel 17). The succession boundaries are marked with blue dashed lines. The top of the major sandstone is marked with a yellow dashed line.

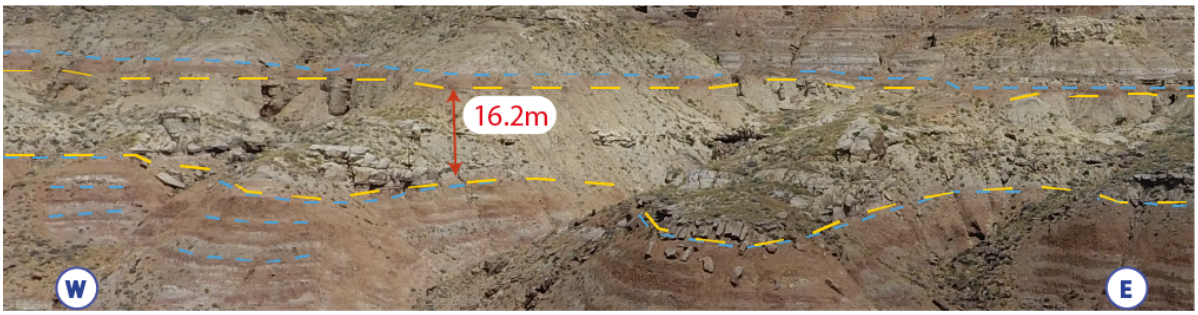

Figure 4.23: Another example of a larger major sandstone as found in the research area (panel 13). The succession boundaries are marked with blue dashed lines. The top and base of the major sandstone are marked with a yellow dashed line.

Minor sandstones

There are many minor sandstones, some panels have only 5, some panels have over 50. These are too many to describe separately and fall outside the scope of the research, therefore only a quantitative analysis is given:

- The minor sandstones are all within the heterolitics, with the exception of some sheet-like sandstones. The minor sandstones do sometimes erode into an overbank deposit (soil) below (figure 4.25).
- Most heterolitic layers with minor sandstones in them, do have more. So laterally there are multiple minor sandstones within an individual heterolitics layer.

Examples of minor sandstones are shown in figure 4.24, 4.25, 4.26.

Figure 4.24: An example of a minor SST (panel 4). The succession boundaries are marked with blue dashed lines. The top and base of the minor sandstone are marked with a yellow dashed line.

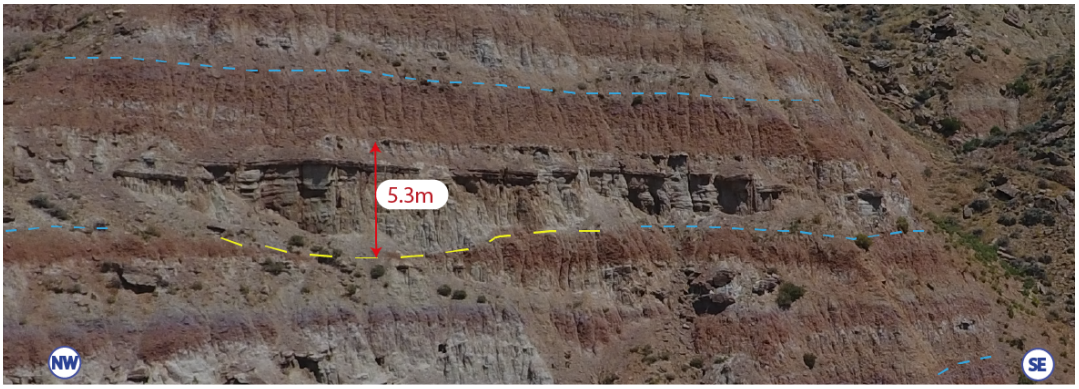

Figure 4.25: An example of a minor SST eroding into the overbank deposits of the succession below (panel 4). The succession boundaries are marked with blue dashed lines. The base of the minor sandstone is marked with a yellow dashed line. Note that where the minor sandstone is truncating, the succession boundary is no longer present.

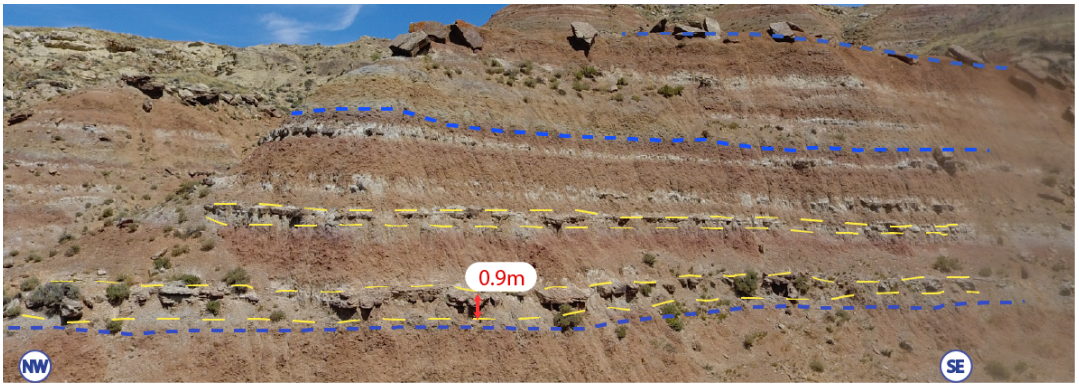

Figure 4.26: An example of two minor sandstone sheets (panel 14). Above are more sheets, but those are less laterally continuous. The succession boundaries are marked with blue dashed lines. The top and base of the minor sandstone are marked with a yellow dashed line.

4.5.2. Qualitative results on the sands

The sands are also evaluated in a qualitative way. This means that visual interpretations of the sands are made, which can be used and/or are necessary for the interpretation of their deposition.

- There are more major sandstones in the panels than shown in the quantitative results. However, they could not be measured, since either the base or the top is not present. The latter is seen most. A top can no longer be determined, or at least it cannot be determined for sure whether the present-day top is equal to the original top of the sand.
- Above every major sandstone, the first overbank phase has a distinctive paleosol.
- Some major sands have a distinct paleosol on top of the sandstone, which is not laterally continuous and which is not the overbank facies forming the top of the succession (figure 4.27).
- The first succession above the major sand is not necessarily a very thin succession. In some cases it is, in some it is not.
- On multiple occasions, there are two major sandstones on top of each other, with only one succession boundary in between. Some of these major sandstones already consist out of multiple stories.

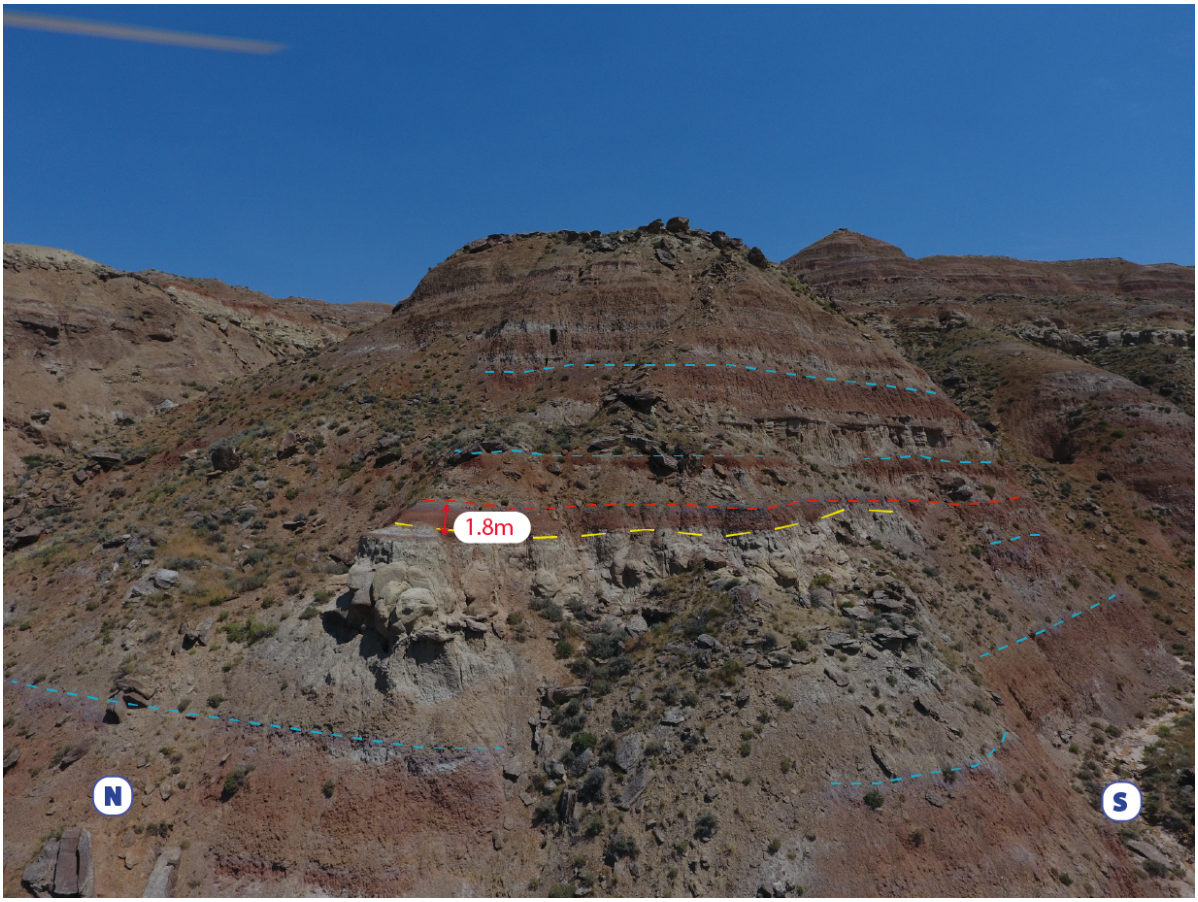

Figure 4.27: A local paleosol on top of a major sandstone (panel 4). The local paleosol is marked with red, the succession boundaries with a blue dashed line. The top of the major sandstone is marked with a yellow dashed line.

5

Discussion

This chapter covers five discussion sections and their resulting recommendations. The first section discusses the approach and reliability of the results. The second section discusses the floodplain successions, the third section the sandstones. The fourth section discusses the synthetic sedimentary model that can be made based on the results. The last section discusses the impact of the results.

5.1. Approach and reliability of the results

5.1.1. The original data

The original data has a few flaws. First of all, a photogrammetry model is never 100% accurate. The resolution of the photopanels is less than preferential. The original photos are of sufficient resolution, but this is lost in the photogrammetry. Due to this loss of resolution, it is recommended to use the best camera as possible. As described in Chapter 3, for panels 15.1, 15.2 and 16 less photos have been used, i.e. a lower photo density. First of all, the panels 15.1, 15.2 and 16 were better to handle by the computer than most others. In that sense it is an improvement. However, the resolution of panel 15.1 is worse than in panel 14 on the section that there is overlap. So the resolution did not improve. The question arises if this is caused by using fewer photos, or by the bad results of 15.1 which was already unable to align initially. An answer cannot be found based on the data available. Multiple photogrammetry panels should be made out of the same panel, each with a different amount of photos, to find an optimum. However, this is outside the scope of this research.

A few notes about the results must be made. Interpretation is, as the word says, not a hard science. One can interpret a geologic feature different than someone else. It must be taken into account that the interpretation of succession boundaries and sands can be slightly different between different authors. With the model being low resolution and data reaching over several hundred meters, the lines that are drawn in Lime on the succession boundaries, can be slightly off (ca. 0.3m). To illustrate the resolution, a screenshot from Lime and the corresponding original photo are compared (figure 5.1). When a change is gradual, it is not always a clear where to mark. Altogether, a line can be ca. 0.3m off. Nonetheless, this does barely influence the average succession thickness, since adding 0.3m to one succession, implies subtracting 0.3m from the succession above or below. The average does not change. However, this does not hold near the edges and there where successions are missing.

Secondly, the GPS data of the panels have been found to be inaccurate. The exact same point in two different panels has different coordinates. This is already the case in Agisoft before converting any coordinates and is therefore embedded in the data. Since it is mainly the height (Z-location) that is off, it is assumed that the errors are caused by an inaccurate GPS in the drone. Within the panels, internal consistency is assumed. Despite, it cannot be proved that there are no errors internally due to the faulty GPS data. It is recommended to take separate GPS coordinates on a separate GPS device of locations on different positions in the panels.

(a) An example from panel 18, to illustrate the resolution.

(b) The actual photo as comparison

Figure 5.1: A comparison of the resolution of the panels in Lime versus the original photo. In both subfigures, the same location is shown. Note the loss of detail in the photopanel, compared to the original photo.

5.1.2. The methodology

The methodology used in this thesis is very time intensive: interpretation of the panels has to be done by hand. Automatizing such a process would enlarge the possibilities. At the moment, there is no suitable software known that is able to do this. Also, geological knowledge is needed for the interpretation, for both the successions and the sandstones. This requires more than distinguishing between colors. An example is debris from sandstones that has fallen down. Software should be able to recognize it as irrelevant for the interpretation, but based on characteristics such as color, it will give the wrong classification. Thus, automatizing the process is difficult. Not only the methodology is time intensive, but the interpretation software Lime has great difficulties in handling the photopanels. Loading a single photopanel can take up to 20 minutes. One option is to split a photopanel in smaller pieces, however, this makes correlation more difficult. It is recommended to use a computer with high memory, preferably 32GB or higher.

In the results, it has already been mentioned that the modelling results are unsatisfying and the interpretation of the results is based on the direct results from Lime. The direct results have as an advantage that the results are a relatively good approximation of the reality, only limited by the photogrammetry and GPS errors. The modelled results are very different in that sense. The model is again an approximation of those direct interpretations in Lime; also subject to limitations of the modelling (e.g. edge effects and smoothing). A summary of the advantages and disadvantages of both methods:

Direct measurements

- [+] Honors data
- [-] Data is lost, since only sample measurements are taken
- [-] Manual work; takes a lot of time

Modelling

- [+] All data available is used
- [+] Interpolation and extrapolation is possible
- [-] Modelling takes a lot of computer power and time
- [-] Does not always honor data
- [-] Bases interpolation and extrapolation on statistics, not on geology
- [-] Has edge effects, influencing the average thickness
- [-] Setting up the model takes a lot of unnecessary manual work

Results show that the modelling in Gocad is only accurate when there is relative large amount of data compared to the size of the model. When there are large gaps in the model, such as when all sets of panels are combined into one model, results are unrealistic (figure 4.6). The two do not provide a similar thickness curve. Also, there are successions present of which the maximum thickness in the model is smaller than the

minimum thickness from the direct measurements, and vice versa. Furthermore, the standard deviation is significantly lower than with the direct results. There are three exceptions where the standard deviation of the model exceeds the direct standard deviation. At the base, the large standard deviation of the model is caused by edge effects of the model, not by the data. Near the middle section and at the top, the amount of data and number of datapoints in the direct results is very limited.

For smaller amounts of data, such as a single set of panels, it provides a moderately accurate model (figure 4.7). Most average thicknesses in Gocad do compare to the average thickness measured directly. There are only a few which differ more than a meter. However, the standard deviation of the modelled results is significantly lower than the standard deviation of the direct measurements.

The model deviates from the direct measurements for a few reasons. First of all, the model has edge effects. This means that a few of the lower layers have layer thicknesses of 0m in their distribution. This causes a decrease in the average layer thickness resulting from the model. Furthermore, it is not able to present the same variances as in the interpretation; results are smoothed in the interpolation and extrapolation. This is an issue, regardless of the settings chosen (as shown in the sensitivity analysis). The thicknesses are largely comparable, but judging by the model, not an extreme good fit of the data. For a geologist, the direct measurements seem more reliable. Furthermore, the added value of being able to extrapolate is lost, since standard deviations do not compare. Lastly, the modelling does only work sufficiently when split up into multiple smaller sections. Because of these limitations, it is recommended to evaluate different software and possibly another modelling method. I.e., instead of making a stratigraphic model, a process based model can be evaluated. This also enables the modelling of the sandstones, such that a better insight on their behavior can be gained.

The final results are biased by the inter- and extrapolation and do not honor the data, therefore it is concluded that the direct measurements from Lime are the most reliable. However, it does not mean that the modelling step has been completely useless. For correlation, mainly within the sets, Gocad is very useful. Lime is not able to import lines from other panels, so Gocad can be used to present multiple panels within a single screen. Since all panels and lines are referenced in GPS coordinates, it can be checked whether the same succession boundaries are interpreted in the overlapping panels. Despite, this cannot easily be used when correlating between the sets of panels, because distances are too large to visually correlate exactly which succession boundaries belong together. However, it does give a good indication, providing a rough estimate.

5.2. The floodplain successions

The results of this thesis show an average succession thickness of 6.9m, with a standard deviation of 1.3m. One must take the uncertainties that are attached to these numbers into account. First of all, two color transitions can follow each other closely (figure 4.2), making it difficult to determine which one to pick. This can be caused by autogenic processes of the sedimentary system. An allogenic cycle in which heterolitics are formed can start, but if the channel due to (small scale) avulsion still shifts somewhere else, again more overbank deposits are deposited, causing the second overbank deposit phase not far from the first one. All in all, it adds to the uncertainty.

Secondly, correlation is difficult, regardless of the panel. Within the sets of the panels, the correlation is of fairly good result. Overlap between the panels and the proximity enable reliable correlation. It is therefore recommended to always include sufficient overlap when photographing the outcrops. Correlation between the sets of panels are even more difficult. Would a mistake in correlation change the results a lot? The average thickness of all measurements individually, is 6.8m. So the sorting into successions only changes this to 6.9m. It is unlikely that a slightly different correlation is going to change the average thickness much. Furthermore, it is shown that the weighted average is almost similar to the non-weighted average. The ranges would be slightly smaller. However, even within a set of panels (in which the correlation is more reliable), there is already a large variation and range of thicknesses measured. Results would therefore not change a lot.

The lateral extensiveness of the data varies per floodplain succession. The largest distance along which a succession is present in the data, is 3.0km parallel to the paleoflow direction and 2.8km perpendicular to

the paleoflow direction, obtained from different locations. These numbers do not refer to the maximum uninterrupted floodplain width along which an individual succession is measured, since data from different locations is added up. If a data bounding box would be used, it would be 3km parallel to the paleoflow direction and 2km parallel to the paleoflow direction. The floodplains do often exceed a width of 20km (Bown and Kraus, 1987). This means that the panels only cover a small part of the total floodplain width.

The relation of the range, standard deviation and average thickness versus the distance along which the data was obtained is essential. The relation between the range (maximum thickness of the succession - minimum thickness of the succession) of each succession and the distance along which that succession has been measured shows that the range becomes larger the longer the distance along which it has been measured (figure 4.10). The same relation is seen when comparing the standard deviation and distance along which the succession has been measured (figure 4.11). This suggests that lateral information is essential when evaluating thickness differences. The relation between the average thickness of a succession and the distance along it was measured, confirms this claim (figure 4.12). When the floodplain distance is small, the average thicknesses of the successions vary a lot. Those successions which have been measured over longer floodplain distances, converge towards the average of 6.9m (though it must be noted that the amount of data with longer floodplain distances is less). This also builds to the hypothesis that thickness differences are only local and therefore also compensated locally (compensational stacking). These plots can also be used to determine what distance a succession must be measured to be classified as laterally consistent. Judging by figure 4.12, around 1250m parallel and perpendicular to the paleoflow direction, the average thicknesses stay close to the average of 6.9m. The amount of data is perhaps too limited to draw unambiguous conclusions, but it is a first indication of how laterally consistent must be defined in this area. The graphs comparing the floodplain distance along which the succession was measured to the statistics all show that there is not a significant difference between the relations when comparing parallel distance and perpendicular distance to each other.

The histogram of the average thickness (figure 4.14) shows a distribution which is far off of a Gaussian distribution. Their frequencies are also limited, often only 1 succession, at most 5 successions. This implies that there is not enough data available.

The results show that thickness differences between successions are not compensated when considering the averages (figure 4.15). However, it has been found that 4 out of the 5 thinnest layers are on top of a purple soil. The purples are formed due to oxidation and in less hydrated conditions than the red soils (Kraus and Gwinn, 1997). A possible explanation is that those purple soils are formed on paleo-highs, which receive less deposition in the following succession; causing a thinner succession on top of the purple soils. It has also been evaluated whether the thickness differences are compensated locally. The analysis shows that in some cases locally a thin succession is followed by a thick succession and vice versa, but this is certainly not always the case. Succession 4 in panel 17 is thin and followed by another thin succession, but the one on top being a major sandstone. Possibly, the two thin layers created a stratigraphic low and for that reason the channel avulsed to that location. Succession 8 is thick in panel 16 and partly compensated by the successions below and above (figure 4.16). The succession which is above that (succession 10) is not present in that section of panel 16 and can therefore not added to the analysis. The same holds for the comparison of succession 12 in panel 4, only one succession above is measurable in that section (figure 4.17). In all sections evaluated, the thickness compensation is never fully done within the next succession. The amount of data which could be quantified is way to less to accurately describe what is observed: locally thick or thin successions are (at least partly) compensated by thickness compensation (compensational stacking), but this is not fully done by the successions on top or below. It can take multiple successions.

In the 'What-If' analysis, multiple variants of determining the succession thickness have been evaluated. In case of only including the laterally extensive successions, i.e. succession 7 to 11, the question arises whether the results in this subset are any different from what has been found in the model as a whole. This is a relevant question, since this area holds the most lateral information, which is relevant for the research question. The results show a slightly smaller average thickness (6.7m). The standard deviation between the average succession thicknesses is only 0.6m, compared to 1.3m when all successions are taken into account. On the other hand, the average standard deviation of an individual successions is 1.4m in the subset, higher than 1.1m when all successions are used. For determining lateral variability, the 1.4m is a more relevant number,

since in the full section also successions with only a few measurements are present (because they are only found in one or a few panels). So, stratigraphically the thicknesses have a smaller standard deviation, while an individual successions has a higher thickness standard deviation when using the subset. Combining the two, it gives the idea that the stratigraphic thickness differences are mainly caused by lateral variations. I.e., the laterally large variations are compensated stratigraphically; so where a layer is locally thin, the successions on top are locally thicker and vice versa. The fact that this subset shows that the lateral standard deviation of individual successions is higher than the stratigraphic standard deviation between multiple successions, also implies that the histogram of all measurements (figure 4.14) is more representative than the histogram of the average thickness measurements (figure 4.13).

The weighted average (6.8m) of the succession thickness is barely different from the un-weighted average of 6.9m. A weighted average is used when not all values have an equal probability to be measured, which is not relevant in this situation. Furthermore, there is no significant difference, so there is also no added value in using the weighted average.

The distinctiveness of the successions has been determined in a qualitative way. There are differences in lighting conditions over the panels, making comparison between distinctiveness in two panels not completely unambiguous. But even when accounting for this, there are differences. This is something that can already be seen in a single photopanel, that a succession boundary can be distinct in one place and less distinct a few hundred meters further. This shows that there is not only a variation in thickness, but also in distinctiveness. Such lateral variation could be caused by e.g. by the distance from the corresponding channel (Bown and Kraus, 1987 or by differences in topography during deposition. When determining which succession boundaries are distinct and which are not, a color index would be preferential; it makes the interpretation unambiguous. Analyzing the colors with software, per individual panel such that relative color differences can be used, could give a possibility to improve. If the lighting conditions become comparable, an independent scale should be used to which the colors are compared. Therefore it is also recommended to photograph the outcrops in similar weather conditions, for as far as that is possible.

For the successions, Abels et al., 2013 is the most comparable research. Performed in the Dear Creek Amphitheater, it is ca. 1.5km north of panel 13, but in the same formation and the same age. It found the successions to be on average 7.1m thick, well within the standard deviation of this thesis. The 6.9m found in this thesis is well within the standard deviation (1.9m) of Abels et al., 2013. However, there are some differences. Abels et al., 2013 bases his results on logs made in the field after digging trenches. On the one hand, this means reliable results, since properties as grainsize and fresh color are known, whereas this thesis has only distant photos where interpretation is based on visibility only. On the other hand, this thesis is much more abundant in data, it covers a larger area (both lateral as stratigraphic) and lateral variability can be much better evaluated. Despite these differences, the average succession thickness is comparable. One would expect that the thickness measured is larger in this thesis, for two reasons: 1. When digging trenches in the field, one often chooses the places where it is easiest to dig. This means digging where there are no sands. And it are the sands that make the successions thicker. When observing from photopanels, one is not biased to choose the easiest sections and therefore one would expect thicker successions. 2. Local events are not included in this thesis. Lateral continuity is vital. But if only a few logs have been made, the lateral element is missing. Therefore, it can be that an event occurs only local, but cannot be interpreted as such. In this thesis, the event is cut out. As a result, it would be expected that the average thickness is thicker. However, this is not supported by the results. The key to why this expectation does not apply, might lay in the lateral component. Abels et al., 2013 finds a pattern which could be related to the presence of 100kyr cyclicity of eccentricity. The sets which are identified in the distinctiveness analysis are similar to what Abels et al., 2013 describes. For Abels et al., 2013 the identification was much easier, his methodology made it easier to determine which successions are distinct and at the same time lacked the lateral variability.

The correlation with Abels et al., 2013 is possible for succession B to O. Succession A and P have not been correlated. As Abels et al., 2013 describes, these are two of the less distinct successions. Furhtermore, there are some uncertainties regarding the correlation. Abels et al., 2013 has reviewed the successions in much larger detail from up close. He finds much more purple soils than that can be seen in photopanel 13. One option would be that succession F as described by Abels et al., 2013 is in fact a combination of two successions; his results do provide a possibility to that. In that case the top section of the correlation would change and shift

one succession up. The average succession thickness in Abels et al., 2013 would then decrease to 6.7m.

Abels et al., 2016 describes hyperthermals in the Willwood Formation in the Bighorn Basin of which the Eocene Thermal Maximum 2 (ETM-2, also known as ELMO), and H2 are also present in the panels used in this thesis; the research areas are partly overlapping. Abels et al., 2016 uses a carbon-isotope approach which requires fieldwork, this thesis has only surface data (photos). There is a ca. 34m cyclicity for the ETM2-I2 interval, which corresponds with a ca. 96kyr cyclicity; very close to the 100kyr eccentricity scale. For the couples (ETM2-H2 and I1-I2), a scale of ca. 405kyr is found, which relates to the eccentricity maximum scales. By showing the presence of these climate driven thermal events, Abels et al., 2016 proves that such events can be found back in fluvial sediments. Furthermore, it builds to the case that the fluvial deposition has been influenced by orbital climate forcing. In this thesis, the 100kyr cyclicity of eccentricity has not been clearly found. Indications are found for the 400kyr cyclicity being present, on a scale that can be considered similarly to Abels et al., 2016.

The sedimentation rate that is found in Abels et al., 2016 is ca. 0.35m/kyr, Abels et al., 2013 finds a geometric mean sedimentation rate of 0.33/kyr based on literature, while Chew and Oheim, 2013 finds ca. 0.439m/kyr. The sedimentation rate of Abels et al., 2013 is used. The reason why it might be a better fit than Chew and Oheim, 2013, is that the by Chew and Oheim evaluated area is more north and a different stratigraphic interval, while the ones from Abels et al., 2013 are based on multiple literature values which are based on nearby areas. Also, the methodology is different. Chew and Oheim, 2013 is fossil-based, Abels et al., 2013 is literature based, while Abels et al., 2016 is based on succession thickness combined with precession. The latter is thus based on the assumption that precession cyclicity is present in the deposits, so it is not a clean number for testing whether precession cyclicity is present in the results from this thesis. Since it is based on multiple literature values from the same area, the fit with the sedimentation rate from Abels et al., 2013 is expected and likely to be realistic. Important to consider is that the sedimentation rates hold for the amount of sediment after compaction. In all described literature, as well as in this thesis, the sedimentation rate is based on the stratigraphy after compaction. This is not the same to the sedimentation rate during deposition and can be influenced by differences in compaction. It is therefore advised to only compare sedimentation rates of the same/nearby areas.

Westerholt et al., 2018 has used core data from the Bighorn Basin. A bandpass filter of 7 meter with a bandwidth of 30% is used. Results from this thesis have shown that this bandwidth is too small. The minimum height of a succession measured is 3.48m and the maximum height of a succession is 12.44m. The bandpass filter of Westerholt et al., 2018 would miss these and is therefore insufficient. Furthermore, Westerholt et al. claims a correlation with Abels et al., 2013. However, this correlation is not actually substantiated; the successions are just pasted on his bandpass results without actual checking if it correlates in reality. Despite, the results could still be correct. Lastly, Westerholt et al., 2018 claims that cyclostratigraphy is straightforward. If there has been one thing that this thesis has shown, it is that cyclostratigrahpy is not straightforward and correlation is very difficult.

Abdul Aziz et al., 2008 has evaluated the nearby Polecat Bench (15km north of the McCullough Peaks) and Red Butte (70km south-east of the McCullough Peaks). The cycle thickness of ca. 8m recorded is thicker than found in this thesis, though still within the standard deviation. The Polecat Bench is 2 Myr older (Abdul Aziz et al., 2008); sedimentation rates could also have been different, explaining the thickness difference. Similarly as to Westerholt et al., 2018, the bandpass filter used is insufficient. The smallest measurements from this thesis would be missed by this bandpass filter, this might be an explanation why the average thickness by Abdul Aziz et al., 2008 is higher. Furthermore, he identifies ca. 3m cycles for individual paleosols, a cyclicity which is not observed in this thesis. The amount of data evaluated is far less, only 7.5 cycles.

A difference compared to all literature, is that others make use of more data than just a visual interpretation. Digging, logging and carbon-isotopes are used to determine the succession boundaries. It cannot be ruled out that the interpretation of the successions is slightly different, explaining the differences in thickness. This thesis does not only differ in size of the area evaluated, but also in method: based on photos only. Furthermore, this thesis is unbiased; the entire area available is evaluated, also on the locations things are difficult to see or are less of a 'textbook example', while for fieldwork one tends to go to the most optimal locations.

The outcome of this thesis is also compared with the preliminary results of the PhD-thesis of Youwei Wang (Delft University of Technology). He constructed a numerical model of the sediment build-up of a river system with cyclicity in sediment supply and water discharge. They confirm the cyclicity in deposition of sediments and the presence of a stable phase and a heavy depositional phase, as long as the two parameters are not in phase. This is also in line with the depositional model of Abels et al., 2013 and the findings in this thesis.

To conclude, the results fit well within literature. Furthermore, with the result of this thesis a strong case has been built, due to the large amounts of data. The size and dimensions of the area evaluated is larger than what has previously been done. Furthermore, the fact that the average succession thickness is close to what is found in literature, means a larger reliability of the new insights obtained by this thesis.

5.3. The sandstones

The sandstones form an essential part of the stratigraphy. Regarding the major sandstones, the amount of data is limited. Only 13 major sandstone bodies could be measured from base to top. For the single story thickness, there are only 8 data entries. More data is necessary. The sandstones are subject to the same limitations as the successions; the resolution of the panels is limited and their outline is determined by the geological interpretation. One of the observations of the major sandstone bodies is that often the top is not present, since the major sandstones are at the top of the outcrop and have partly been eroded. This is not unexpected, since sandstones are the toughest, hardest to erode lithology in the outcrop and therefore prone to form the top.

A research focusing on the sands in the Willwood Formation is Foreman, 2014. Apart from his paper in 2014, he recently also performed fieldwork leading to relevant results, as obtained in personal communications with H.A. Abels (2018). Near the McCullough Peaks, Foreman finds an average sandbody thickness of 8.6m, with a standard deviation of 3.4m, based on 48 measurements. Near Sand Coulee, Foreman finds an average sandbody thickness of 10.8m with a standard deviation of 6.7m, based on 34 measurements. These average thicknesses are smaller than what has been found in this thesis; 14.0m. First of all, near the McCullough Peaks the lowest value measured is 4.0m and near Sand Coulee the lowest value measured is 4.3m. These values fall below the cut-off used in this thesis and would be classified as minor sandstones. This partly explains why the results from Foreman show a lower thickness. One should also take into account that, as described in this thesis, major sandstones are sometimes multistory. When comparing the single story thickness as found in this thesis, 9.6m, results correlate better.

Owen et al., 2017 obtained results from both the Willwood Formation and the older Fort Union Formation. A distinction is made between 5 different channel body geometries (massive, semi-amalgamated, internally amalgamated, offset stacked channel body and isolated channel body geometry) and 2 floodplain sandstone geometries (floodplain sheets and floodplain ribbons); in this thesis there is only a distinction between 'minor' and 'major'. Roughly, the floodplain sandstone geometries correspond with the minor sandstones and the channel body geometries correspond with the major sandstones. The ribbon floodplain sandstone thickness is on average 1.2m with a maximum of 3.4m; sandstone sheets do not exceed 2m thickness (Owen et al., 2017). The minor sandstones in this thesis exceed these maximum thicknesses significantly. Therefore it is likely that what Owen et al., 2017 defines as channel body geometry is in some cases classified as minor sandstone in this thesis. The channel body thicknesses as defined by Owen et al., 2017 range from 1.7m to 47.5m. The average thickness found in this thesis, for the major sandstones, is 14.0 meter. What is classified as a major sandstone in this thesis, is likely to be a mix of all five geometries described by Owen et al., 2017, as well as some of the thinner channel bodies being defined as minor sandstones in this thesis. The massive channel body geometry of Owen et al., 2017 is defined as massive and lacking story surfaces; the minimum lateral extent measured is 1.5km. These are not seen in the major sandstones measured in this thesis; all major sandstones do show story surfaces to some amount and the lateral extent is often below the described scale. However, they do seem to be present near the top of the panels, where they have been partly eroded. Semi-amalgamated channel bodies, internally amalgamated channel bodies and isolated channel bodies are seen in this thesis. Owen et al., 2017 describes the first as channel deposits with up to 50% contact with the floodplain and the rest with other channel deposits; the second as laterally extensive, having a simple

geometry and the latter as single story channel bodies. It is possible that the other types are also present in the area evaluated. The average thickness found by Owen et al., 2017 is 7.5m for semi amalgamated bodies, 11.0m for internally amalgamated and 4.2m for isolated bodies. Though the ranges are very large, the average thickness of all classes is significantly smaller than what is found in this thesis. The average thickness of isolated bodies would be defined as a minor sandstone in this thesis, so many of the lower measurements would be excluded. Therefore, it is not a fair comparison. Furthermore, it is possible that the other classes defined by Owen et al., 2017 are also present. However, since the number of major sandstones measured in this thesis is relatively low (13 compared to 184 by Owen et al., 2017), the data is insufficient to draw any conclusions on thickness differences.

Kraus and Gwinn, 1997 proposed a model with ribbon sandstones and sheet sandstones. The distinction between the two is very similar to the division observed in this thesis; minor and major sandstones. Kraus and Gwinn, 1997 suggest thicknesses larger than a succession to larger than multiple successions, which also fit to the results of this thesis. Though it must be taken into account that for this thesis, the thickness of the sandstone versus the thickness of the successions is partly inherited by the definition of major sandstone; it already excludes most sandstones thinner than the successions. The minor sandstones show slightly different results than the ribbon sandstones by Kraus and Gwinn, 1997. This thesis show the minor sandstones to always be in the heterolitics, with an exception of eroding into the paleosol beneath and a few sheet-like deposits, whereas Kraus and Gwinn, 1997 also show them in the paleosols (though they are dominantly in the heterolitics).

Neasham and Vondra, 1972 show a thickness of channel deposits in the Willwood Formation to be up to 100ft (ca 33m). This thesis found a maximum sandbody thickness of 22.9m. It is well within the range of Neasham and Vondra, but there is still a large gap between the two. Neasham and Vondra, 1972 evaluates a section in the central Bighorn Basin, almost 50km to the south-east from this thesis' area. Despite the distance, the results from Neasham and Vondra, 1972 suggests that even thicker sandstone bodies are present in the area.

The outcome of this thesis is also compared with the preliminary results of the PhD-thesis of Youwei Wang (Delft University of Technology). His results show a similar set of sandstones: minor sandstones and major stones. Major sandstones have a maximum thickness of ca. 10m; before diagenesis (compaction). The decompaction ratio for sandstones of 10m initial thickness is 1.2 at a burial depth of 1km, up to 1.7 at a burial depth at 8km (Perrier and Quiblier, 1974). Therefore, after compaction the thickness is expected to be only one or a few meters smaller. This is significantly smaller than thickness of the major sandstones found in this thesis. However, they are all single story channels, while in this thesis most of the major sandstones are multi-level sandstones. If a major sandstone in the model would erode into a major sandstone below, also a multi-level sandstone would be formed. With that being the case, thicknesses would become comparable.

All in all, comparing the sandstones to literature is difficult, due to the differences in interpretation and definition of the sandstone bodies. Results from this thesis fall within the (large) range of what is shown in literature, but the average thickness is not an immediate match.

5.4. Synthetic sedimentary model

5.4.1. Astronomical cycles in practice

The floodplain successions show cyclicity. Thicknesses stay mostly within the same range and also visually, the successions are cyclic. Nevertheless, not all successions have a similar thickness; the range is still quite large. There are two possibilities. First of all, they can be caused by the astronomical cycles as well. As discussed before, apart from precession, they include obliquity and eccentricity. Eccentricity has a large influence on precession and can therefore be a cause of differences in precession cycles. Precession can be exert a strong effect or a weak effect, which largely corresponds with the eccentricity cycle. Secondly, the difference in thickness of the successions can be caused by autogenic controls, i.e. river dynamics.

Astronomical cycles

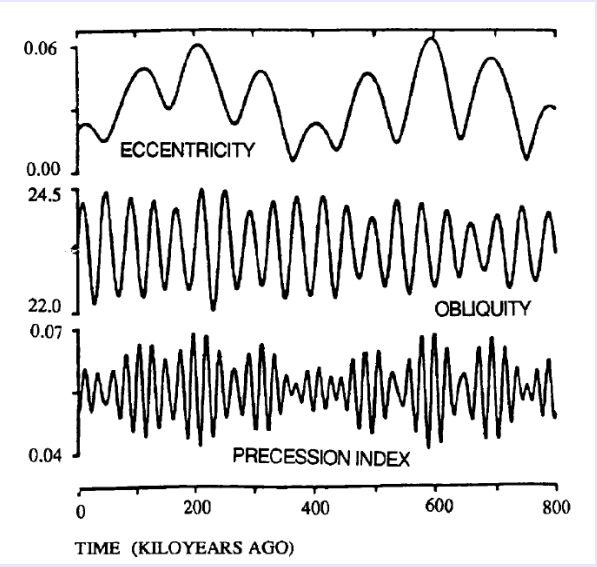

The insolation cyclicity of the astronomical cycles (Milankovitch Cycles) (Fischer and Bottjer, 1991).

Milankovitch proposed three astronomical cycles that influence the climate on earth.

- Precession - The earth not rotating along its axis perfectly (wobbling).
- Obliquity - The earth's axis not always having the same angle.
- Eccentricity - The earth's orbit around the sun differing in shape (circular to ellipse shape).

All three influence the climate on earth, since the amount and/or distribution of solar radiation on earth changes (Zachos et al., 2001). They are so usable in this research, because of their predictable cycles. Precession has a period of ca. each 20 kyr, obliquity ca. 40 kyr and eccentricity of ca. 100 kyr (Zachos et al., 2001, Merlis et al., 2013, Deitrick et al., 2018). Obliquity has mainly influence around the poles, so it is less relevant in this research. Eccentricity is on a large scale, but can also be found back due to its influence on precession. An eccentricity high increases the range of precession, an eccentricity low deafens the contrast in precession.

Precession
If precession is the control behind the succession cyclicity, the cyclicity should be around 20kyr (Merlis et al., 2013; Deitrick et al., 2018). The sedimentation rate as described in Abels et al., 2013 is ca. 0.33m/kyr. With the average succession thickness of 6.9m, this implies an average cycle duration of 20.9kyr, which is very close to the precession cycle duration. When the sedimentation rate of Abels et al., 2016 is used (0.35m/kyr), an average cycle duration of 19.7kyr is found.

The standard deviation of the average thickness measurements is 1.3m, however, when only successions 7 to 11 are taken into account (which cover laterally the largest area), it reduces to 0.4m. It must be taken into account that this new standard deviation is based on only 5 successions. With only 5 cycles, not the full scale of variability caused by orbital climate forcing can be captured. It is therefore in line with expectations that the standard deviation is lower.

Eccentricity
For further determining the influence of orbital climate forcing, it is evaluated whether eccentricity is seen as well. Eccentricity has two cyclicities, a cyclicity at 100kyr scale and another cyclicity at 400kyr scale (Zachos et al., 2001). Precession events are grouped in eccentricity on the 100kyr timescale in bundles of 3 to 6 (Berger

et al., 1992). Similarly, these bundles are bundled in itself on the 400kyr timescale in bundles of 3.5 to 5 (Berger et al., 1992). Therefore, to compare the results from this thesis to eccentricity, an effect every 3 to 6 successions should be visible to prove 100kyr eccentricity. For the 400kyr timescale, an effect every 3.5 to 5 times larger should be visible, i.e. ca. every 15 to 25 successions. This corresponds with the amount one would expect based on a simple calculations; a cyclicity of every ca. 20kyr within a cyclicity of every 100kyr and 400kyr. As shown in Abels et al., 2013, the pattern found could be related to the eccentricity 100kyr scale. The pattern being a few distinct successions, followed by one or two less distinct successions. A pattern similar to the description by Berger et al., 1992. This distinctness is based on lithology and color records. In this thesis there are distinct successions and less distinct successions, based on color only (figure 4.20). However, a clear pattern as in Abels et al., 2013 has not been found. More data is needed, such that the local variations do not take up such a large part of the data. It will then be easier to determine an overall distinctiveness for each successions. Based on the results it is determined that the presence of 100kyr cyclicity is possible, but cannot be confirmed.

Regarding the 400kyr cyclicity, it must be determined if that is even possible to be visible in the successions. There are likely to be ca. 35 successions in total in the photopanels evaluated by this thesis (if the unmeasured intervals in the middle of the section are considered as well), of which 28 have thickness measurements. 35 successions, which have just been related to precession, i.e. 35 precession cycles. With a precession cycle duration of 20kyr, this would mean that there is already for 700kyr of data. The base of the panels was not chosen arbitrary when photographing in the field. It was started above an interval with large sandstones, where the distinctive paleosols were hardly observable. It could be that there is an eccentricity low on the 400kyr cycle on that stratigraphic height. In the middle of the section that this thesis evaluates (successions 15-17), there are also large sandstones present and the succession boundaries have barely been observed. This implies that there is another eccentricity low on the 400kyr cycle, which also fits with the timing. This would also suggest that the next eccentricity low on the 400kyr scale is at the top of the section, just outside the range that this thesis evaluates. Hopman, 2013 does evaluate that section in his MSc Thesis and shows those successions to be more sandy and to have less paleosol development than average, backing up to the suggestion. This implies a pattern similar to the 400kyr cyclicity of eccentricity.

5.4.2. Depositional model

What has become clear from the thickness data, is that the floodplain successions are not of constant thickness. They are laterally continuous, but thickness and color intensity can change with several meters over a distance of a few hundred meters to several kilometers.

The depositional model as proposed by Abels et al., 2013 (figure 1.1) forms also the basis for this thesis. The hypothesis, which is partly based on this model, can be confirmed: a pattern similar to the astronomical cycles are (partly) recognizable in the successsions. The depositional model seems in line with the results, the results do not indicate that anything should be changed about this model. However, the results do add to the model. More is known about the lateral variability, which can be included. The depositional model shows a rather perfect cyclicity, where consequently mainly allogenic controls are dominant. Lateral variability of individual successions (on average a standard deviation of 1.1m) is a measure of events during a cycle and therefore of autogenic controls. Ranges go up to 8.0m, meaning that autogenic controls should get a place in the depositional model as well. This means that more attention should be given to local events and variabilities.

One of the observations of the major sands, that sometimes a distinct soil is present at the top which is not lateral continuous, can also be explained by the depositional model. The channel being a topographic high, it sees less sedimentation for a significant amount of time. When conditions are good, a soil can develop well on top, since it is not buried rapidly by fresh sediment. This can also explain the observation that multiple major sands are formed on top each other. If the amount of sediment deposition on the location of the paleochannel is so low, it can become a topographic low again. Therefore, it would be prone to be the next location of a new channel. If this is the case, one would expect the succession on top of the lowest major sand to be thin. As has been shown in Chapter 4, this is not necessarily the case.

The minor sandstones being in the heterolitics correspond with the hypothesis. During the heterolitics phase,

the river is very unstable with a lot of avulsions. This means that the channels often do not get the chance to grow and build up. The result is smaller sandstone bodies. During the subsequent overbank phase, the river is stable again. Most of the minor channels have been abandoned again, so there is no longer sedimentation. Soils develop on top of these minor sandstones. This is exactly as is seen in the results, the minor sandstones stay within the heterolitics. Furthermore, there can be numerous minor sandstone bodies within an individual heterolitics layer. Some thin, sheet-like sandstone deposits can be present in the overbank deposits and are an exception. They are interpreted as crevasse splays. These can occur even within a phase of relative channel stability and thus be in the overbank facies, without compromising the depositional model.

One of those minor sandstone channels of avulsion, will be the new path of the main channel, being stable in the overbank phase. This then builds up to become a major sandstone. Regarding the major sandstones, the hypothesis is repeated and illustrated.

Hypothesis - sandstone deposition

The hypothesis regarding the sandstone deposition can be summarized as: The base of a major sandstone is somewhere halfway in the heterolitics phase. It is then stays stable during the overbank phase. In the next heterolitics phase, the river avulses and there is not a lot of new sedimentation. However, the channel was topographically higher than the floodplain during the overbank phase, due to its levees and bars. Therefore, one would expect that the sand is slightly higher than the end of the overbank phase, approximately halfway up the heterolitics phase. All in all, the total thickness of the major sandstone is half a heterolitics phase, a full overbank phase and half a heterolitics phase; i.e. ca. the full thickness of a single succession (figure 5.2). When the channels erodes down, it might even exceed the thickness of a single succession.

This hypothesis cannot be confirmed based on the data. There is simply not sufficient data on the major sandstones available. Furthermore, based on these photopanels it cannot be determined where the top and the base of the major sandstone are, with respect to the floodplain successions. At this moment, the base of the major sandstone body is defined as the color transition from overbank deposits to heterolitics. Therefore, due to this measurement methodology, its stratigraphic position is predefined. According to the depositional model, there is an initial phase in which the channel has a high avulsion frequency, before the channel stabilizes. This initial phase cannot be distinguished from the latter main channel, based on the current methodology and definition. The hypothesis can therefore not be properly tested. This also implies that, if the hypothesized depositional model is correct, the major sandstone bodies are in fact thinner than measured. The lower section with heterolitics should be subtracted. This also means that the average thickness of the major sandstones would come closer to the hypothesized thickness (so similar to the succession thickness). A better, more accurate definition of top and base of the sandstone are necessary. Interpreting the boundary between the top of the heterolitics and base of the overbank deposits could help with better distinguishing the two and is therefore recommended. Another reason why the found major sandstone thickness of 14.0m exceeds the hypothesis of a thickness close to the succession thickness, is that if a channel avulses towards a topographic low, it has a relatively larger accommodation space. This additional accommodation space can result in larger sediment stacking and therefore thicker sandstones.

The hypothesized depositional model is strengthened by the minor sandstones. They have been observed to be in the heterolitics facies. Since they do not progradate into the overbank deposits on top, a depositional model with high avulsion frequency fits. The minor sandstones can be interpreted as avulsion channels of the main channel, which did not grow out to be the new main channel in the preceding stable phase.

The depositional model does not always hold, in one of the major sandstones (1), the sandstone originates from the overbank deposits (figure 5.3). This directly contradicts the depositional model, but is seen in only 1, possibly 2 of the 13 major sandstone bodies. Furthermore, what is seen is that the channelbody is eroding downwards and barely aggradational. Most other major sandstones do have a larger aggradational component. Despite above observations, there is not enough data on the major sandstones to determine whether this is an exception (which is still possible under the depositional model), or that the hypothesized

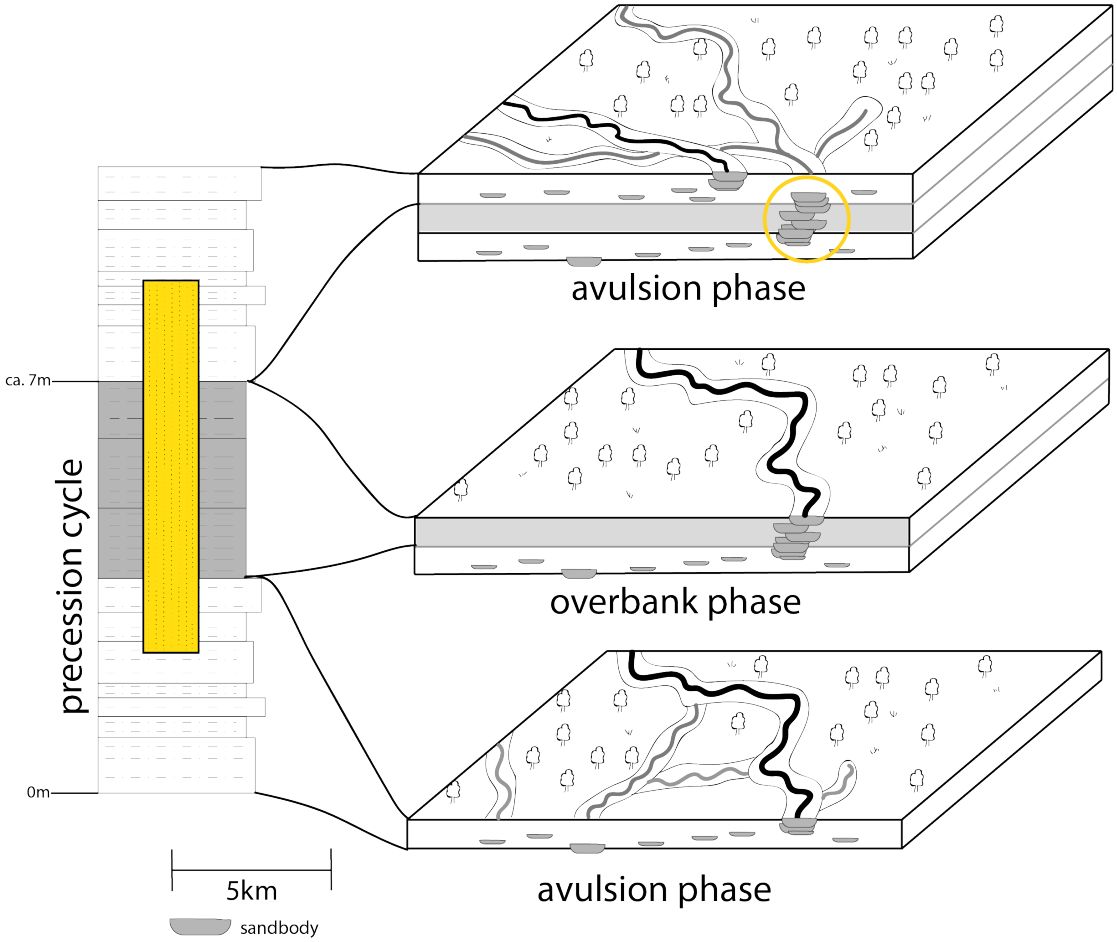

Figure 5.2: The hypothesized depositional model for the major sands. The yellow circle shows the stratigraphic position of the major sandstones. The yellow box in the stratigraphic column shows the approximate position a major sands would have. The depositional model is based on and adjusted from Abels et al., 2013.

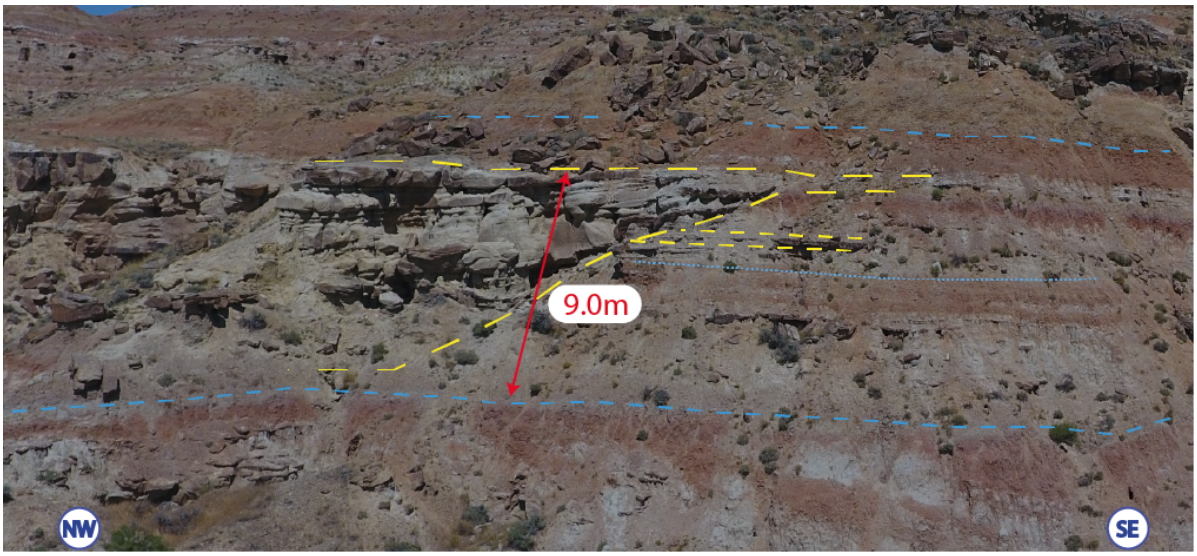

Figure 5.3: A major sandstone originating in the overbank deposits (panel 2). The succession boundaries are marked with blue dashed lines. The top and base of the major sandstone are marked with a yellow dashed line, as well as a minor sandstone. The blue dotted line in between is a possible succession boundary, however, in this interval it has not been interpreted since there is no lateral inconclusive interpretation.

depositional model should be adjusted. However, what can be said based on the results, is that a major sandstone exceeds the thickness of a single succession and most single stories are close to the average thickness of a succession. Therefore, the hypothesis regarding the major sandstones also isn't rejected; it is possible based on the results. For the minor sandstones, the hypothesis can be confirmed, they are only located within the heterolitics.

Furthermore, some sandstone bodies do provide an insight in their relation to stratigraphy (figure 5.4). The splaychannel is clearly originating in the heterolitics facies of the upper succession. It has been truncating the succession below. The original succession boundary can still be seen on the right. This observation builds to the hypothesis; the original action occurs in the heterolitics facies.

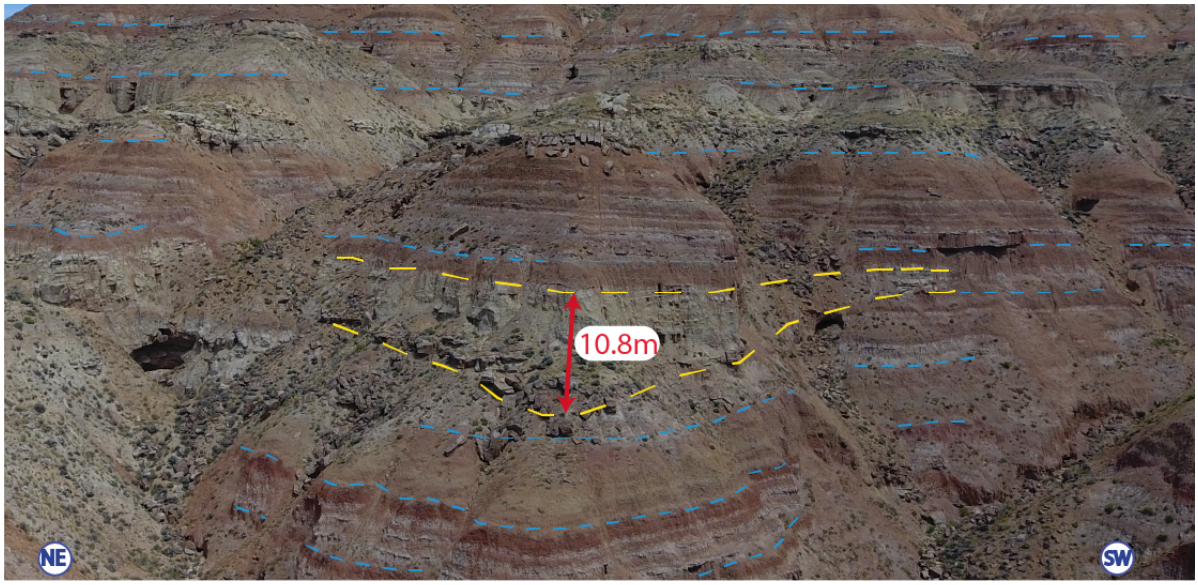

Figure 5.4: An example of a splay channel (panel 13). The succession boundaries are marked with blue dashed lines. The top and base of the splaychannel are marked with a yellow dashed line. Note that the thickness of the major SST is larger than the thickness of the splay channel (which is marked).

5.5. Impact of the results and interpretation

The results from this thesis provide a lateral understanding of the floodplain successions. Previous studies evaluated the thickness of the successions in a stratigraphic sense (vertically). This thesis shows that those thickness measurements only have limited meaning. On average, the succession thickness found in this thesis and those of e.g. Abels et al., 2013 are very similar. At which location you measure the succession thickness does not necessarily matter, as long as one has sufficient data. However, the range of the succession thicknesses also show that the individual succession thickness at only a single location (a 1D section) is not necessarily representative. One should not compare thickness differences between successions based on only measurements at a single location. Furthermore, what is sufficient data to represent succession thicknesses? How many floodplain successions are needed to get a representative average thickness from a 1D section? A simple test can be used to get a rough indication. The required sample size can be calculated as:

$$n \geq \frac{Z^2 \cdot \sigma^2}{d^2}$$

With n being the sample size, Z the reliability level based on a normal distribution, σ the standard deviation of the population and d the maximum error allowed. A reliability of 95% makes Z=1.96, the standard deviation of the population is unknown. The standard deviation based on the direct results can be used as an approximation, being 1.3m. The number of samples needed are then 7 if a maximum error of 1.0m is allowed; 26 samples are needed if a maximum error of 0.5m is used. So based on the maximum error one is willing to allow, it can be determined how many successions should be measured. Note that this method assumes a normal distribution and only an approximation of the population standard deviation is known.

However, this thesis also shows the importance of lateral information on the floodplain successions. A succession should be followed for ca. 1250m in order to obtain a lateral representative indication of the thickness of that succession. A 1D section will not give a representative thickness of individual successions.

The range of thicknesses a floodplain succession can have, can also be used for further research in the Willwood Formation. The width a bandpass filter needs to have, is now better known. Furthermore, the described results build to the depositional model, as described by Abels et al., 2013. It can also be generalized for other formations. The results from this thesis show a laterally extensive cyclicity of two facies: heterolotics and overbank deposits. They have been interpreted as a phase where the channel is instable (having a high avulsion frequency), versus a phase where the channel is stable. In other formations at other locations with fluvial origin, one would expect to find cyclicity and phases of channel stability and instability. Dimensions and ranges can be completely different, due to differences in sedimentation rate and/or diagenesis; as well as different net-to-gross ratios.

Furthermore, the sandbodies provide knowledge about the deposition and also about where sandstones (and therewith potential reservoirs) can be found. The minor sandstones have been observed to be in the heterolitics facies of the floodplain successions. They are likely to be stratigraphically isolated, since an overbank facies is on top. Whereas minor sandbodies can have reservoir properties, the overbank facies on top is likely to be a flow barrier, due to its lithology, as described in Chapter 2. Despite, the minor sandbodies are of less interest by themselves, due to the small dimensions. However, they help in the development of the depositional model. This depostional model is essential for finding the major sandstones, which are larger potential reservoirs. An insufficient amount of data is present on the major sandstones to draw indefinite conclusions. However, based on the data that is available, some predictions can be made. First of all, based on the stratigraphic position of the major sandstones, there are stratigraphic intervals which do contain a large amount of major sandstones compared to other intervals. As has been discussed before, this might be related to 400kyr cyclicity of eccentricity. Related to this, is that on multiple occasions the major sandstones are found almost on top of each other. This implies that the major sandstones can be found in vicinity of each other, which is useful information for finding potential reservoirs.

6

Conclusions

This research interprets and analyses a section of the fluvial deposits of the Willwood Formation in the Bighorn Basin (WY, USA). The formation consists of three facies: heterolitics, overbank deposits and sandstone channels. The heterolitics and overbank deposits form floodplain successions, which can be distinguished by their color; heterolitics dominantly being light brown/grey and the overbank deposits dominantly being dark brown/red/purple. In order determine the lateral and vertical persistency of the floodplain successions and how the sandstones fit in, a quantitative and qualitative analysis of the successions and sandstones has been made. On three locations, several photopanels were made in the field, which have been analyzed and interpreted in this thesis.

In total, 28 complete successions have been found in the panels. Most succession boundaries can be found in all three sets of panels, however some are only present in one or two. Approximately 700kyr of data is stored in those successions, which is a large and sufficient amount. However, lateral correlation between the sets of panels have proven to be difficult. For determining distinctiveness of the successions and to determine when a succession is laterally consistent, more data is needed. Obtaining data in between the current sets is advised. Stratigraphic modelling of the successions in Gocad, in order to obtain a stratigraphic and thickness model, does not have any added value. Evaluating alternative software is advised. The direct measurements are more reliable. They show an average thickness of a succession of 6.9m, with a standard deviation of 1.3m. The floodplain succession are laterally consistent, though one must take into account that local events are present. Variability is quite large, even on small distances, the thickness of a single succession can change up to a few meters. The average cycle thickness ranges between a minimum of 4.2m and a maximum of 9.9m. Individual measurement even exceed those extreme values. The longer the distance along which the succession has been measured, the larger the range and standard deviation. Furthermore, when the distance along which the succession has been measured exceeds ca. 1250m, the more the average succession thickness converges towards the average thickness of 6.9m. More data is needed to further specify this behavior. Results do not inconclusively show that a thinner (part of a) succession is followed by a thicker one and vice versa. This thickness compensation is likely to be spread over multiple successions. The large lateral variability within a succession do indicate that they are caused by autogenic controls and therefore a relation with the channel belt must be present.

Sandstone geometry ranges from small meter-scale features, up to large stacked channels of 10s of meters in height and hundreds of meters wide. A distinction is made between minor and major sands. In total, 13 major sandstones have been identified and measured in the panels, with an average thickness of 14.0m and standard deviation of 3.9m. More major sandstones are present on top and at the base of panels, such that they are only partly visible. Of the minor sandstones, no quantification is made. Per panel, minor sandstones can be present at a frequency of ca. 10, up to over 50 minor sandstones; such that a sufficient amount of data is available. The minor sands are present in the heterolitics of the succession. In some cases, they do erode into the underlying overbank deposits from the preceding succession. The minor sands have a variable width and often multiple are present in the same heterolitics layer. The stratigraphic position of the major sands cannot be determined based on the data, there is an insufficient amount of major sandstones which could been measured. However, mainly the single story thickness of 9.6m provides a thickness that fits with the

depositional models proposed in this thesis and in literature.

The depositional model described by Abels et al., 2013 holds under the results found in this thesis. As a result of the measurements of the successions combined with the sedimentation rate, the cycle duration is 20.9kyr, in line with precession cycle duration. Patterns are found that could be linked to 100kyr and 400kyr eccentricity cycles, however the amount of data is insufficient to confirm this. An addition to the depositional model is hypothesized, such that the position of the sandstone bodies is included. There is not sufficient data on the major sandstonebodies to accept, reject or update this hypothesized model. It is recommended to also interpret the heterolitics to overbank deposits boundary, such that a depositional model can be confirmed.

The results have shown that when the distance along which the floodplain successions are measured exceeds 1250m, average thickness converges to the average of 6.9m. The main thickness variations are therefore expected locally. Sandstone bodies with a large variation in thickness can be expected. Minor sandstones, with the exception of some sheets, can be found in the heterolitics facies. Major sandstones are often multistory, their location in relation with the floodplain cannot be accurately predicted based on the results. However, there are intervals with large amounts of major sandstones and there are intervals with fewer major sandstones, which are possibly linked to the 400kyr cyclicity of eccentricity.

With these findings, there is sufficient basis to answer the main research question:

Answer to the research question

What is the lateral and vertical persistency of externally-driven floodplain successions and how do the fluvial sandstones relate to these successions?

The floodplain successions have an average thickness of 6.9m, which is comparable to 1D analyses in other researches. Succession thicknesses range from 3.5m to 12.4m; a large lateral variation is present, indicating autogenic variability. Thickness variability has a large lateral component, ca. 1250m of floodplain distance is needed to find an accurate average thickness. The successions show a trend similar to precession, through which the allogenic component can be extracted. Minor sands are found in the heterolitics of the successions and are present abundantly. They fit the depositional model that the heterolitic deposits form in an avulsion phase; while the main channel is stable in the overbank phase. For testing the depositional model on major sandstones and their relation to the floodplain successions, more data should be gathered.

The results of this thesis show new insights into climate forcing of fluvial sediments. These insights can be used in the petroleum industry; finding and characterization of reservoirs. It can also be used for geothermal reservoirs and storage of CO_2, both need reservoirs. Finally, it is not only practical, it is also much more fundamental. It provides an insight in how climate has influence on fluvial systems.

Bibliography

[1] Abdul Aziz, H. , Hilgen, F.J. , Luijk, G.M. van , Sluijs, A. , Kraus, M.J. , Pares, J.M. , and Gingerich, P.D. . Astronomical climate control on paleosol stacking patterns in the upper Paleocene–lower Eocene Willwood Formation, Bighorn Basin, Wyoming. *The Geological Society of America*, 36:531–534, 2008.

[2] Abels, H.A. , Clyde, W.C. , Gingerich, P.D. , Hilgen, F.J. , Fricke, H.C. , Bowen, G.J. , and Lourens, L.J. . Terrestrial carbon isotope excursions and biotic change during palaeogene hyperthermals. *Nature Geoscience*, 5:326–329, 2012.

[3] Abels, H.A. , Kraus, M.J. , and Gingerich, P.D. . Precession-scale cyclicity in the fluvial lower Eocene Willwood Formation of the Bighorn Basin, Wyoming (USA). *Sedimentology*, 60:1467–1483, 2013.

[4] Abels, H.A. , Lauretano, V. , Yperen, A.E. , Hopman, T. , Zachos, J.C. , Lourens, L.J. , Gingerich, P.D. , and Bowen, G.J. . Environmental impact and magnitude of paleosol carbonate carbon isotope excursions marking five early Eocene hyperthermals in the Bighorn Basin, Wyoming. *Climate of the Past*, 12:1151–1163, 2016.

[5] Agisoft LLC, Agisoft LLC . *Agisoft PhotoScan User Manual: Professional Edition, Version 1.2*, 2016.

[6] Beerbower, J.R. . Cyclothems and cyclic depositional mechanisms in alluvial plain sedimentation. *Kansas Geological Survey*, 169:31–42, 1964.

[7] Bemis, S.P. , Micklethwaite, S. , Turner, D. , James, M.R. , Akciz, S. , Thiele, S.T. , and Ali Bangash, H. . Ground-based and UAV-Based photogrammetry: A multi-scale, highresolution mapping tool for structural geology and paleoseismology. *Journal of Structural Geology*, 69:163–178, 2014.

[8] Berger, A. , Loutre, M.F. , and Laskar, J. . Stability of the astronomical frequencies over the earth's history for paleoclimate studies. *Science*, 255:560–566, 1992.

[9] Bown, T.M. and Kraus, M.J. . Integration of channel and floodplain suites, I. Developmental sequence and lateral relations of alluvial paleosols. *Journal of Sedimentary Petrology*, 57.4:587–601, 1987.

[10] Chew, A.E. and Oheim, K.B. . Diversity and climate change in the middle-late Wasatchian Willwood Formation, central Bighorn Basin, Wyoming. *Palaeography, Palaeoclimatology Palaeoecology*, 369:67–78, 2013.

[11] Clyde, W.C. , Hamzi, W. , Finarelli, J.A. , Wing, S.L. , Schankler, D. , and Chew, A. . Basin-wide magnetostratigraphic frame work for the Bighorn Basin, Wyoming. *GSA Bulletin*, 119:848–859, 2007.

[12] Deitrick, R. , Barnes, R. , Quinn, T.R. , Armstrong, J. , Charnay, B. , and Wilhelm, C. . Exo-Milankovitch Cycles. I. Orbits and rotation states. *The Astronomical Journal*, 155:60:1–21, 2018.

[13] Fischer, A.G. and Bottjer, D.J. . Orbital forcing and sedimentary sequences. *Journal of Sedimentary Petrology*, 61:1063–1069, 1991.

[14] Foreman, B.Z. . Climate-driven generation of a fluvial sheet sandbody at the Paleocene-Eocene boundary in north-west Wyoming (USA). *Basin Research*, 26:225–241, 2014.

[15] Foreman, B.Z. and Straub, K.M. . Autogenic geomorphic processes determine the resolution and fidelity of terrestrial paleoclimate records. *Science Advances*, 3:1–11, 2017.

[16] Google Maps, Google LLC. Google Maps, 2018. URL `maps.google.com`.

[17] Gouw, M.J.P. . Alluvial architecture of fluvio-deltaic successions: a review with special reference to Holocene settings. *Netherlands Journal of Geosciences*, 86:3:211–227, 2007.

[18] Hajek, E.A. , Heller, P.A. , and Schur, E.L. . Field test of autogenic control on alluvial stratigraphy (Ferris Formation, Upper Cretaceous–Paleogene, Wyoming). *Geological Society of America*, 124:1898–1912, 2012.

[19] Hopman, T. . New constraints on Early Eocene hyperthermals; Terrestrial I1 and I2 hyperthermals solve the relation between marine and continental carbon isotope excursion magnitudes. Master's thesis, Universiteit Utrecht, The Netherlands, 2013.

[20] Kim, W. , Petter, A. , Straub, K. , and Mohrig, D. . Investigating the autogenic process response to allogenic forcing: experimental geomorphology and stratigraphy. *International association of sedimentologists*, 46:127–138, 2014.

[21] Kraus, M.J. and Gwinn, B. . Facies and facies architecture of Paleogene floodplain deposits, Willwood Formation, Bighorn Basin, Wyoming, USA. *Sedimentary Geology*, 114:33–54, 1997.

[22] Kraus, M.J. and Riggins, S. . Transient drying during the Paleocene–Eocene Thermal Maximum (PETM): Analysis of paleosols in the Bighorn Basin, Wyoming. *Palaeogeography, Palaeoclimatology, Palaeoecology*, 245:444–461, 2007.

[23] Lawton, T.F. . Chapter 12: Laramide sedimentary basins. In *Sedimentary Basins of the World*. Elsevier, Jordan Hill, Oxford, UK, 2008.

[24] Merlis, T.M. , Schneider, T. , Bordoni, S. , and Eisenman, I. . The tropical precipitation response to orbital precession. *Journal of Climate*, 26:2010–2021, 2013.

[25] Miall, A.D. . Reservoir heterogeneities in fluvial sandstones: Lessons from outcrop studies. *The American Association of Petroleum Geologists Bulletin*, 72:682–697, 1988.

[26] Neasham, J.W. and Vondra, C.F. . Stratigraphy and petrology of the Lower Eocene Willwood Formation, Bighorn Basin, Wyoming. *Geological Society of America Bulletin*, 8:2167–2180, 1972.

[27] Nicholas, A.P. , Aalto, R.E. , Sambrook Smith, G.H. , and Schwendel, A.C. . Hydrodynamic controls on alluvial ridge construction and avulsion likelihood in meandering river floodplains. *The Geological Society of America*, 46:7:639–642, 2018.

[28] Owen, A. , Ebinghaus, A. , Hartley, A.J. , Santos, M.G.M. , and Weissmann, G.S. . Multi-scale classification of fluvial architecture: An example from the Palaeocene-Eocene Bighorn Basin, Wyoming. *Sedimentology*, 64:1572–1596, 2017.

[29] Perrier, R. and Quiblier, J. . Thickness changes in sedimentary layers during compaction history; methods for quantitative evaluation. *The American Association of Petroleum Geologists Bulletin*, 58:507–520, 1974.

[30] Seeland, D. . Late Cretaceous, Paleocene and Early Eocene Paleogeography of the Bighorn Basin and Northwestern Wyoming. *Wyoming Geological Assocation*, 49:137–165, 1998.

[31] Shanley, K.W. and McCabe, P.J. . Perspectives on the sequence stratigraphy of continental strata. *AAPG Bulletin*, 78:544–568, 1994.

[32] Slingerland, R. and Smith, N.D. . River avulsions and their deposits. *Annual Review of Earth and Planetary Sciences*, 32:257–285, 2004.

[33] Smith, N.D. , Cross, T.A. , Dufficy, J.P. , and Clough, S.R. . Anatomy of an avulsion. *Sedimentology*, 36: 1–23, 1989.

[34] Stouthamer, E. and Berendsen, H.J.A. . Avulsion: The relative roles of autogenic and allogenic processes. *Sedimentary Geology*, 198:309–325, 2007.

[35] Vandenberghe, J. . Climate forcing of fluvial system development: an evolution of ideas. *Quaternary Science Reviews*, 22:2053–2060, 2003.

[36] Westerholt, T. , Rohl, U. , Wilkens, R.H. , Gingerich, P.D. , Clyde, W.C. , Wing, S.L. , Bowen, G.J. , and Kraus, M.J. . Synchronizing early Eocene deep-sea and continental records cyclostratigraphic age models for the Bighorn Basin coring project drill cores. *Climate of the Past*, 14:303–319, 2018.

[37] Willis, B.J. and Behrensmeyer, A.K. . Fluvial systems in the Siwalik Miocene and Wyoming Paleogene. *Palaeogeography, Palaeoclimatlogy, Palaeoecology*, 115:13–35, 1995.

[38] Wyoming State Geological Survey. Stratigraphic nomenclature chart of the Laramide Basins, Wyoming, 2018. URL `http://www.wsgs.wyo.gov/docs/wsgs-web-basin-stratigraphy.pdf`.

[39] Wyoming State Geological Survey. Geologic map of the Bighorn Basin, Wyoming, 2018. URL `http://www.wsgs.wyo.gov/docs/wsgs-web-bhb-geologic-map.pdf`.

[40] Zachos, J. , Pagani, M. , Sloan, L. , Thomas, E. , and Billups, K. . Trends, rhythms, and aberrations in global climate 65 Ma to present. *Science*, 292:686–693, 2001.

[41] Zachos, J.C. , Shackleton, N.J. , Revenaugh, J.S. , Palike, H. , and Flower, B.P. . Climate response to orbital forcing across the Oligocene-Miocene boundary. *Science*, 292:274–278, 2001.

A

Appendix Photogrammetry

Photogrammetry - how does it work

This appendix further elaborates on the methodology of photogrammetry, for those unfamiliar with photogrammetry or those who seek further knowledge.
The reason why photographing with a drone is preferable, can be seen with the following figure A.1 from the Agisoft Photoscan manual:

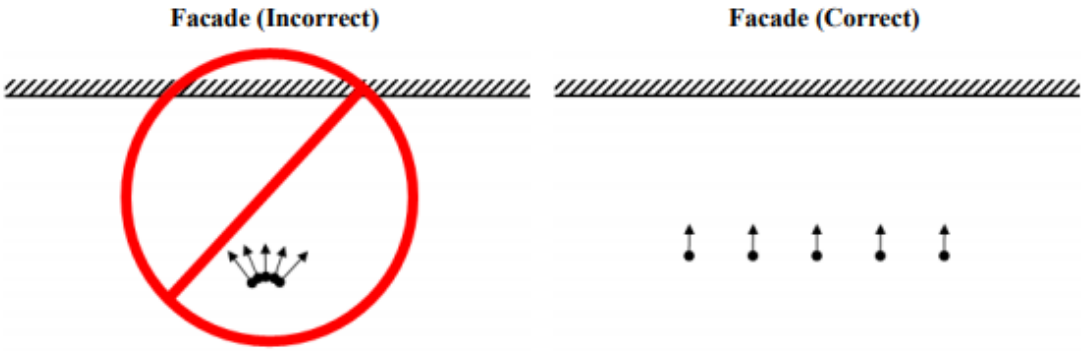

Figure A.1: How a facade should be photographed for optimum photogrammetry results. Source: Agisoft LLC, 2016

Since in geology the terrain is often difficult to walk, it would be almost impossible to photograph a panel in the manner displayed on the right in figure A.1. Even if this would be laterally possible when walking, to capture the full height of the outcrop will be difficult without photographing multiple times from the same point, as displayed on the left side.

What is essential in photogrammetry is that all photos have overlap with at least one another. A 3D model can only be formed when the same spot is photographed from (at least) two different locations; the same spot photographed from different angles (figure A.2). Ground control points are created in the field as well, to improve the photogrammetry results.
In photogrammetry, if a spot is photographed in both photos, the location relative to the camera of that spot can be determined (Bemis et al., 2014). This, step by step, builds a 3D model. With the camera positions known by GPS, points can be georeferenced.

The workflow used from fieldwork to resulting photopanel is described by Bemis et al., 2014 and shown in figure A.3.

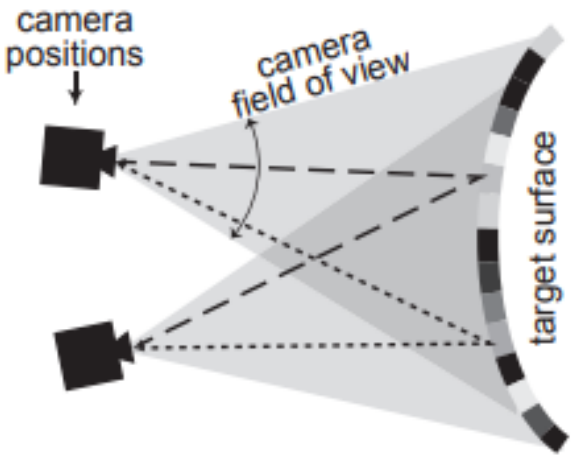

Figure A.2: The principle of photogrammetry. Source: Bemis et al., 2014.

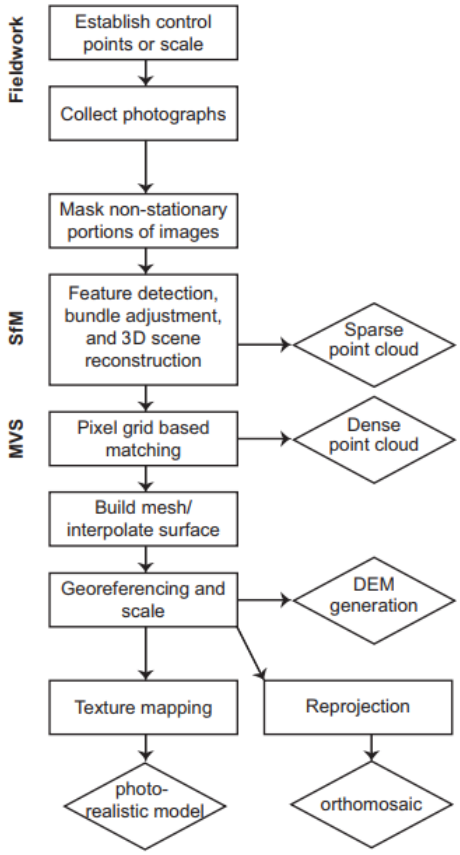

Figure A.3: The photogrammetry workflow from fieldwork to photopanel ('photorealistic model'). Source: Bemis et al., 2014.

The software that has been used for the photogrammetry is Agisoft Photoscan Professional version 1.4 from Agisoft LLC.

B

Appendix Lime interpretation

In this appendix each panel is shown with the interpretation from Lime. Each succession boundary is numbered separately. The scale is shown by the red line in each panel, with a length of 50m. Please note that the models are 3D, so it cannot be used as a scale bar.

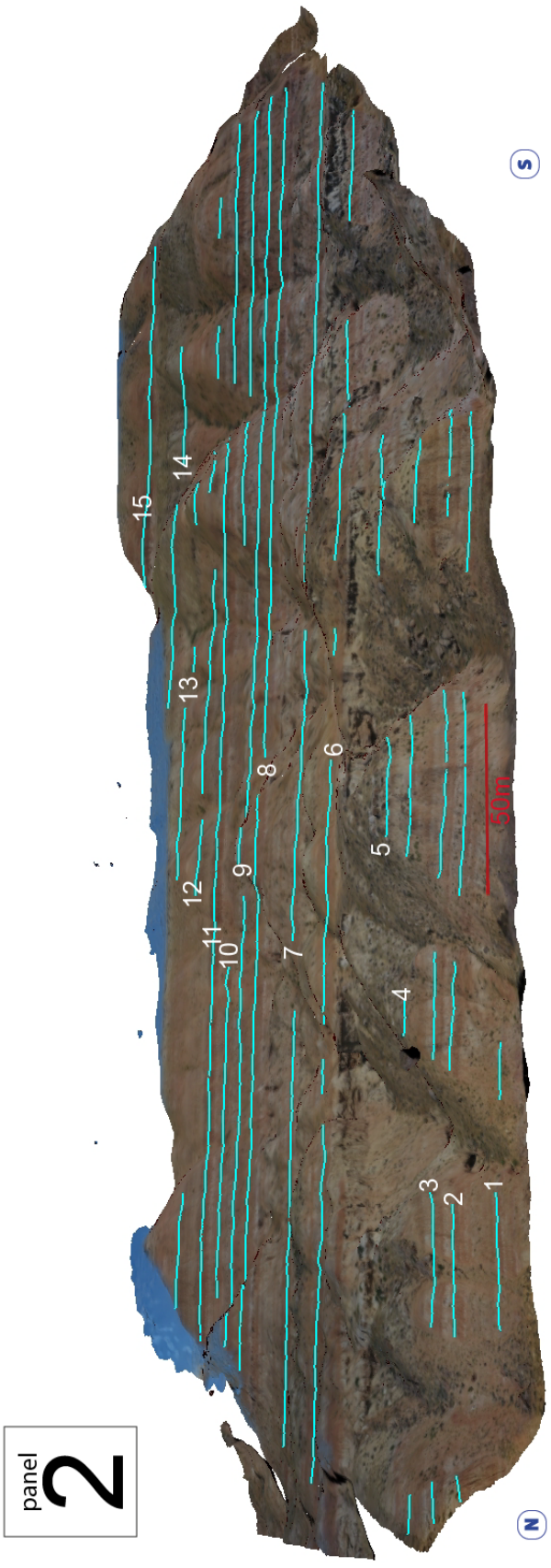

Figure B.1: The interpretation of panel 2. The succession boundaries are marked with a blue line and numbered from base to top. A line with a length of 50m is shown in red, which can be used as scale.

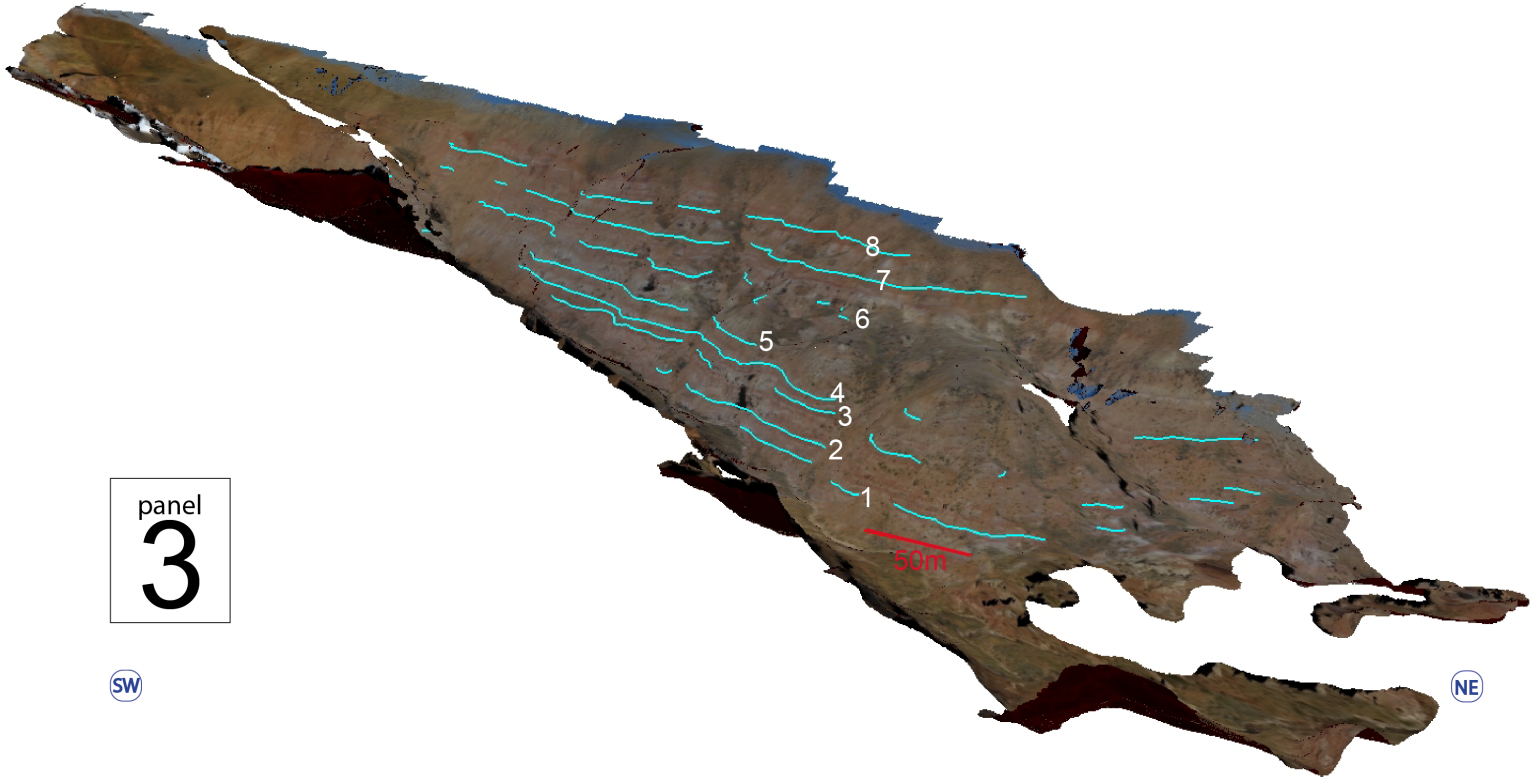

Figure B.2: The interpretation of panel 3. The succession boundaries are marked with a blue line and numbered from base to top. A line with a length of 50m is shown in red, which can be used as scale

Figure B.3: The interpretation of panel 4. The succession boundaries are marked with a blue line and numbered from base to top. A line with a length of 50m is shown in red, which can be used as scale

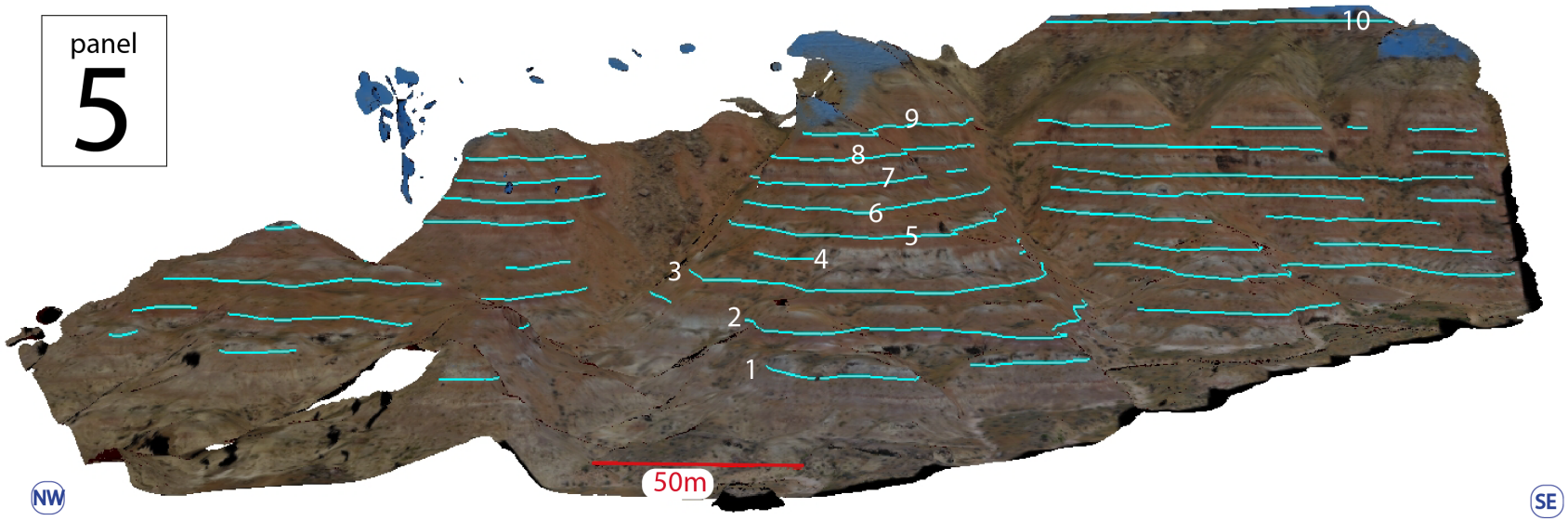

Figure B.4: The interpretation of panel 5. The succession boundaries are marked with a blue line and numbered from base to top. A line with a length of 50m is shown in red, which can be used as scale

Figure B.5: The interpretation of panel 13. The succession boundaries are marked with a blue line and numbered from base to top. A line with a length of 50m is shown in red, which can be used as scale

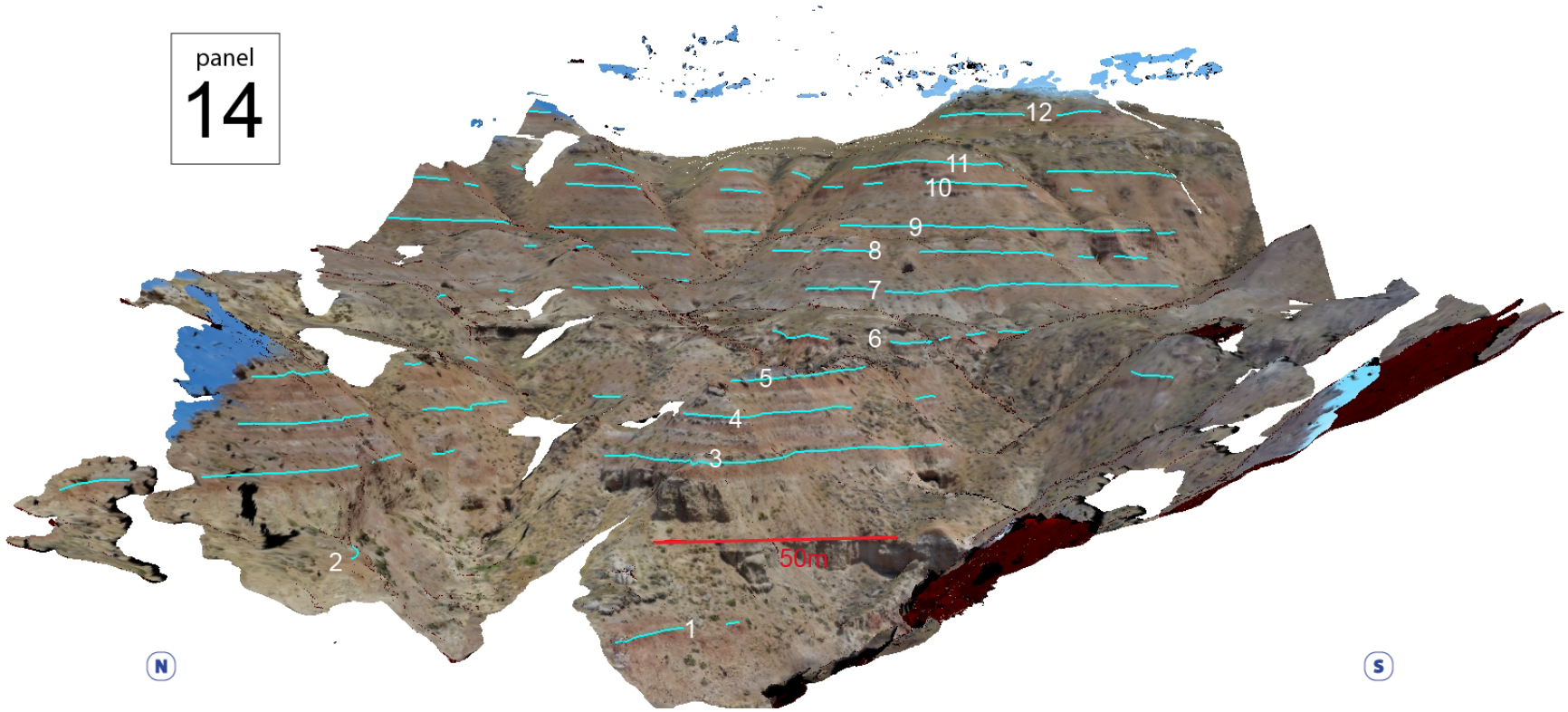

Figure B.6: The interpretation of panel 14. The succession boundaries are marked with a blue line and numbered from base to top. A line with a length of 50m is shown in red, which can be used as scale

Figure B.7: The interpretation of panel 15.1. The succession boundaries are marked with a blue line and numbered from base to top. A line with a length of 50m is shown in red, which can be used as scale

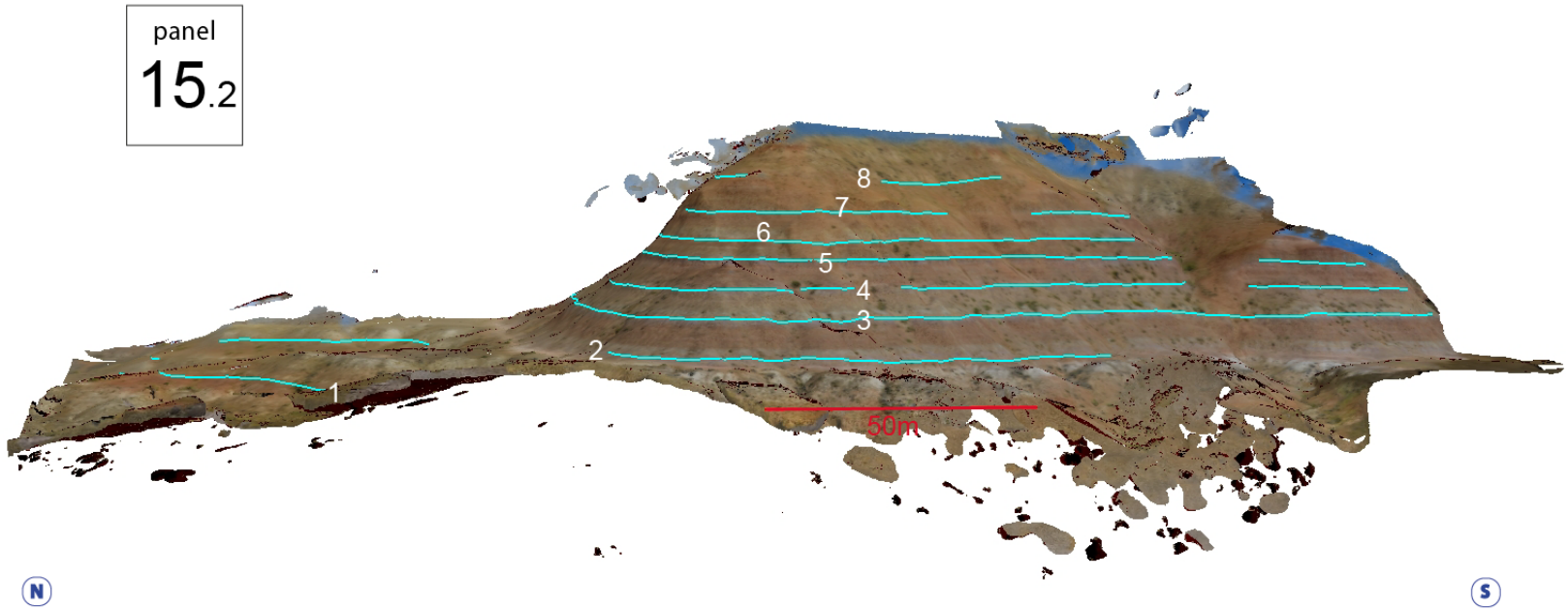

Figure B.8: The interpretation of panel 15.2. The succession boundaries are marked with a blue line and numbered from base to top. A line with a length of 50m is shown in red, which can be used as scale

Figure B.9: The interpretation of panel 16. The succession boundaries are marked with a blue line and numbered from base to top. A line with a length of 50m is shown in red, which can be used as scale

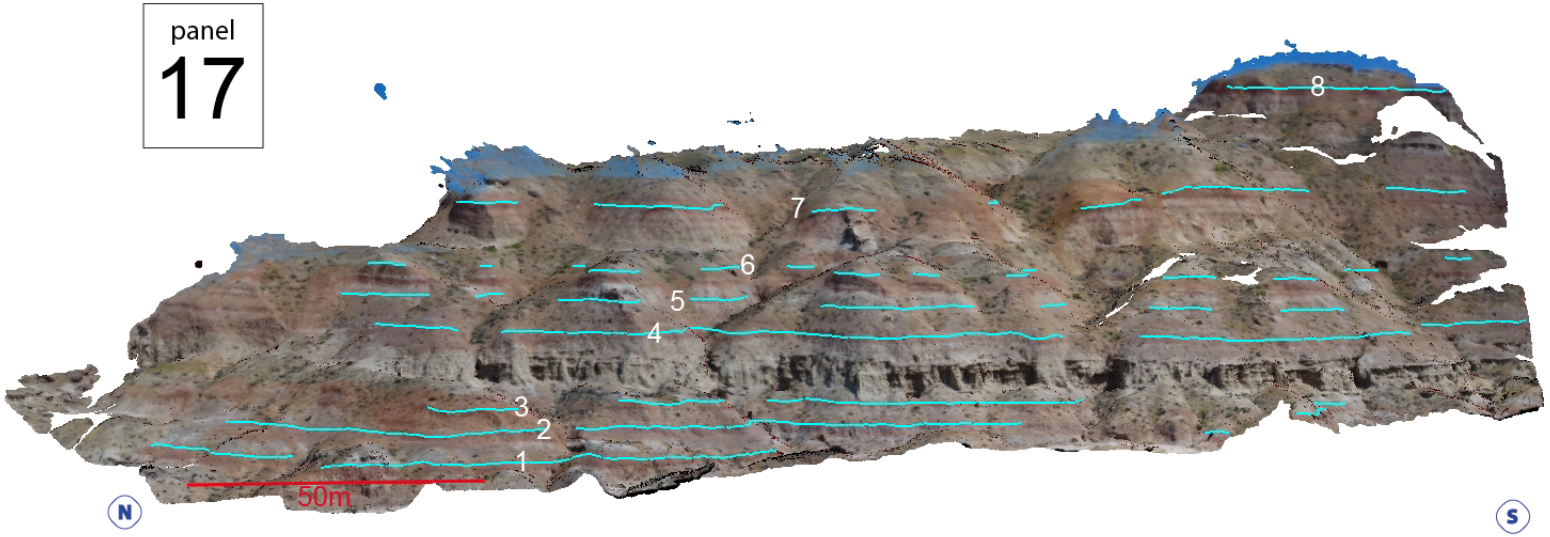

Figure B.10: The interpretation of panel 17. The succession boundaries are marked with a blue line and numbered from base to top. A line with a length of 50m is shown in red, which can be used as scale

Figure B.11: The interpretation of panel 18. The succession boundaries are marked with a blue line and numbered from base to top. A line with a length of 50m is shown in red, which can be used as scale

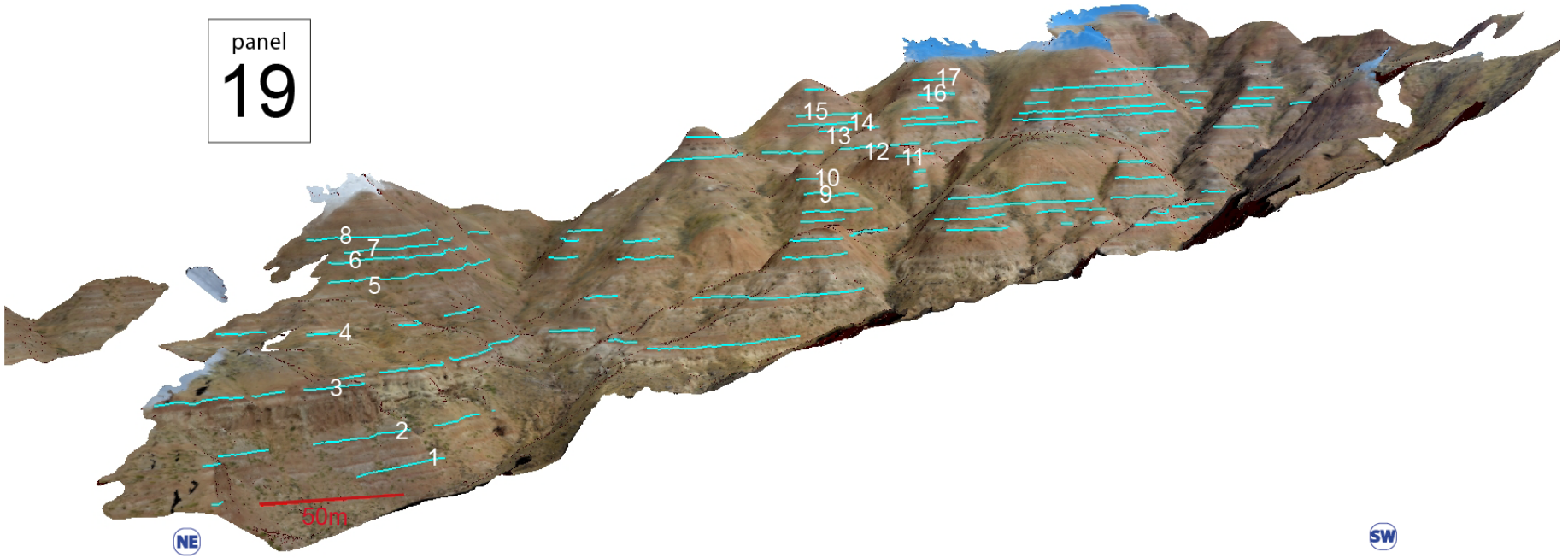

Figure B.12: The interpretation of panel 19. The succession boundaries are marked with a blue line and numbered from base to top. A line with a length of 50m is shown in red, which can be used as scale

C

Appendix Adjustment interpretation for consistency

As described, the coordinates in the panels, mainly the Z-location, were not consistent and corresponding with reality. Therefore they have been adjusted with Matlab, in order to retain this consistency. The changes made are shown per panel in table C.1.

Table C.1: The changes made in meters, for all of the lines in each panel.

Panel	**x-location**	**y-location**	**z-location**
2	0	0	-17.6
3	-1.0	-1.0	+6.3
4	0	0	-5.5
5	-0.4	+2.0	-4.2
13	-1.2	-2.0	+12.8
14	-0.5	-1.0	+9.5
15.1	0	0	+6.1
15.2	-22.0	-2.0	+1.0
16	0	0	-7.5
17	+0.7	-1.4	-16.0
18	0	0	-21.9
19	0	-2.0	-14.0

D

Appendix Original thickness measurements in Lime

This appendix shows all the separate thickness measurements from Lime, which are used for the average thickness calculation. Bottom section shown in figure D.1, top section in figure D.2.

Succession	Measurements thickness (m)										
10	5.02	5.99	5.67	4.87	4.71	5.82	4.82	6.07	7.09	7.08	7.71
		6.92	7.07	7.49	7.54	7.82	7.73	8.75	8.75	7.14	6.26
		5.93	6.29	6.7	7.61	6.68					
9	5.33	4.53	4.16	4.99	4.66	6.8	6.16	5.36	4.98	7.16	7.29
		6.35	5.28	6.46	4.23	5.7	5.64	6.11	5.57	6.05	5.94
		6.72	5.18	4.81	5.33	5.39	5.27	5.86	7.06	4.4	6.2
		6.02									
8	6.75	8.59	6.97	7.94	8.92	6.22	5.93	6.47	6.86	6.11	6.55
		11.1	10.88	12.06	11.42	11.02	10.8	11	11.68	11.59	8.33
		8.59	6.54	6.9	4.35	8.35	8.3	8.45	7.72	9.25	9.58
		6.55	6.65	5.39	5.72	7.06	7.43	6.9	6.17	5.4	6.18
		5.68	6.23	5.9	7.18	6.69	5.85	5.76	5.39	5.58	6.12
		5.39	4.46	4.09							
7	5.24	5.45	5.73	4.99	5.73	4.44	5.77	6.09	5.79	5.54	5.35
		5.69	8.82	8.85	9.72	7.88	8.18	6.25	5.91	5.45	4.97
		9.14	9.03	8.98	7.47	8.2	8.75	8.86	8.34	8.54	9.25
		9.35	8.99	8.71	8.4	6.28	7.07	6.87	6.39	6.65	6.47
		7.07	6.44	6.56	7.25	6.86					
6	9.29	11.22	12.25	12.44	11.73	12.37	8.23	6.71	5.23	6.62	4.56
		4.71	5.67	5.63	5.23	6.09					
5	4.62	4.12	3.68	3.55	5.93	6.14	6.38	6.84	6.69	6.55	6.49
		8.31	6.4	6.9							
4	3.79	3.68	3.81	4.07	5.11	5.94	5.2	4.38	5.25	4.23	4.74
		4.07	4.19	3.58	3.48	3.76	4.34				
3	8.02	7.59	8.7	6.99	7.38	8.57	7.92	6.28	6.88	6.43	6.34
		7.18									
2	6.34	6.17	7.03	6.3	6.79	7.19	8.38	6.41	6.4	6.25	6.39
		6.66	7.3	7.72	6.8	9.08	7.82	7.04			
1	8.91	9.13	8.9	8.66	8.92	9.4	9.16	8.18	8.64	8.5	

Figure D.1: The thickness measurements of the successions (bottom section).

Succession	Measurements thickness (m)										
33	9.55	9.78	10.22								
32	8.88	8	7.99	7.28	6.58	6.72	8.59	7.55	9.54		
31	6.45	5.8	6.05	6.35	5.92	6.12	6.38	6.56	6.35	6.69	6.35
		6.5									
30	4.4	4.37	3.89	3.93	4.26	4.33	4.38	4.03	4.02	3.78	3.88
		4.38	4.93								
29	6.66	6.45	6.02	6.03	6.5	5.76					
28	5.3	5.87	6.26	6.38	6.92	5.82	5.9	6.2			
27	6.5	6.03	6.81	7.03	8.27	8.88	8.75				
26	8.8	7.04									
25	7.74	8.77	7.75	8.72	8.3	9.43	9.89	8.39	6.22		
24	9.53	7.58	5.03	7.33	9.19	8.98	9.4	8.48	7.69	7.39	7.09
		6.09	5.19	5.64	6.02	6.96					
23	7.08	6.06	5.32	5.04	5.01	4.26	5.14	5.98	5.87	5.47	6.28
		6.63	7.92	6.89	6.53	6.59	6.56				
22	4.5	5.15	4.84	4.58	4.72	5.41	5.77	4.31	5.9	5.54	5.16
		6.37	5.7	4.89	4.51	6.36	6.4	5.53	4.97	6.22	5.23
21	7.39	8.95	8.21	9.08	8	8.68	7.22	6.39	4.78	5.1	5.18
		4.47	5.15	5.89	6.2	5.36	5.26	4.69	5.22	4.42	6.13
		4.71	5.4								
20	17.44	17.02	18.24	17.34	16.61	14.96	15.21	15.15	15.2	14.99	14.58
		14.41	12.81	14.14	14.13	12	12.52	13.68	13.29	12.53	
19											
18	8.32	9.16	7.18	7.65	8.31	7.91	7.92	5.68	5.78	7.8	8.1
		9.44	8.64	9.93	9.48	9.6	7.26	10.14	12.15	11.04	9.14
		10.49									
17											
16											
15											
14	5.48	5.93	7.53								
13	6.25	6.12	5.58	5.36	7.42	7.84	8.84	8.43	8.09		
12	7.48	4.3	4.9	5.52	7.37	8.35	8.18	8.62	8.33	8.73	6.54
		7.57	5.79	5	5.14	4.71	4.82	5.57			
11	6.59	5.82	5.27	6.28	4.99	4.91	9.94	10.64	9.36	7.03	7.5
		6.95	7.43	8.21	6.39	6.77	7.57	7.17	6.25	7.5	7.49
		5.4	8.15	8.46	7.61	6	4.51	4.41	4.08	5.30	6.26
		4.86									

Figure D.2: The thickness measurements of the successions (top section). Note that the measurements from succession 20 are discarded, since they are assumed to be no longer the result of a single succession.

E

Appendix Software used

The following software has been used in this thesis:

- Agisoft Photoscan Professional version 1.4.0.5650
- Lidar Interpretation and Manipulation Environment v1.0.1 (Lime)
- Paradigm 17 SKUA-GOCAD (version March 2017)
- Microsoft Office - Excel 2010
- Microsoft Office - PowerPoint 2010
- Microsoft Office - Word 2010
- Adobe Illustrator 2017 & 2018
- Matlab R2015b

This thesis is made in ShareLaTeX / Overleaf v2.